ISTANBUL TECHNICAL UNIVERSITY ★ GRADUATE SCHOOL

DESIGN OF A NEW LAMINAR SOIL CONTAINER AND ITS NUMERICAL VERIFICATION FOR SSI AND LIQUEFACTION TESTS

Ph.D. THESIS

Omid BAGHERI

Department of Civil Engineering

Earthquake Engineering Programme

JULY 2024

ISTANBUL TECHNICAL UNIVERSITY ★ GRADUATE SCHOOL

DESIGN OF A NEW LAMINAR SOIL CONTAINER AND ITS NUMERICAL VERIFICATION FOR SSI AND LIQUEFACTION TESTS

Ph.D. THESIS

Omid BAGHERI
(802172204)

Department of Civil Engineering

Earthquake Engineering Programme

Thesis Advisor: Assoc. Prof. Dr. Esra Ece BAYAT

JULY 2024

ISTANBUL TEKNİK ÜNİVERSİTESİ ★ LİSANSÜSTÜ EĞİTİM ENSTİTÜSÜ

YENİ BİR LAMİNER ZEMİN KONTEYNERİNİN TASARIMI VE SSI VE SIVILAŞMA TESTLERİ İÇİN SAYISAL DOĞRULAMASI

DOKTORA TEZİ

Omid BAGHERI
(802172204)

İnşaat Mühendisliği Anabilim Dalı

Deprem Mühendiliği Programı

Tez Danışmanı: Doç. Dr. Esra Ece BAYAT

TEMMUZ 2024

Omid BAGHERI, a Ph.D. student of İTU Graduate School student ID 802172204 successfully defended the dissertation entitled “DESIGN OF A NEW LAMINAR SOIL CONTAINER AND ITS NUMERICAL VERIFICATION FOR SSI AND LIQUEFACTION TESTS”, which he prepared after fulfilling the requirements specified in the associated legislations, before the jury whose signatures are below.

Thesis Advisor:	**Assoc. Prof. Dr. Esra Ece BAYAT** Istanbul Technical University	**….....**
Jury Members:	**Prof. Dr. Recep İYİSAN** Istanbul Technical University	**….....**
	Prof. Dr. Pelin ÖZENER Yildiz Technical University	**….....**
	Assist. Prof. Dr. Berrak TEYMÜR Istanbul Technical University	**….....**
	Assoc.Prof. Dr. Kubilay KELEŞOĞLU Istanbul University-Cerrahpasa	**….....**

Date of Submission : 22 May 2024
Date of Defense : 10 July 2024

to my dearest MUM,

I dedicate this work to you with ALL MY LOVE AND GRATITUDE.

FOREWORD

The journey of designing and manufacturing the Enhanced Transparent Impermeable Laminar (ETILam) soil container has been both challenging and rewarding. My deep interest in numerical modeling and eagerness to perform hands-on laboratory studies motivated me throughout this project. Creating a unique and innovative soil container was a key goal, aiming to advance geotechnical engineering and provide practical solutions for future research.

I am deeply grateful to my advisor, Assoc. Prof. Dr. E. Ece BAYAT, for her unwavering support and the opportunity to work on this topic. Her guidance has been invaluable. I also extend my thanks to my steering committee members, Prof. Dr. Recep İYİSAN and Prof. Dr. Pelin OZENER.

A special acknowledgment goes to Prof. Dr. Recep İYİSAN, whose support went beyond academic guidance. His fatherly concern for my well-being and his continuous encouragement played a crucial role in helping me navigate the challenges of this journey.

Thanks are also due to everyone who assisted with the laboratory studies in the Soil Mechanics Laboratory and the Earthquake Engineering Laboratory. Your help was vital to the successful execution of the experimental work.

The PhD journey comes with its challenges, particularly maintaining mental relief amid financial constraints. Completing a PhD requires significant mental and emotional resilience, and this journey has undoubtedly shaped my perspective as a researcher. Here I thank the BAP (Financial Coordination Office for Research Projects of Istanbul Technical University) for providing financial support through the project ID of 42629.

This study provides new insights into the design and manufacturing of laboratory test setups. The ETILam soil container represents a significant advancement in conducting accurate soil performance tests in a laboratory setting, offering practical and efficient means to study soil behavior under various conditions.

Looking ahead, I believe the ETILam soil container will serve as a valuable tool for researchers, contributing to a deeper understanding of soil behavior and better-informed engineering practices.

In conclusion, this dissertation reflects years of hard work and the support of mentors, colleagues, and friends. I hope the findings and innovations in this study will inspire future research and contribute to the advancement of geotechnical engineering.

Thank you to everyone who has supported me on this journey. Your encouragement has been invaluable, and I am deeply grateful for your contributions.

July 2024 Omid BAGHERI

TABLE OF CONTENTS

Page

ABBREVIATIONS

ETILam	**:**	Enhanced Transparent Impermeable Laminar
SDOF	**:**	Single Degree of Freedom
SSI	**:**	Soil Structur Interaction
1G	**:**	1 g Gravity test conditions
NG	**:**	More than 1 g Gravity test conditions
ESB	**:**	Equivalent Shear Beam
3D	**:**	3 dimensional conditions
1D	**:**	1 directional condition
PGA	**:**	Peak Ground Acceleration
PGD	**:**	Peak Ground Displacement
FSM	**:**	Flexible Sealant Mechanism
RM	**:**	Roller bearing Mechanism
R&FSM	**:**	Roller bearing and Flexible Sealant Mechanism
CSSLB	**:**	Cyclic Simple Shear Liquefaction Box
LVDT	**:**	Linear Variable Differential Transformer

SYMBOLS

E	**:**	Elastic modulus
G	**:**	Shear modulus
K	**:**	Bulk modulus
υ	**:**	Poisson ration
Dr	**:**	Relative density
γ	**:**	Unit weight
ø	**:**	Internal friction angle
σ_v	**:**	Verical stress
Vs	**:**	Shear wave velocity
k_n	**:**	Normal Stiffness
k_s	**:**	Shear stiffness

LIST OF TABLES

Page

LIST OF FIGURES

Page

DESIGN OF A NEW LAMINAR SOIL CONTAINER AND ITS NUMERICAL VERIFICATION FOR SSI AND LIQUEFACTION TESTS

SUMMARY

This dissertation presents the design, development, and evaluation of an Enhanced Transparent Impermeable Laminar (ETILam) soil container for laboratory soil tests. The research addresses the challenges in replicating prototype responses under static and dynamic conditions, which are crucial for geotechnical engineering applications. By conducting a comprehensive review of existing soil test setups and various types of laminar soil containers, the study aims to enhance the design and functionality of soil containers, particularly for dynamic tests using shaking tables and centrifuges.

The research begins by identifying the key aspects and essential characteristics of laboratory test setups. It emphasizes the importance of soil container boundary conditions on test performance. Different types of soil containers and their specifications are examined, concluding that laminar soil containers are the most effective for replicating prototype conditions in laboratory settings. The study then explores the limitations that need to be considered during the design of a laminar soil container, leading to the development of an initial design concept.

To ensure the effectiveness of the design, potential materials for the laminar soil container were tested in the laboratory. Characteristic parameters of these materials were evaluated for use in numerical modeling. Plexiglas and Sikaflex Pro3 flexible sealant paste were selected for the container construction. The performance of the lamina frame under maximum stresses induced during dynamic loadings was verified using structural software, and the locations of lateral support points were determined.

A new method was developed for preparing the required soil sample with the proper relative density. This method evaluates the relative density of the soil based on the diameter of the sieve opening and the height of raining, leading to the design of a new sand pluviation mechanism. Through numerical modeling, the effect of boundary type and expansion on the soil sample was studied. Different sinusoidal motions were

applied to the model, and the proper motion was selected for numerical evaluations of the laminar soil container design.

Based on a review of available containers and their movement mechanisms, various numerical models were developed and their performances compared with free-field test responses. An enhanced movement mechanism was developed to provide a response more closely resembling free-field conditions. This mechanism employs roller bearings and a flexible sealant moving mechanism between the laminas.

The study also examined the effect of the lateral support system on the behavior of the laminar soil container. It was found that vertical support, in addition to lateral support, provides a better response for the laminar soil container. The expected performance of the laminar soil container during laboratory tests was studied using generated models. The soil-structure interaction performance was evaluated, and the effect of a Single Degree of Freedom (SDOF) system on soil performance was assessed.

The design process, through numerical modeling, resulted in the manufacturing of the ETILam soil container. Its performance was evaluated through tests on an empty container on a shaking table and with soil samples during multiple tests. For studying the soil-structure interaction (SSI) effect, a test setup representing a pile-supported SDOF system was designed and manufactured. A series of laboratory tests were performed on this system, and some of the results were presented.

The performance of the empty ETILam soil container was compared with numerical model results, revealing that the numerical results closely resemble the laboratory test results. However, the results obtained from the laboratory tests on the soil sample inside the container indicated that increasing the input motion frequency and acceleration led to discrepancies between the numerical model and laboratory results, necessitating more detailed analytical studies on the soil models in the software.

In conclusion, this dissertation demonstrates the development and validation of the ETILam soil container. The study highlights the effectiveness of combining roller bearings and flexible sealant for laminar movement, the importance of proper boundary support, and the need for detailed numerical and laboratory analysis to accurately replicate real-site conditions for soil-structure interaction and liquefaction tests. The ETILam soil container represents a significant advancement in geotechnical

engineering laboratory testing, providing a more accurate and reliable method for studying soil behavior under dynamic conditions.

YENİ BİR LAMİNER ZEMİN KONTEYNERİNİN TASARIMI VE SSI VE SIVILAŞMA TESTLERİ İÇİN SAYISAL DOĞRULAMASI

ÖZET

Bu tez, laboratuvar zemin testleri için Geliştirilmiş Saydam Geçirimsiz Laminer (Enhanced Transpaerent Impermeable Laminar) (ETILam) zemin konteynerinin tasarımını, geliştirilmesini ve değerlendirilmesini sunar. Araştırma, Geoteknik mühendisliği uygulamaları için statik ve dinamik koşullar altında prototip yanıtlarının tekrarlanmasında karşılaşılan zorlukları ele almaktadır. Mevcut zemin test düzeneklerinin ve çeşitli laminer zemin konteynerlerinin kapsamlı bir şekilde incelenmesi yoluyla, özellikle dinamik testler için sarsma tablaları ve santrifüjler kullanılarak zemin konteynerlerinin tasarımı ve işlevselliği geliştirilmiştir.

Inşaat mühendisliğinde, laboratuvar test düzenekleri genellikle prototip modellerin hem statik hem de dinamik koşullarda tepkilerini tekrarlamakta zorluklarla karşılaşır. Dinamik testlerde bu zorlukları ele almak için araştırmacılar sarsma masaları (1G) veya santrifüjler (NG) kullanır, böylece serbest alan sınır koşullarını taklit eden koşullar simüle edilir. Zeminler üzerinde doğru laboratuvar testleri yapabilmek için gerçek saha koşullarını yakından taklit eden zemin konteynerlerine ihtiyaç vardır. Laminer zemin konteynerleri, prototip koşullara benzer şekilde zemin performansını simüle edebilme yetenekleri nedeniyle özellikle tavsiye edilir. Ancak, laminer zemin konteynerinin optimal tipi ve lamineler arası hareketi kolaylaştıran mekanizmalar konusunda sıkça sorular gündeme gelir.

Araştırma, laboratuvar test düzeneklerinin anahtar yönlerini ve temel özelliklerini belirleyerek başlamaktadır. Test performansı üzerindeki zemin konteyneri sınır koşullarının önemini vurgular. Farklı türde zemin konteynerleri ve bunların özellikleri incelenmiş ve laboratuvar ortamlarında prototip koşullarını tekrar eden en etkili tür olarak laminer zemin konteynerleri seçilmiştir. Çalışma, laminer zemin konteynerinin tasarımı sırasında dikkate alınması gereken sınırlamaları araştırarak, başlangıç tasarım konseptinin geliştirilmesine yol açmıştır.

Tasarımın etkinliğini sağlamak için laminer zemin konteyneri için potansiyel malzemeler laboratuvarda test edilmiştir. Bu malzemelerin karakteristik parametreleri, sayısal modelleme adımlarında kullanılmak üzere değerlendirilmiştir. Konteynerin yapımı için Plexiglas ve Sikaflex Pro3 esnek birleştirici macunu seçilmiştir. Dinamik yüklemeler sırasında maksimum stresler altında lamina çerçevesinin performansı, yapısal yazılım kullanılarak doğrulanmış ve yan destek noktalarının yerleri belirlenmiştir.

Gerekli zemin numunesini uygun rölatif yoğunlukta hazırlamak için yeni bir yöntem geliştirilmiştir. Bu yöntem, elekten geçen malzemenin çapı ve yağmurlama yüksekliğine dayalı olarak zeminin rölatif yoğunluğunu değerlendirmekte olup, yeni bir kum serme mekanizmasının tasarlanmasına yol açmıştır. Sayısal modelleme yoluyla, sınır türü ve genişlemesinin zemin numunesi üzerindeki etkisi incelenmiştir. Modele farklı sinüzoidal hareketler uygulanmış ve laminer zemin konteyneri tasarımının sayısal değerlendirmeleri için uygun hareket seçilmiştir.

Mevcut konteynerler ve hareket mekanizmaları üzerine yapılan incelemelere dayanarak, çeşitli sayısal modeller geliştirilmiş ve performansları serbest saha test sonuçları ila karşılaştırılmıştır. Serbest saha koşullarını daha yakından taklit eden bir sonuç sağlamak için geliştirilmiş bir hareket mekanizması üretilmiştir. Bu mekanizma, laminalar arasında hareketli esnek birleştirici macunu ve makaralı rulmanlar kullanır.

Çalışma ayrıca yan destek sisteminin laminer zemin konteynerinin davranışı üzerindeki etkisini incelemiştir. Dikey desteğin, yan desteğe ek olarak, laminer zemin konteynerinin daha iyi sonuç vermesini sağladığı bulunmuştur. Laboratuvar testleri sırasında laminer zemin konteynerinin beklenen performansı oluşturulan modeller kullanılarak incelenmiştir. Zemin-yapı etkileşimi performansı değerlendirilmiş ve Tek Dereceli Serbestlik (Single Degree of Freedom) (SDOF) sisteminin zemin performansı üzerindeki etkisi araştırılmıştır.

Sayısal modelleme yoluyla tasarım süreci, ETILam zemin konteynerinin imalatıyla sonuçlanmıştır. Performansı, sarsma tablasında boş konteyner üzerindeki testler ve çeşitli testler sırasında zemin numuneleri ile değerlendirilmiştir. Zemin-yapı etkileşimi (Soil Structure Interaction) (SSI) etkisini incelemek için, prototip koşulları temsil eden kazık destekli SDOF sistemi tasarlanmış ve üretilmiştir. Bu sistem üzerinde çok sayıda laboratuvar testi gerçekleştirilmiş ve bazı sonuçlar sunulmuştur.

Boş ETILam zemin konteynerinin performansı, sayısal model sonuçlarıyla karşılaştırılmış ve sayısal sonuçların laboratuvar test sonuçlarına oldukça benzediği bulunmuştur. Ancak, konteyner içindeki zemin numunesi üzerindeki laboratuvar testlerinden elde edilen sonuçlar, giriş hareketi frekansı ve ivmesi arttıkça, sayısal model ile laboratuvar sonuçları arasında tutarsızlıklar gösterdiğini ve yazılımdaki zemin modelleri üzerinde daha ayrıntılı analitik çalışmalara ihtiyaç duyduğunu göstermiştir.

Sonuç olarak, bu tez, ETILam zemin konteynerinin geliştirilmesini ve doğrulanmasını göstermektedir. Çalışma, lamina hareketi için makaralı rulmanlar ve esnek birleştirici macununun kombinasyonunun etkinliğini, uygun sınır desteğinin önemini ve zemin-yapı etkileşimi ve sıvılaşma testlerini doğru bir şekilde tekrar etmek için detaylı sayısal ve laboratuvar analizine olan ihtiyacı vurgulamaktadır. ETILam zemin konteyneri, dinamik koşullar altında zemin davranışını incelemek için daha doğru ve güvenilir bir yöntem sağlayarak Geoteknik mühendisliği laboratuvar testlerinde önemli bir ilerlemeyi temsil etmektedir.

1. INTRODUCTION

1.1 Purpose of Dissertation

In geotechnical earthquake engineering, gaining a better understanding of phenomena such as site amplification, dynamic soil behavior, and soil–structure interaction (SSI) is crucial, especially with the growing emphasis on performance-based design. Earthquake geotechnical studies employ various methodologies, including dynamic soil element tests, scaled model tests, numerical and analytical models, and full-scale field tests. When conducted correctly, scaled model tests offer economic and realistic insights into ground amplification, changes in pore water pressure, soil non-linearity, failure occurrence, and soil–structure interaction.

Both full-scale field tests and scaled model tests are vital for examining soil response and SSI during earthquakes and for validating analytical models. Full-scale field experiments provide the advantage of considering realistic site conditions, while model tests offer a controlled environment conducive to economic parametric studies. Typically, scaled seismic model tests are performed either in a centrifuge (N-G) or on a shaking table (1-G). Centrifuge testing is particularly advantageous as it can replicate a gravitational stress field similar to in-situ conditions, accurately simulating the prototype stress state. For sands, where stress–strain behavior depends on confining stress, an appropriate gravitational stress field is essential. However, modeling overburden stresses is less critical for studying the seismic response of clays compared to sands, making the use of a centrifuge less necessary for undrained cohesive soils.

Figure 1.1 shows a schematic diagram of a laminar container. The typical design of a laminar soil container involves a series of laminae individually supported by bearings and a steel guide connected to an external frame. The key design principle of a laminar box is to minimize the lateral stiffness of the container, allowing the soil to control the response of the soil-box system.

While the most common shape for these containers is rectangular, for two-dimensional shaking tests, the box can also be square, circular, or even a 12-sided polygon.

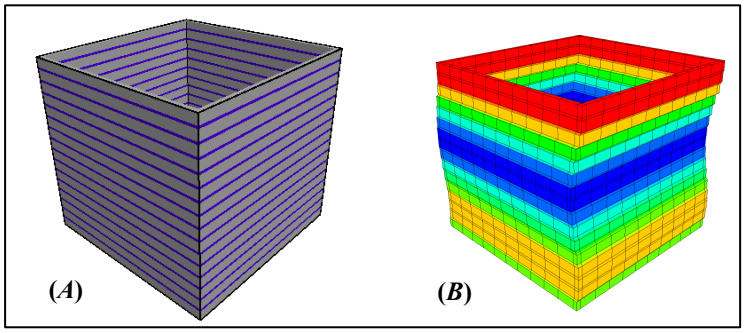

Figure 1.1:(A) Sketch of a typical laminar soil container modeled in this study (B) an example of a laminar soil container deformed shape in the numerical analysis.

As all the laminar containers manufactured to date may have been designed to address specific problems, there is currently no comprehensive design specification encompassing all possible effective parameters. Thus, this thesis aims to evaluate all possibilities and parameters to design the most appropriate and optimized box, incorporating all effective parameters before its manufacture. The objective is to develop a novel design for a laminar soil container to be used on the shaking table for testing soils under SSI effects or liquefaction behavior.

1.2 Unique Aspect of the Study

There are different types of soil containers which could be used to develop a model for performing tests. These multiple types include:

1- Rigid container

2- Rigid container with flexible boundaries (e.g. duxseal or sponge)

3- Rigid container with hinged end-walls

4- Equivalent Shear Beam (ESB) container

5- Laminar container

6- Active boundary container

While each type of laminar soil container has its own advantages and disadvantages, they meet different design requirements to varying extents. Given that tests in laminar containers represent the optimal execution method for model box tests, the focus should be on the performance of these types of boxes. To comprehend the function of the laminar box, it is essential to recall that its design principle is to minimize the

container's lateral stiffness, ensuring that the soil governs the response of the soil-box system.

This dissertation aims to cover the following aspects by reviewing the advantages and disadvantages of existing boxes and studies:

1- This research will provide valuable information about the steps toward designing and modeling a soil container suitable for SSI tests and further understanding of models under dynamic loadings.

2- The numerical modeling of the box will offer insights into its performance, including the effects of the materials used and various load cases.

3- Through numerical modeling, an outline of the box's performance can be achieved before the preparation of the physical model.

4- Numerical modeling allows for further modifications to the test setup and can include multiple parameters that would be costly to model physically.

5- The suitability of the materials used for the laminar box will be verified to ensure their capability of transferring lateral loads to the upper layers.

6- The mechanism used between the laminas should facilitate load transfer to the layers with minimal energy loss, closely replicating free-field conditions.

7- Typically, laminar soil containers are made of rigid, non-transparent materials. Using transparent materials will allow for better understanding and monitoring of soil performance inside the container during tests.

8- The shape of the container will be designed to accommodate multiple types of test setups.

9- Flexible sealant is planned to be used to separate the laminas, providing an impermeable boundary for saturated soil cases and liquefaction tests, potentially eliminating the need for a membrane.

10- Additionally, using flexible sealant between the laminas will prevent soil grains from penetrating the gaps between laminas, as seen in roller bearing laminar boxes, making maintenance easier.

1.3 Impact of the Study

As previously mentioned, this thesis aims to present a novel design concept for the laminar soil container, which is expected to have the following impacts:

1- Domestically, there are a limited number of laminar soil containers in Turkey. This design will not only be larger in dimension but also provide more detailed information about the soil's performance inside the box.

2- The use of this box will serve as an excellent educational tool for academic courses.

3- The test preparation and execution procedures will offer younger students an opportunity to become familiar with laboratory work and soil behavior during tests.

4- In the future, various cases could be modeled using this box, allowing for the verification and potential replacement of existing regulations with better results and instructions.

5- Worldwide, numerous laminar soil containers exist, but none offer such comprehensive specifications in a single design.

6- To date, there has been no extensive 3D numerical modeling verification of laminar soil containers that thoroughly examines different parameters and the dynamic performance of the box.

7- The transparency of the designed box is a significant aspect, providing the ability to monitor the performance of the box and the sample inside it.

8- In addition to sensor data, visual processing can be incorporated during every test conducted in the box.

9- The ability to observe the soil sample inside the box during tests will enhance awareness of soil performance and may lead to a deeper understanding of the complex characteristics of soil.

2. LITERATURE REVIEW AND STUDY METHOD

2.1 Key Aspects of Soil Containers for Dynamic Testing

While prototype soil layers extend infinitely in lateral directions, model setups are confined, presenting a challenge in replicating prototype conditions. Figure 2.1 illustrates the conceptual movement of the soil body when lateral loading is applied at the bedrock level, generating shear waves within the soil stratum. The movement mode shapes are influenced by the shear modulus variation with depth, characterizing the soil body as a shear beam. Thus, designing a soil container must include features that ensure the stress distribution during lateral loading at the base closely mimics the infinite boundary condition (Fardis, 2011).

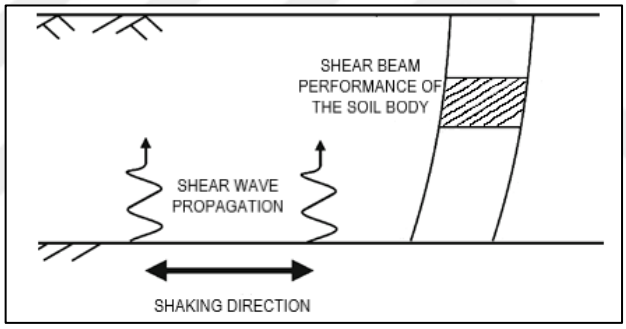

Figure 2.1: Conceptual soil body movement during the application of a lateral load to the Bedrock (Bhattacharya, 2012).

There are some key aspects and specifications that containers have to satisfy to properly represent the soil performance during the tests. These conditions that some of them are mentioned by Campbell et al. (1991) and Zeng and Schofield (1996), are summarized in the following sections.

2.1.1 Stress distribution and resemblance considerations

The horizontal loads applied at the base of the soil layer generates shear stresses in vertical and horizontal planes in the soil body. Free body diagram of the affecting loads during the shaking represents the generation of the soil mass inertia force that can be defined by a horizontal force (Fh) concentrated at the center of the inertia of the soil layer.

Figure 2.2 illustrates the generation of an overturning moment due to base shaking, which must be balanced to stabilize the system. The balancing forces arise from shear forces acting at the soil body's boundaries, a condition expected to occur in the soil sample within the container. The similarity of stress conditions near the boundary and the center of the container depends on the friction properties between the container walls and the soil materials. Frictionless end walls lead to a distortion of the stress field in the soil body, unlike prototype conditions. Placing the test setup in the middle of the container can minimize the end-wall effect. However, the impact range of the boundaries varies with the container's shape and dimensions, which should be determined through experimental tests and numerical modeling.

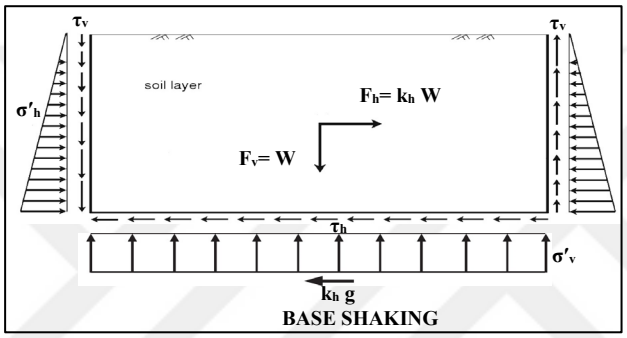

Figure 2.2: Representations of stresses generated within the soil body during the shaking (Zeng and Schofield, 1996).

2.1.2 Transfer of the ınput motion to the soil sample

To accurately simulate seismic loading conditions on a soil sample, it is essential to establish a frictional interface between the soil and the container boundaries. This interface ensures the effective transfer of applied wave energy from the shaking table to the soil sample. Typically, this is achieved by using a rough surface on the base of the container, which facilitates the transmission of horizontal wave energy. Consequently, stress is generated throughout the entire soil sample, rather than being concentrated only at the container's base.

2.1.3 Strain distribution

When subject to a one-dimensional horizontal dynamic load at the base of the soil layer, soil particles move in a planar manner. This same condition must be replicated in soil containers to accurately simulate soil behavior. To achieve this planar movement during one-dimensional motion application, the container's side walls parallel to the movement direction should be smooth and frictionless. This ensures that a two-dimensional condition, resembling that of the free field, is represented.

2.1.4 Wave propagation and reflection problems

When shear waves are applied to the base of a container, they propagate through the soil body and encounter the container boundaries. The interaction results in refraction and reflection due to the Snell effect, especially noticeable in waves hitting boundaries of different stiffness. This phenomenon includes the P-wave component, which must be considered in test analysis. The use of stiffer materials for container walls creates a reflective surface, reducing the stress and displacement amplitudes of the reflected wave compared to the incident wave.

In a homogeneous linear elastic infinite material layer, stress waves propagate without alteration. However, in free field conditions, waves attenuate over distance due to various material properties, such as viscous and hysteretic damping, as well as radiation damping (Kramer, 1996).

2.1.5 Impermeable property

For saturated conditions, the test setup necessitates impermeable container boundaries. These impermeable boundaries retain water within the container, facilitating the generation of proper pore water pressure, particularly crucial in liquefaction test samples.

2.1.6 Laminated performance of the soil body

Accurately studying the performance of a soil layer requires acknowledging that soil in its natural state consists of discrete elements. However, confining soil within finite boundaries may cause it to behave more like a continuous cantilever column experiencing lateral motion. This behavior is influenced by the container's movement mechanism and end-wall specifications. To address this, containers can be fabricated using multiple laminas separated by supports, enabling the laminas to move relative to each other. This approach allows for the discretization of the soil sample, ensuring that it can more precisely regulate the performance of the soil container.

2.1.7 Laterally rigid end-walls

To ensure zero lateral movements and strains in the boundaries of the container boundaries during spin-up in centrifuge tests, and to enhance effective gravity and stresses, the container material must exhibit proper rigidity, preventing excessive lateral deformation during testing. However, achieving this ideal condition may not always be feasible. Hence, it's essential to meticulously select the dimensions of both

the container and model to minimize the boundary effect at the test setup location as much as possible.

2.1.8 Settlement of the end-walls

In centrifuge tests during spin-up, soil material experiences settlement. Thus, it's crucial for the end-walls to move along with the soil layer to prevent initial shear stress between the soil body and frictional end-walls. This prevents any adverse impact on the vertical normal stress at the boundaries, consequently safeguarding the base of the container.

2.2 Types of Containers and their Specifications

Various types of soil containers have been developed and employed in dynamic soil testing, each with its distinct advantages and drawbacks, depending on how effectively they meet essential criteria. These containers can be classified into different categories based on their boundary conditions and end-wall performance:

2.2.1 Rigid container

This type of soil container is made of rigid material, forming a complete box with no flexibility or permission to deform in the side and end walls (Figures 2.3A and 2.4A).

2.2.2 Rigid container with absorbing boundaries

To mitigate the reflection of P-waves from the end-walls in rigid boundary containers, a solution involves covering the end-walls with a flexible and compressible material like duxseal or sponge (Duxseal or Sponge (Coe 1985)) (Figure 2.3B). This measure reduces the stress and displacement amplitudes of the reflected waves, while also minimizing the risk of damage to the end-walls resulting from repeated application of dynamic loads.

2.2.3 Rigid container with hinged end-walls

Given that the soil's behavior resembles that of a shear beam and entails lateral deformation, a hinge connection is employed between the end-walls and the base of the container (Figures 2.3C and 2.4B). This hinge mechanism allows for rotational flexibility at the end-walls, enabling them to laterally move along with the soil sample. This approach is adopted in the container utilized by Eseler-bayat (2016) in CSSLB.

2.2.4 Equivalent shear beam (esb) container

Typically, ESB containers are constructed by assembling multiple individual frames stacked atop one another, employing sliding materials such as Teflon or flexible materials like rubber. This design facilitates the division of the soil sample into distinct layers, with the objective of imparting realistic shear strains within the soil layers (Figures 2.3D and 2.4F).

2.2.5 Laminar container

In a laminar container, ball bearings are typically employed between the lamina frames. While the performance concept resembles that of equivalent shear beam containers, the soil response differs due to the entirely frictionless movement of the frames facilitated by the ball bearings. Nonetheless, laminar containers are more susceptible to residual deformation of the container and sliding of the frames (Figures 2.3E, 2.4C, and 2.4D).

2.2.6 Active boundary container

The active boundary container (Takahashi 2001) shares similarities with laminar soil containers in construction but diverges in the method of applying lateral loads. While other container types feature a fixed base on a shaking table with motion applied from below, the active boundary container utilizes a set of actuators affixed to the container's side to exert forces or deformations on the frames. This design affords greater control over boundary conditions and enables simulation of more intricate loading scenarios. However, the container's design and construction can be more intricate and costly compared to other container types (Figures 2.3F and 2.4E).

When deciding on a soil container for laboratory testing, it's crucial to consider key factors that ensure responses akin to free field conditions. Table 2.1 summarizes the pros and cons of each container type. Additionally, the capacity, applicable load amplitude, and frequency limitations of the dynamic load application system used in the test setup should be taken into account. Therefore, researchers are advised to select a container that best meets these limitations and characteristics to ensure a faithful simulation of free field conditions.

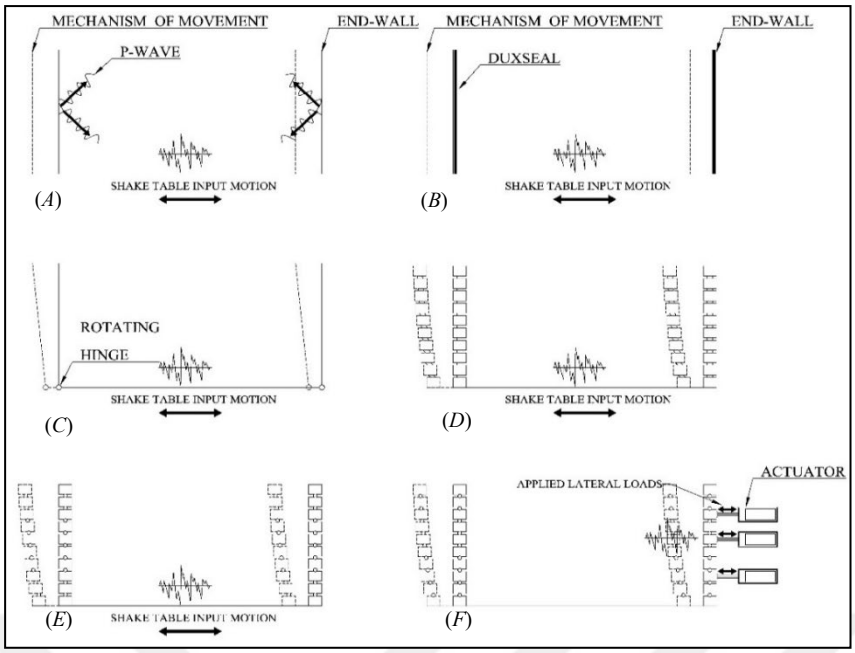

Figure 2.3: Sketch of mechanisms of movement for (A) Rigid container (B) Rigid container with absorbing boundary (C) Rigid container with hinged end walls (D) Equivalent shear beam (E) Laminar soil container (F) Active boundary container.

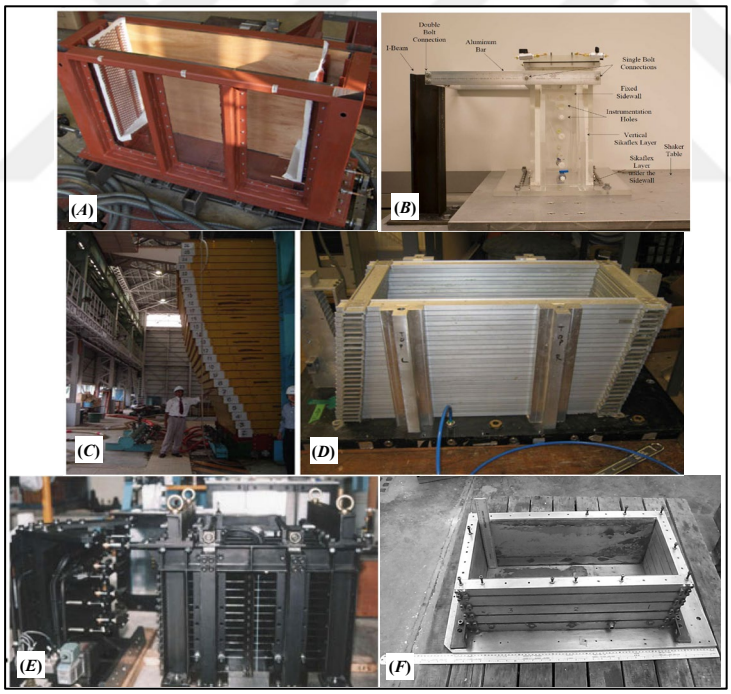

Figure 2.4: Examples of soil containers in the literature: (A) Rigid box used in the shaking table at the University of Oxford (B) Simple shear container with hinged end walls (CSSLB, Eseler-bayat, 2016) (C) Large laminar container used in 1-G testing in Tsukuba, Japan (D) Laminar container used in centrifuge, University of Cambridge (Brennan and Madabhushi, 2006) (E) Active boundary laminar container (Courtesy of Professor Akihiro Takahashi, Tokyo Institute of Technology, 2001) (F) ESB container at Cambridge (Zeng and Schofield, 1996).

The advantages outlined in Table 2.1 indicate that laminar soil containers may be the most suitable option for laboratory testing setups and dynamic evaluations of soil samples. These containers afford precise control over the soil sample, rendering them ideal for laboratory testing and dynamic assessments of soil behavior.

Table 2.1: Detailed specifications of each type of soil container.

Type of the Container	Advantages	Disadvantages
Rigid Boundary Containers	-Stress resemblance -Motion transfer to the soil -Strain distribution -Impermeable boundary -Zero lateral wall displacement	-Reflection of the P-wave -Non-compressible end-walls -Performance of the soil body like a continuous cantilever column -Requiring more length to height ratio to eliminate boundary effect
Rigid Container with Absorbing Boundaries	-Stress resemblance -Motion transfer to the soil -Strain distribution - Impermeable boundary -Less P-wave reflecting side-walls -Zero lateral wall displacement	-Non-compressible end-walls -Performance of the soil body like a continuous cantilever column - Requiring more length to height ratio to eliminate boundary effect -Effect of softer material on actual boundary conditions
Rigid Container with Hinged End-Walls	-Stress resemblance -Motion transfer to the soil -Strain distribution - Impermeable boundary -Zero lateral wall displacement	-Reflection of the P-wave -Non-compressible end-walls -Performance of the soil body like a continuous hinged column - Requiring more length to height ratio to eliminate boundary effect
Equivalent Shear Beam (ESB) Container	-Stress resemblance -Motion transfer to the soil -Strain distribution - Impermeable boundary (in case of using internal membrane) -No P-wave reflecting side-walls -Zero lateral wall displacement -Compressible end-walls in high vertical stresses -Laminated soil performance controls the container movements -Less boundary effect due to the movement of the frames	-Linear performance of the rubber material between the frames in contrary to soil nonlinearity - Difference between the stiffnesses of the laminas and the adjacent soil material -Excessive relative displacement of the frames -Rocking of the container at high values of displacement amplitude -Local failure of soil sample in mid-heights of the container -Excessive compression of the rubber layer under high gravity conditions in N-G
Laminar Container	-Stress resemblance -Motion transfer to the soil -Strain distribution - Impermeable boundary (in case of using internal membrane) -No P-wave reflecting side-walls -Zero lateral wall displacement -Compressible end-walls at high vertical stresses -Laminated soil performance controls the container movements -Less boundary effect due to the movement of the laminas -Supports between the laminas enforce the laminas to move horizontally without rocking	-Linear performance of the rollers in contrary to soil nonlinearity -Difference between the stiffnesses of the laminas and the adjacent soil material -Improper transfer of the input motion to higher layers -Vertical supports don't compress at high gravity conditions in N-G, resulting in initial shear stress between the soil and end walls
Active Boundary Laminar Container	-Stress resemblance -Motion transfer to the soil -Strain distribution - Impermeable boundary (in case of using internal membrane) -No P-wave reflecting side-walls -Zero lateral wall displacement -Compressible end-walls at high vertical stresses -Laminated soil performance controls the container movements -Less boundary effect due to the movement of the laminas -Supports between the laminas enforce the laminas to move horizontally without rocking -Lateral actuators apply the predicted motion	-Linear performance of the rollers in contrary to soil nonlinearity - Difference between the stiffnesses of the laminas and the adjacent soil material - Vertical supports don't compress at high gravity conditions in N-G, resulting in initial shear stress between the soil and end walls - Controlling the laterally applied motion amplitude is complicated for different depths of the model

2.3 Laminar Containers Published in Literature

The primary objective of employing laminar soil containers is to enable the soil sample to dictate the behavior of the soil-container system during lateral shaking, as emphasized by Bhattacharya (2012). Laminar soil containers typically comprise multiple lamina frames, each separated by a mechanism facilitating the unrestricted lateral movement of individual laminas relative to one another. This section reviews various laminar containers documented in the literature, summarizing their design, testing specifications, and performance results in Table A1.

2.4 Study on the Limitations of the Design

In order to decide on the dimension and the limits for laminar box to be constructed, there would be some limitation due to available bearing load on the shaking table.

So by checking the shaking table specification, the maximum applicable load will be confirmed.

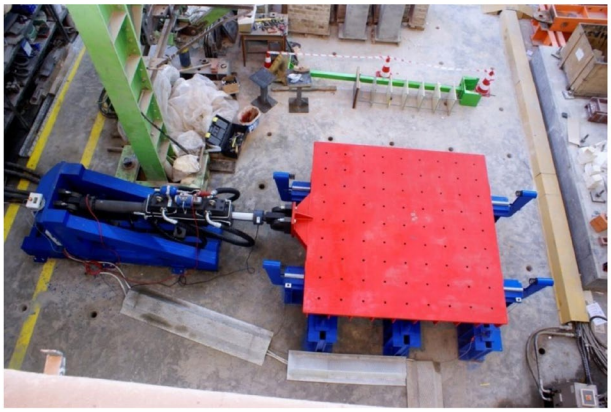

Figure 2.5: An overview of the shaking table.

Table 2.2: Characteristics of the shaking table.

Parameter	Value	Unit
Dimension of Table (B×L)	235×235	cm
Displacement Limit	±32.5	cm
Maximum Theorical Velocity	100	Cm/sec
Maximum Acceleration	2.0 g	(g=9.81 m/s^2)
Maximum Actuator Force	300	kN
Engine Power	75	kW
Maximum Vertical Capacity	200	kN

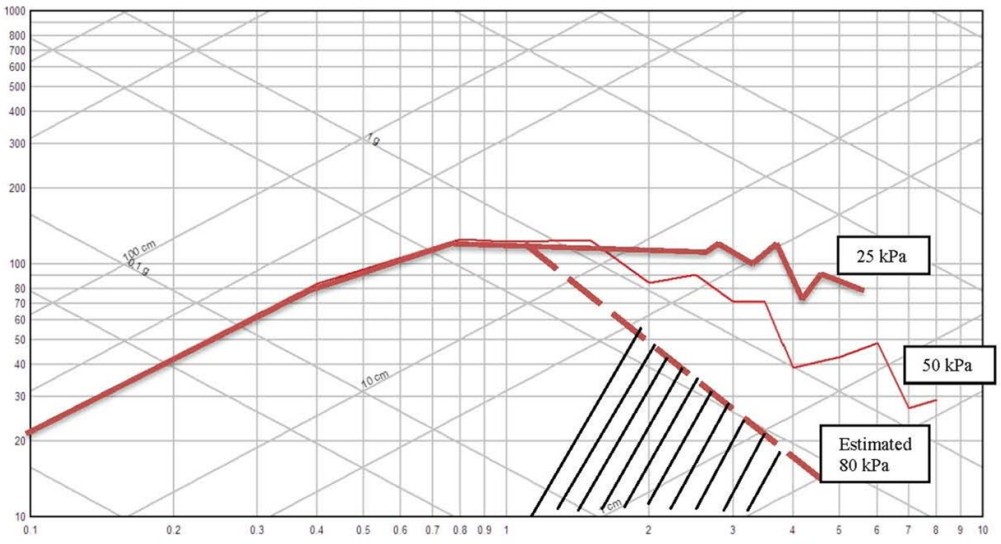

Figure 2.6: Performance diagram of shaking table carrying 25 and 50 kPa (x10e-1 tons) overload, and estimated range for the 80 kPa (8 tones).

In Table 2.4, the range of parameters of applicable loads for applying to the laminar soil container by the shaking table during the numerical modelling and laboratory tests are presented.

Table 2.3: Maximum applicable load parameters by the shaking table to the box.

Maximum full box weight	Range of Frequency	Range of displacement	Range of acceleration
8 tones	0~ 4 Hz.	0.5 ~ 5 cm	0.05 ~ 0.7 g

2.5 Methods and Techniques

To start designing the laminar soil container and having a proper conjecture for designing the box and performing the tests, it would be necessary to have a relevant notion about the performance of the box which will be verified by the numerical modelling of the box and intended design through the FLAC3D which is a finite difference program.

The steps toward the preparation of the box may be listed as follow:

2.5.1 Considerable steps for designing a laminar soil container

The steps that should be studied in this thesis would be as follow:

1- Selection of the materials which could be used to prepare the laminar soil container including Plexi-Glass, flexible sealants or any other required material.

2- Defininig the best performing mechanism of movement for the container based on the connection between the laminas and type of interaction among them by using bearing connection or rubber-like material to fill the gaps between the laminas.

3- Understanding the performance of the material during construction of the box, through static analysis of the box by modelling sequential construction of the laminas, and also checking the compression and lateral deformation of the flexible material due to the excess loads, which are transferred to them during the box preparation, and also placement of soil material inside the box.

4- Checking the performance of the box under the dynamic load which is applied to the base of box on shaking table.

5- Defining the limits of the dynamic loads which could be applied to the box by the shaking table.

6- Comparison of the box model with the free-field condition to confirm the resemblance of the performance.

7- Checking the performance of the box with different laminar materials and dynamic load cases.

8- Numerical modelling of tests for studying the SSI effects on the surface or buried foundation.

After numerical study of the laminar container, and confirming the proper performance of the box for the intended case studies, the experimental tests would be triggered and will be compared with the numerical models.

2.5.2 Necessary steps for experimental tests in the laboratory

To perform the experimental tests, the following steps are mandatory;

1- Prepare the laminar container design specifications and provide the proper material for the intended purpose based on the initial specifications attained from the numerical modelling.

2- Manufacturing the box and preparation of the laminar soil container

3- Calibrate the box based on the numerical analysis procedure and study the performance of the box under the same conditions as the numerical modelling for verifying the properties which is used during the numerical simulation, and if required

change the initial parameters and capture close results as the experimental tests will provide us.

4- Define a procedure to prepare soil sample in the box so that the intended parameters could be attained for the tests. In this section different procedures which has been used in the previous works, might be used or a new procedure could be defined based on the requirements.

Procedures have been used already based on the literature, may include:

a- Using hopper and nozzle to pure the material inside the box in continuous rows and layers.

b- Using raining box to pour the material in layers over each other.

It should be considered that different height of pouring will result in different densities in the box. So for the selected method, some tests should be run in order to calibrate the sample preparation method.

5- Prepare the test setup and sensor location and define the best monitoring system on the box. The sensors may include accelerometers, displacement gauges, pore pressure sensors, laser displacement sensors and visual analysis cameras.

6- Comparison of the results gained from the experimental tests with the numerical model and confirm the proper performance of the tests.

2.6 Discussions and Conclusions

In this chapter the following key points are covered:

1- The key aspects and essential characteristics which should be considered during soil dynamic laboratory tests are presented.

2- Different types of soil containers and their specifications are studied and the laminar soil containers are selected as the best performing type of containers for the laboratory test setups.

3- Laminar soil containers avaliable in the literature are reviewed and their specifications are summarized.

4- Main effective parameters on the design and manufacturing of a soil container are studied.

3. LABORATORY STUDIES FOR CONFIRMING THE REQUIRED PARAMETERS FOR NUMERICAL EVALUATION OF THE CONTAINER DESIGN

The main idea during designing the laminar soil container is to use flexible sealant material between the laminas to fill the gap and also, provide the chance of laminas to move separately form each other to represent the freefield condition. So, for the purpose a polyurethane based aditive paste namely SikaFlex Pro-3 is selected based on the elastic deformation potensials of the material and elaongation capability which is provided through the datasheets provided by the manufacturing company.

The connection and adhesion of the material to the surface of the lamiar frame is required to be studied. For this purpose the SikaFlex Pro-3 is used to attach the pieces of plexiglas and also aluminum together and tested by applying extension loading.

3.1 Shear and Compression Tests on the Flexible Sealant

To confirm the properties which is used during the numerical modeling and also the durability and flexibility range of the sealant, some tests are carried out in the laboratory. Figure 3.1 shows the attachment mechanism which is planned to be used for the test samples.

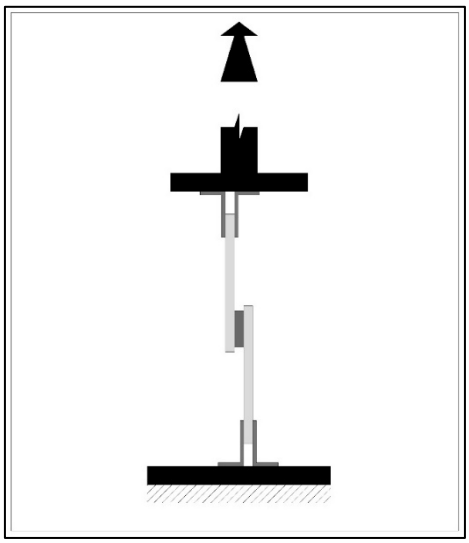

Figure 3.1: Test setup details of the samples.

The results of the tests are presented in the charts in the Figures 3.2 and 3.3. Obviously, the shear force applied to each sample will be different from the other samples and based on the adhesion surface the performance will be different too.

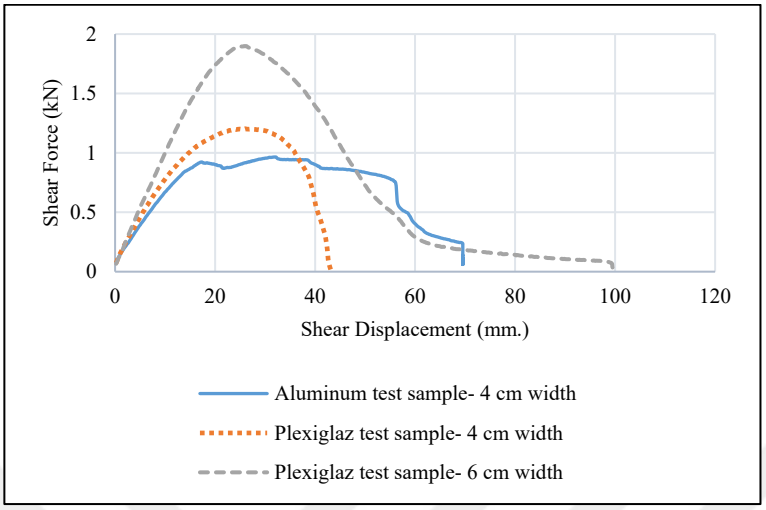

Figure 3.2: The applied shear force to the test samples for evaluation of the cohesion between the flexible sealant and laminar frame base material.

It is evident that the test sample with a greater adhesive surface will exhibit higher resistance when subjected to shear forces. Consequently, employing a larger adhesive surface contributes to increased durability against laterally applied shear loads. To obtain a reliable comparison for determining the suitable material for different faces of the container, shear stresses are computed and juxtaposed. This allows for the evaluation and comparison of material resistance per square centimeter. The findings indicate that the aluminum face demonstrates significantly higher resistance and offers sufficient adhesion, preventing the flexible sealant from detaching from the surface of the aluminum base material. However, there is minimal discrepancy between the results of test samples utilizing Plexiglas as the base material. Additionally, shear stresses closely resemble those observed in the test sample employing an aluminum base material at the point of separation from the surface.

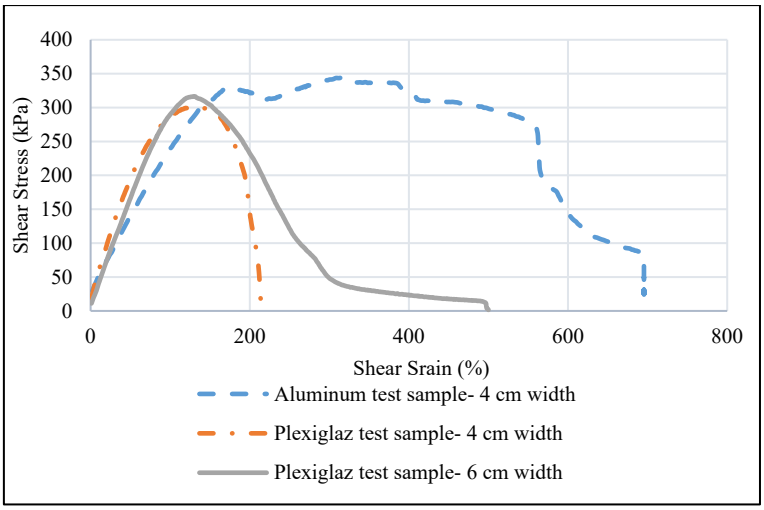

Figure 3.3: The applied shear stress to the test samples for evaluation of the cohesion between the flexible sealant and lamina base materials.

Given the superior adhesion of the flexible sealant to the aluminum surface, opting for aluminum as the base material for laminar frame fabrication appears advantageous. The separation of the flexible sealant occurs through the tearing mechanism between the adhesive surfaces. Therefore, considering the separation of the flexible sealant, the shear modulus of the flexible sealant can be calculated by dividing the shear stress by the shear strain. As such, for each range of lateral displacement, a shear modulus value is computed. As illustrated in Figure 3.4, an increase in shear displacement and shear force correlates with a decrease in shear modulus, indicating plastic behavior and residual deformation.

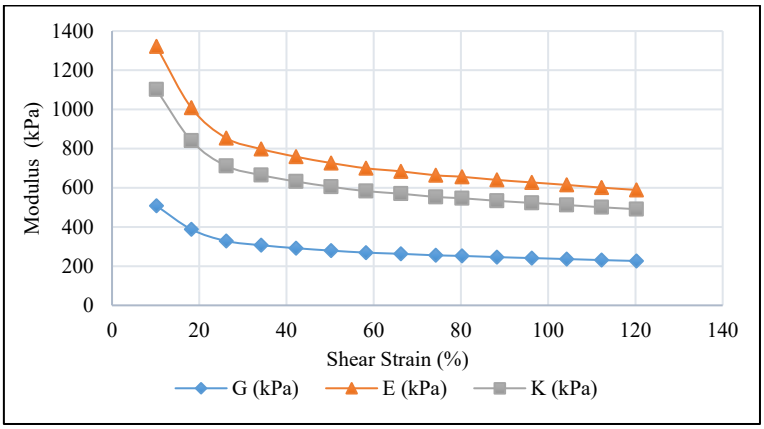

Figure 3.4: Modulus values calculated by the shearing test on the aluminum base material sample for Sikaflex PRO-3.

Based on the test results the parameters which should be used during the numerical modeling of the flexible sealant material could be summarized as presented in Table 3.1.

Table 3.1: Properties of the Flexible Sealant (SikaFlex-Pro3).

Property	Value	Units (S.I.)
Density	1.26	Mg/m3
Bulk Modulus	0.63	MPa
Poisson's Ratio	0.45	-
Shear Modulus	0.29	MPa

3.2 Verification of the Parameters and Performance of the Plexiglas

3.2.1 Flexural testing of the short length plexiglas

To assess the parameters utilized in the study for Plexiglas, a compact sample of the material is prepared for examination under a flexural test setup. The decision to use a compact sample is driven by the need to precisely validate the performance of Plexiglas within a more controlled loading environment and with a highly accurate hydraulic jack. Loading of the Plexiglas sample progressed until failure occurred, marked by cracking at the loading point. The test setup is depicted in Figures 3.5 and 3.6.

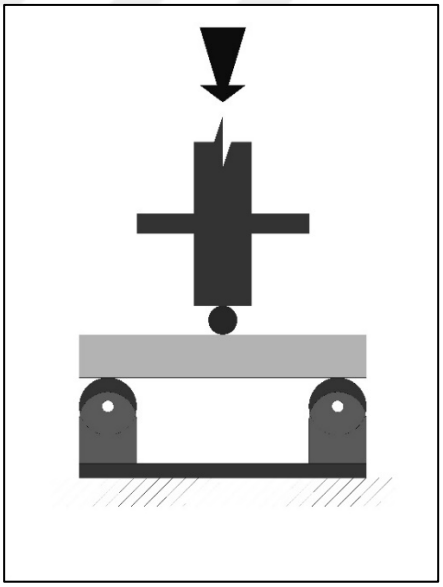

Figure 3.5: Flexural test setup scheme of the Plexiglas.

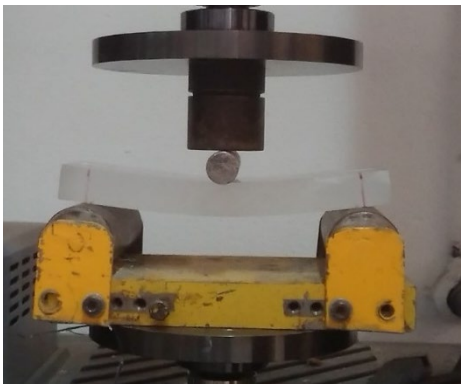

Figure 3.6: Deformed Plexiglas during the application of flexural loading.

The data acquired from the flexural bending test conducted on Plexiglas is utilized to construct stress-strain diagrams and explore the variation of elastic modulus with strain rate. Figure 3.7 illustrates that Plexiglas can withstand stress levels of approximately 70 MPa with a strain range of nearly 3.5%. Additionally, an examination of the correlation between stress range and strain values allows for the evaluation of the elastic modulus of Plexiglas, revealing a peak value of approximately 3.2 GPa at a strain rate of around 1.5% (Figure 3.8).

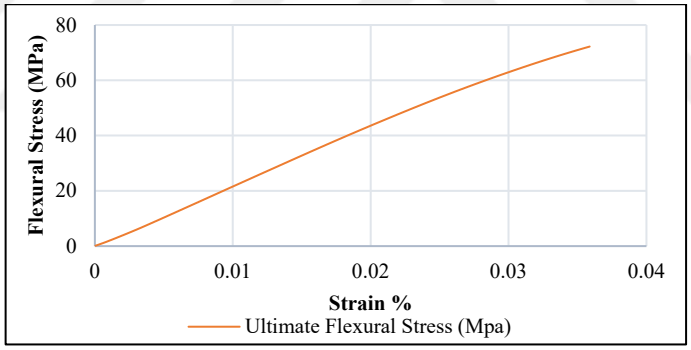

Figure 3.7: Diagram of the Flexural stress of Plexiglas versus strain.

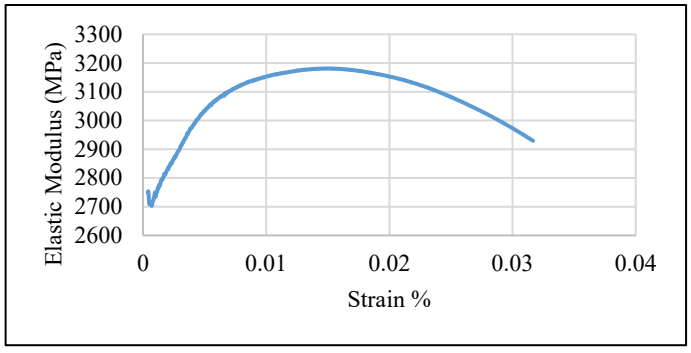

Figure 3.8: Diagram of the Elastic modulus of Plexiglas versus strain for the short sample.

Based on the results obtained from the laboratory tests the parameters of the flexible sealant and the plexiglas is summarized in Table 3.2.

Table 3.2: Properties of the Plexiglas.

Property	Value	Units (S.I.)
Density	1.185	Mg/m3
Bulk Modulus	2.50	GPa
Poisson's Ratio	0.3	-
Shear Modulus	1.15	GPa

3.2.2 Flexural testing of the long length plexiglas

In another test conducted on Plexiglas, a sample with dimensions intended for container use undergoes testing. The sample, with a distance of 1.6 meters between supports and a section of 8×4 cm, exhibits consistent elastic modulus values of approximately 3.2 GPa. However, excessive deflection is observed during loading, indicating potential structural limitations.

Figure 3.9: Flexural test setup for the long sample of Plexiglas.

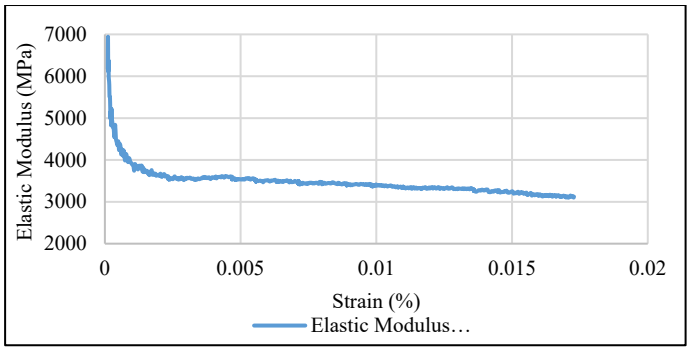

Figure 3.10: Diagram of the Elastic modulus of Plexiglas versus strain for the long sample.

3.2.3 Flexural testing of the triple jointed long length plexiglas

Since the analysis and tests were conducted on a single beam element with a length of 1.6m, the supportive influence of other laminas was disregarded. However, another factor potentially impacting the bearing capacity of the lamina frame is the connection between laminas using flexible sealant. To examine this effect, a test setup was

arranged, adhering 3 Plexiglas beam elements together with Sikaflex Pro3. This configuration simulates a set of laminas representing the loading mechanism on the end-wall of the container during testing on the shaking table, as depicted in Figure 3.11.

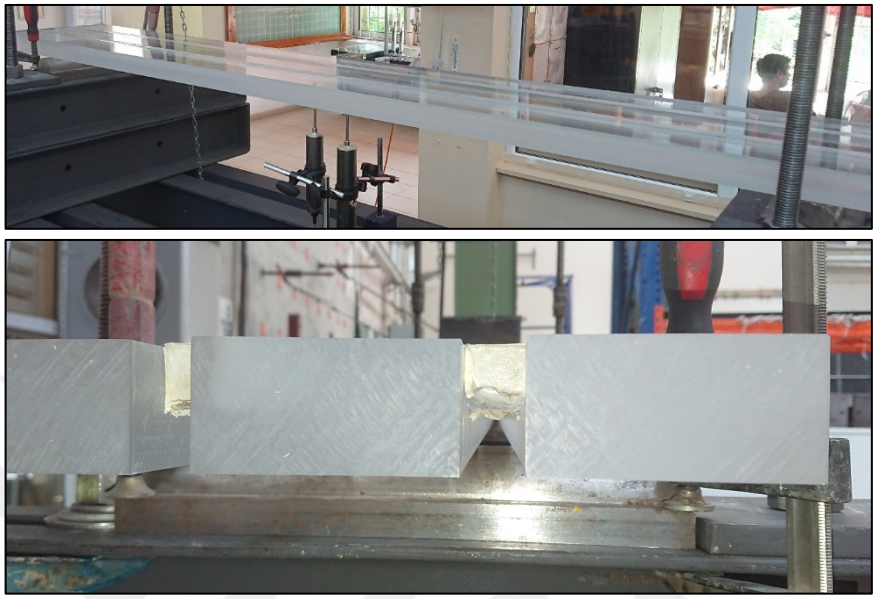

Figure 3.11: Attached lamina beams to verify the effect of simultaneous performance of the frames.

The test sample is configured to mimic the side wall of the container, with a reduced thickness of flexible sealant set at 2 cm. A lateral load is exclusively applied to the middle beam element to ascertain the impact of the two attached elements on enhancing the bearing capacity of the middle one. The loading setup is illustrated in Figure 3.12.

Figure 3.12: Loading over the middle beam element of the three attached Plexiglas beams test sample.

As anticipated, the additional attachment of elements to the middle beam significantly increased its bearing capacity compared to a single Plexiglas beam. Throughout the test, there was no indication of separation in the flexible sealant. However, a minor

residual deformation appeared in the Sikaflex layer immediately after the test, which dissipated after the setup was released from lateral loading.

Displacement measurements were conducted using two displacement transducers, positioned beneath the middle and side beams, allowing for the assessment of relative displacement between the two beams. While the addition of side elements enhances the setup's bearing capacity, it was anticipated that the relative displacement would remain minimal, with all three attached beams moving in unison. The subsequent figure illustrates the displacement values recorded during lateral loading of the test setup.

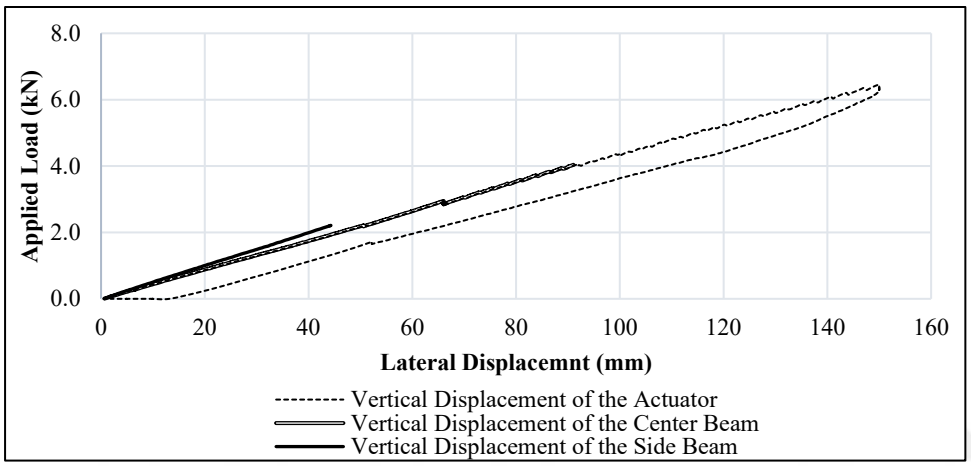

Figure 3.13: Vertical performance of the three attached Plexiglas beam setup.

The conducted tests indicate that attaching beam elements enhances support for the laminas and augments the bearing capacity of the end-walls, thus establishing a suitably rigid boundary for the system. Consequently, any potential increase in concentrated stress values within the soil body would be effectively mitigated, as the frames would collectively distribute the load, preventing stress levels from surpassing the required thresholds for container stability.

Moreover, the performance of the laminas as a unified frame is noteworthy, as it amplifies the system's capacity compared to scenarios where only a single beam is subjected to lateral loading.

3.3 Verification of the Lamina Frame Performance

Considering the movement direction of the container, the most deformable lamina beam would be the ones in the moving direction without any side support.

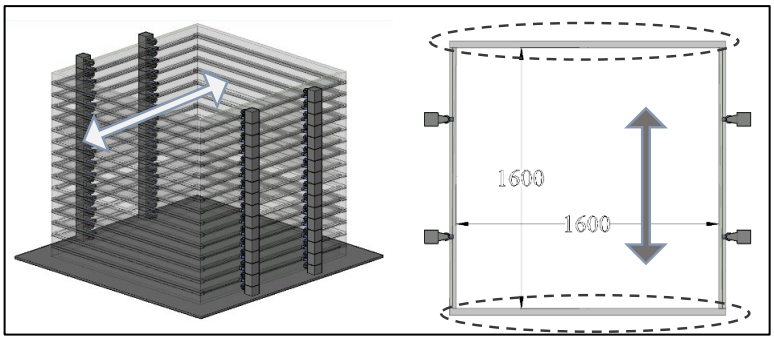

Figure 3.14: Highest deformable frame's beam elements in the moving direction.

Evaluation of the beam under the average applied load from the soil body to the movinng side of the container, shows that the displacement of the beam for a 40 kPa load at the center is approximately 24 cm. To verify this, the beam's deformation was analyzed using ETABS software, confirming a displacement of 25.3 cm at the center. This analysis aids in refining the design of the frame and supporting points for the structure.

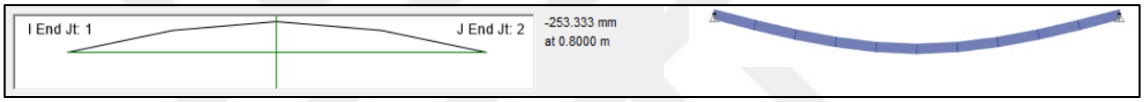

Figure 3.15: Deformation of the Plexiglas beam using the ETABS.

The other deformable part of the container is the fixed boundary (side wall) which is parallel to the moving direction of the container.

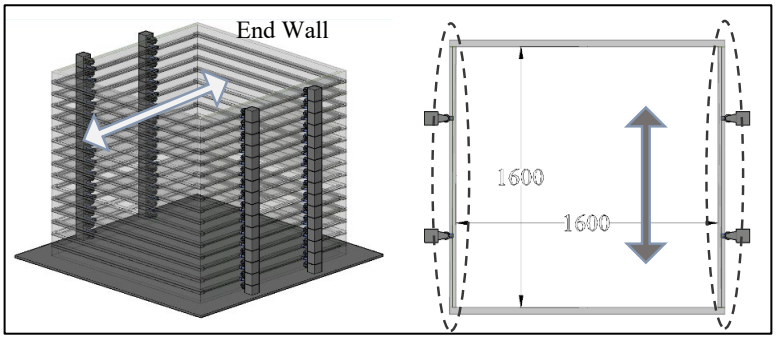

Figure 3.16: Lowest deformable frame's beam elements in the fixed direction.

For this case, where transparency is required, the deflection of the Plexiglas beam is tested to assess its behavior. Limiting deflection in this direction is crucial because excessive lateral deformation can restrict the movement of the laminas over the lateral support when the container moves laterally. Therefore, it's essential to ensure that lateral deformation does not hinder the movement of the laminas, while also providing visual observation through the laminas.

In the first case, with lateral support located 40 cm from each end, the maximum deflection at the middle of the lamina is approximately 2.1 mm.

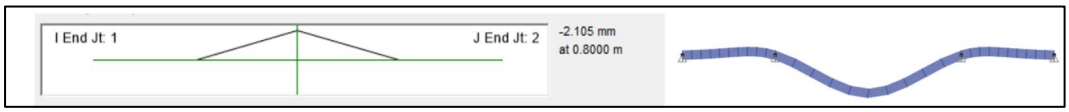

Figure 3.17: Deformation of the laterally supported Plexiglas beam at 40cm from the end points using the ETABS.

In the second case the distance is selected to be 50 cm from each end. In this case, the deflection is around 0.06 mm. which is almost zero.

Figure 3.18: Deformation of the laterally supported Plexiglas beam at 50cm from the end points using the ETABS.

In this case, since the deformation of the lamina in different spans, are almost the same, and also the middle span of 60 cm., will be a proper opening for the observation intentions, it will be recommended to set the lateral supports in the distance of the 50 cm from each end of the boundary in the fixed side of the container.

To assess the deformation of the container boundaries under the influence of internal forces, a comprehensive model of the lamina frame is constructed and analyzed. In this model, all elements of the frame, both fixed and movable, are transparent and made of Plexiglas.

The load applied to the frames corresponds to the maximum applied load to boundaries during tests with a saturated soil sample and during liquefaction tests, which is 80 kPa. The deformed shape of the frame is illustrated in the following figure.

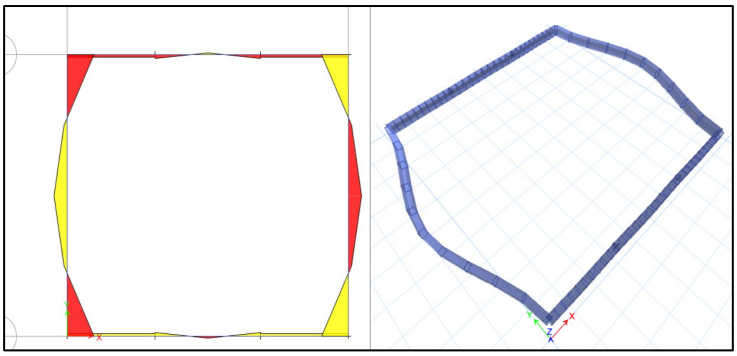

Figure 3.19: Deformed shape of the lamina fram and internal forces.

It could be seen that the maximum moment for the end walls happened in the middle of the beam and causes 80 mm displacement. By controlling the moments and shear

values in the beam element, the sufficiency of the element to bear the lateral loads is confirmed.

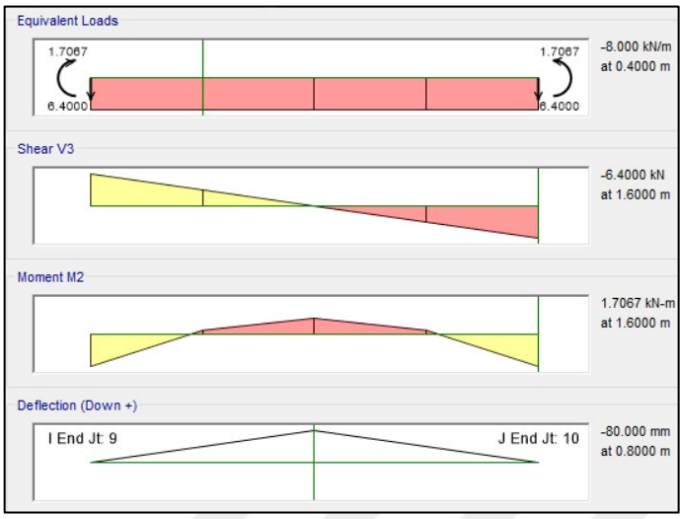

Figure 3.20: Distribution of internal forces and deformation in the moving element of the frame.

Also, for the fixed wall, the lateral displacement is zero and the values of the shear and moment, are calculated to be less than ultimate values of the bearable loads by the Plexiglas.

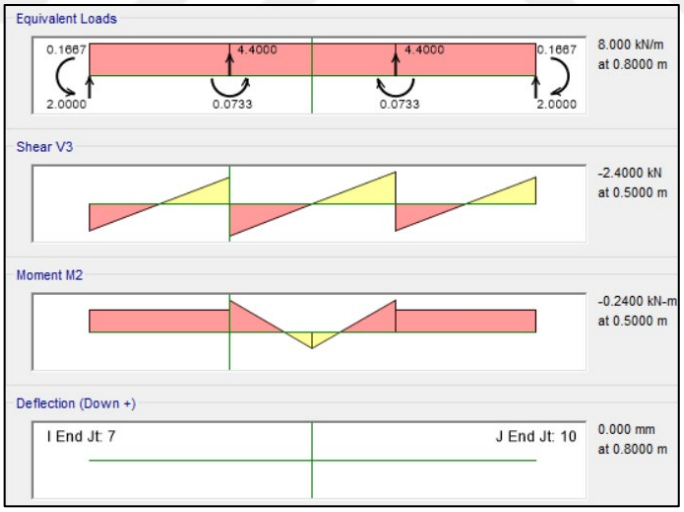

Figure 3.21: Distribution of internal forces and deformation in the moving fixed of the frame.

It could be said that, the frame performance of the Plexiglas will decrease the deformation of the boundary and connection between the laminas by using the flexible sealant between them provides a satisfying extent for lateral deformation potensial of the end-walls during the dynamic testing on the shaking table.

3.4 Sand Pluviation Mechanism Design and Preparation

To prepare the laminar soil container for testing on the shaking table, it's essential to fill it with sand in a manner that ensures the required soil parameters are met for the test conditions. Achieving this entails controlling the sand parameters during the pluviation process. To facilitate this, a test setup is devised to mimic the expected soil parameters for the test conditions.

The setup, depicted in Figure 3.22, enables the depletion of sand from various heights and the control of relative density of the sample based on factors such as hole diameter, number of holes, and their distribution on the pluviator plate.

In order to examine the impact of hole diameters, holes with diameters of 6 mm and 10 mm are drilled into the plate, with a spacing ratio ranging from 2.5 to 5 times the diameter of the holes. The best results are observed with a hole diameter of 6 mm, providing a denser soil sample with a spacing ratio of 5 times the diameter, and a looser soil sample with a denser hole pattern spaced at 2.5 times the diameter of the holes.

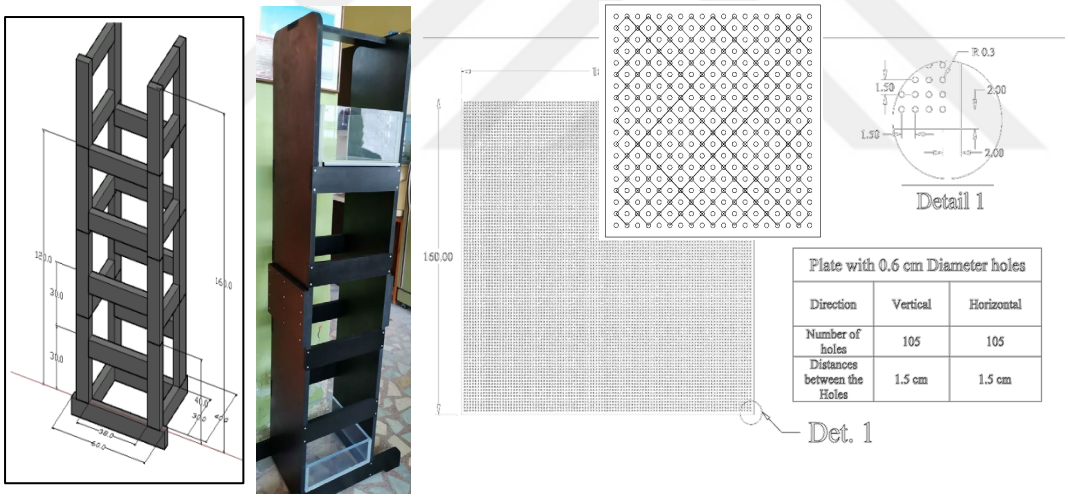

Figure 3.22: Initial sand pluviation test setup design and prepared test setup.

Following the analysis of results, the sand pluviation mechanism's final design will be formulated. Through a series of tests conducted on the initial sand pluviation test apparatus, the optimal hole pattern, diameters, and height range for achieving the desired relative density of the soil sample are determined. Figure 3.23 illustrates the designed mechanism for pluviation of the sand sample into the container.

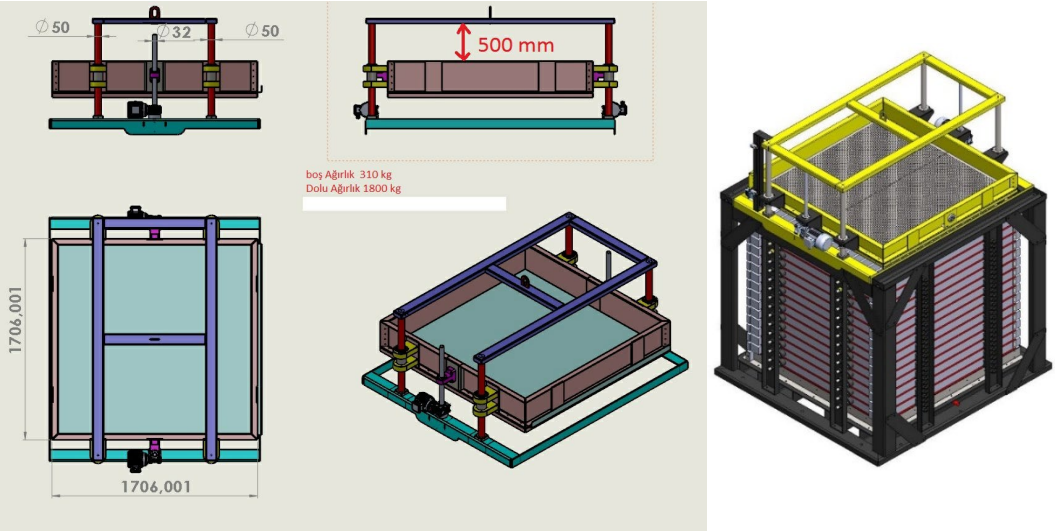

Figure 3.23: Sand pluviation mechanism detail design and location on the external support system.

3.5 Discussions and Conclusions

1- The materials intended for use in the manufacturing of the laminar soil container are tested through laboratory experiments.

2- Flexible sealant materials, specifically Sikaflex Pro3, are selected, and their adherence strength to different base materials is verified.

3- Plexiglas is chosen for the beam elements of the laminas, and its flexural strength is validated through laboratory tests.

4- The performance of the lamina frame under the maximum stresses induced during dynamic loadings is verified using structural software, and the locations of lateral support points are determined.

5- A sand pluviation test setup is developed, and laboratory tests are conducted to design the required patterns for the sieve of the pluviator mechanism.

4. NUMERICAL MODELLING OF THE ENHANCED LAMINAR SOIL CONTAINER

4.1 Numerical Modelling Software, FLAC3D

FLAC3D, short for Fast Lagrangian Analysis of Continua in three Dimensions, is a specialized software application designed for numerical analysis of geotechnical problems in three dimensions. It utilizes explicit finite-difference methods to address a wide range of geotechnical issues, particularly those involving nonlinear and large-strain behaviors. Additionally, FLAC3D includes a powerful programming language known as FISH, allowing users to develop custom functions and variables tailored to their specific needs. The software's nomenclature is aligned with other programs used for stress analysis, ensuring consistency and compatibility across different platforms.

In this research, two models are utilized: the Elastic model and the Mohr-Coulomb model, which will be examined in the following section.

Elastic models exhibit reversible deformation upon unloading, with stress and strain having a linear relationship. These models include both isotropic and anisotropic behaviors. Isotropic elastic models follow Hooke's law, where stress increments are proportional to strain increments. In FLAC3D, isotropic elastic models require inputs such as bulk modulus and shear modulus. For dynamic analysis of sand samples, the Mohr-Coulomb model is employed to study their behavior. The key objective is to observe consistent shear strain across the sample's height, validating its simple shear behavior. Dynamic input in FLAC3D can be applied through acceleration record, velocity record, stress record or force record.

Once the parameters are selected and the numerical modeling of the container is complete, it's crucial to validate the results against the Seed & Idriss (1970) data for sand or clay. This verification step ensures an initial assessment of the container's performance before proceeding to laboratory tests. Additionally, decisions regarding the box design and the construction material can be finalized based on these verified results. Also, the parameters to be evaluated during the tests and modelling procedure are listed in the Table 4.1.

Table 4.1: Parameters to be evaluated by numerical modelling.

Outputs	Vertical strain	Shear strain	Compression stress	Shear stress	Fundamental frequency	Dampin g value	Displacement, Acceleration
Plexi-glass	×	×	✓	✓	×	✓	×
Flexible sealant	✓	✓	✓	✓	×	✓	✓
Interface	×	×	×	×	×	×	×
Box (empty and full)	×	×	×	×	✓	✓	×
Soil parameters in different layers	✓	✓	✓	✓	✓	✓	✓

4.1.1 Soil properties

In addition to the initial model parameters, detailed information about the soil material is essential for accurate analysis. Specifically, for Medium Dense sand, the soil parameters will be determined based on the Relative Density and Effective Stress using Formula 4.1 as outlined by Seed and Idriss (1970).

$$G_{max} = 21.7\ (K_2)_{max} P_a \left(\frac{\sigma'_m}{P_a}\right)^{0.5} \tag{4.1}$$

Using the parameters provided in Table 4.2, the soil parameters for the soil sample are calculated for various depths in the model with a depth of 1.5 meters. These calculated values are summarized and presented in Table 4.3. For the initial design of the Laminar Soil Container, the medium dense sand parameters will be chosen during the analysis.

Table 4.2: Sand Parameters for the different study cases.

Range of Parameters for SAND			
Parameters	Loose	Medium dense sand	Dense
Relative density (D_r)	30	45	75
Unit Weight (kPa)	17	17.5	18
Friction Angle (φ)	30	35	40
Poisson Ratio (υ)	0.42	0.38	0.38
K_0	0.50	0.43	0.36
K_{2max}	33.79	44.28	62.25

Table 4.3: Sand Parameters for the different depth.

1.5 m Depth Model	Depth	σ'_v	σ'_h	σ'_m	Gmax (Pa)	V_s (m/s)	K (pa)
Parameters for Medium Dense Sand	0.15	2.6	1.1	1.6	1.22E+07	84	4.69E+07
	0.45	7.9	3.4	4.9	2.12E+07	110	8.12E+07
	0.75	13.1	5.6	8.1	2.74E+07	125	1.05E+08
	1.05	18.4	7.8	11.3	3.24E+07	136	1.24E+08
	1.35	23.6	10.1	14.6	3.67E+07	145	1.41E+08

4.1.2 Input motion and boundary effect

Free-Field analyses are performed with the model having the lateral range of boundary chosen to be 20 times the selected range for the box. Choosing this wide range is due to exclude the effect of boundaries on the results of the analysis.

To find the range of input motion frequency that should be applied to the model and have an initial notion about the range of frequency on which the resonance or maximum amplification of the input motion will happen in the model, the free vibration analysis by using the Free-Field boundary condition is carried out.

The scheme of the model is presented Figure 4.1 which uses the parameters presented for the Medium Dense Sand as the input parameters.

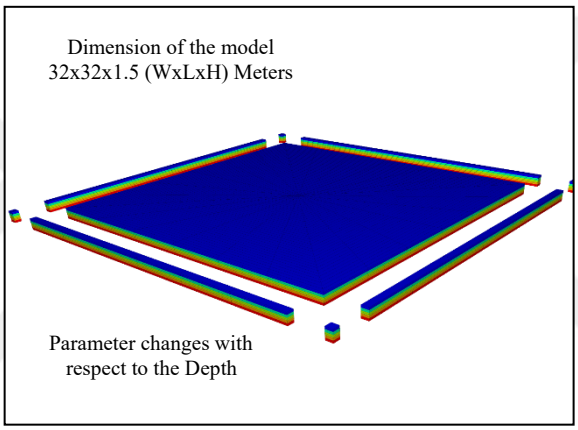

Figure 4.1: Wide range boundary Free-Field model.

The Free-Vibration Analysis of the model, shows amplitude spectrum presented in Figure 4.2 and reveales the fundamental frequency of the model equal to 22Hz.

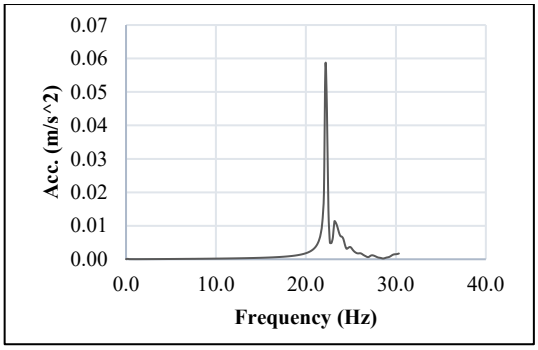

Figure 4.2: Range of fundamental frequency of the wide boundary model.

Based on the free vibration analysis of the model and the fundamental frequency which is found to be 22 Hz, the applied input motion will have the specifications presented in Table 4.4.

Table 4.4: Range of input motion.

Range of Frequency (Hz)	Range of Acceleration Amplitude (m/s^2)
1~22	3.0

After running the analyses for different input motion frequencies, the resulting transferred motion to the surface of the model (Z=1.5 m) is recorded and compared with the applied motion to the base of the model at Z=0.0 m.

Figure 4.3 represent the change of the input motion from the bottom of the model toward the top of the model. During this transfer the amplification happens for different input frequencies. As the input frequency increases the amplification increases and the higher values of acceleration are recorded on top of the model. The highest acceleration values are recorded prior to achieving the fundamental frequency of the model which is around 15 Hz and after that the acceleration amplification ratio decreases.

As presented in the acceleration records, the maximum amplification will happen around the 15 Hz input frequency which is obvious based on the amplitude spectrum for different input frequencies in the Figure 4.4.

The same parameters which have been used in the first step are used to define a model in Deep-Soil and analyses are performed to understand the resemblance of the results of FLAC3D. The model showed the fundamental frequency of the soil layers is equal to 19.5 Hz which is a bit different from the value obtained from the FLAC3D model. The comparison between the FLAC3D results with the DEEP-SOIL analysis, show a considerable difference between the values of the PGA for frequencies more than 10 Hz and close to the natural frequency of the model. In Deep-Soil, the maximum PGA of the input load will be obtained around 12.5 Hz, which is different from what is obtained from FLAC3D analyses.

After studying the performance of the model with the 1.5-meter depth with the wide range boundaries, the performance of the Free-Field response with the dimension of the box will be studied. The shape of the model with the parameters for the medium dense sand is presented in Figure 4.5.

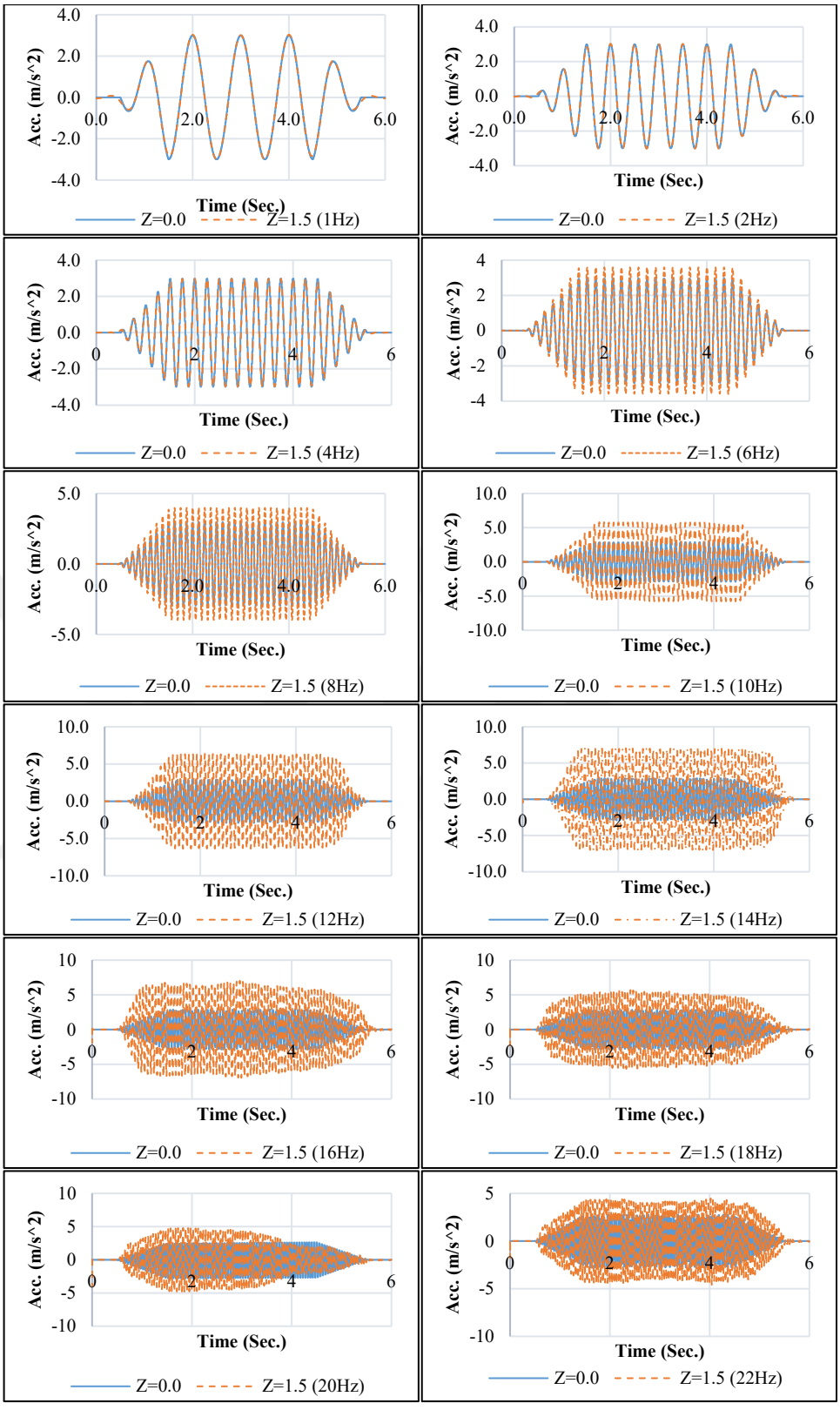

Figure 4.3: Acceleration records for different frequencies of input motion.

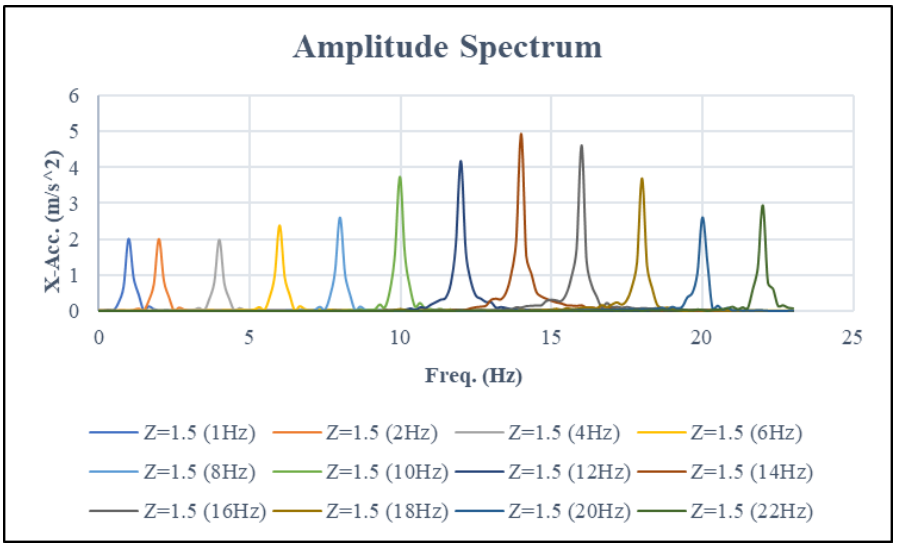

Figure 4.4: Amplitude Spectrum for different input motion frequencies.

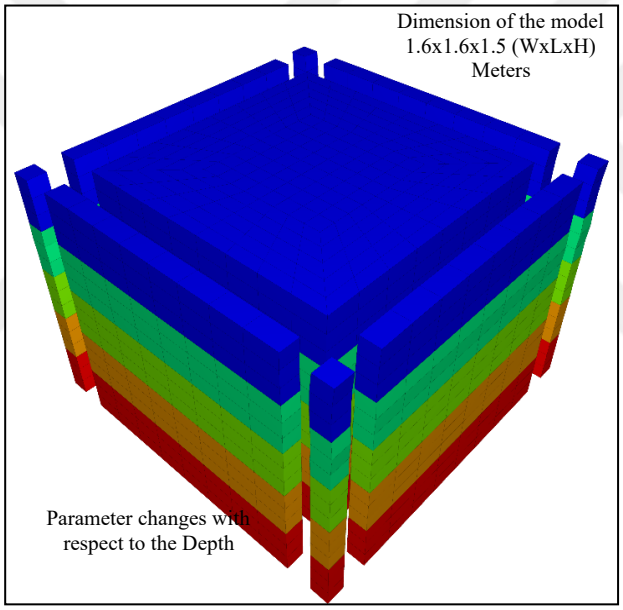

Figure 4.5: Box Size Free-Field model.

Since the available shaking table only provide support excitation in one direction, then there would be a need to study the performance of the Free-Field model, having only free-field boundaries in one direction which resembles the 1 directional (1-D) movement of the model (Figure 4.6). The results are compared with those attained from the 3D performance of the model.

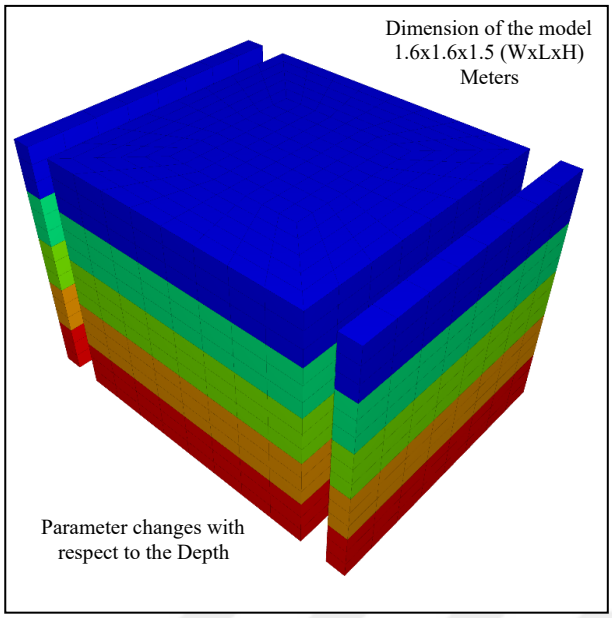

Figure 4.6: Box Size 1-D Free-Field model.

The results obtained in the previous steps, are summarized in the Figure 4.7. It is seen that, up to almost 10 Hz of motion input frequency, the responses are mostly alike and follow each other. Yet, the Box-Sized model have less amplification with respect to the wide range boundary and Deep-Soil results, which is due to higher natural frequency of the model effected by the boundary.

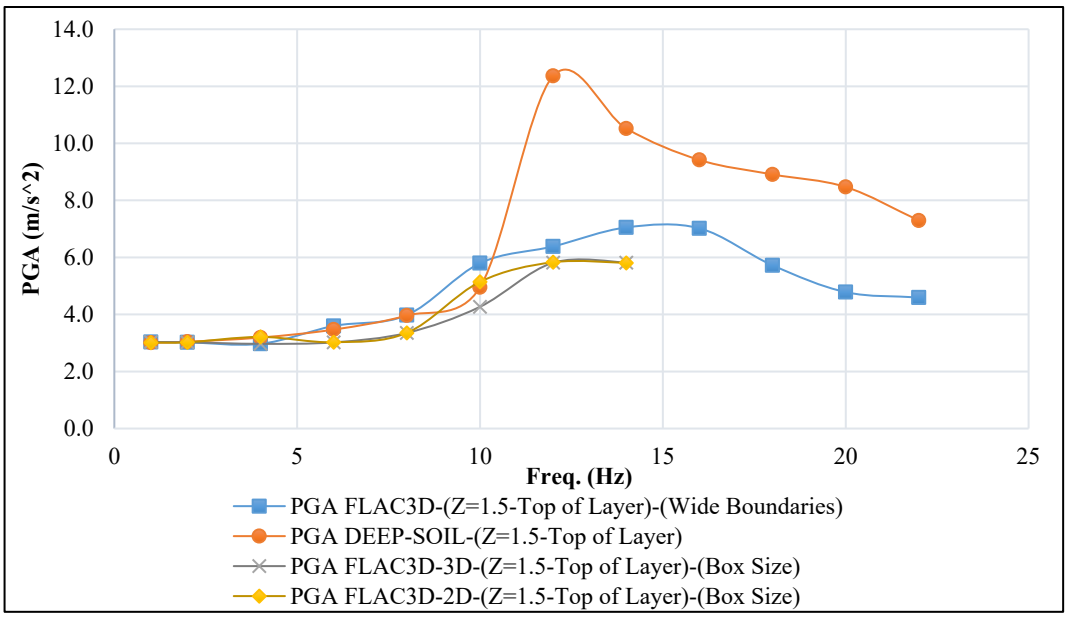

Figure 4.7: Peak Ground Acceleration Comparison between the results of the different boundary conditions.

As mentioned previously, due to the limitation during the laboratory tests, originated by the capacity of the shaking table, the maximum applicable frequency would be

around 8~10 Hz. So, for the further analysis, the highest applicable frequency which may resemble the free-field conditions, could be selected as 8 Hz.

4.2 Modeling Different Mechanisms of Movement for Laminar Soil Containers

Based on the limitation of the shaking table which was mentioned previously, the initial dimension of the box is chosen in such a way to contain soil sample with the size of 1.6×1.6×1.5 meters (W×L×H). For the initial evaluation of the soil container it is supposed to contain soil material with the specifications of medium dense sand, presented previously.

4.2.1 Interface parameters of the materials used for the container design

Parameters selected for the interface of the attaching faces for both soil and container boundary and also the material used in manufacturing the laminar container itself, including the plexi-glass and the flexible material, are defined based on the instructions provided by the FLAC3D Version 7.0 user manual.

It's advisable to select the lowest stiffness that maintains minimal interface deformation. A general guideline is to set kn and ks at ten times the equivalent stiffness of the stiffest neighboring zone. The apparent stiffness, measured in stress-per-distance units, of a zone in the normal direction is given by:

$$max\left[\frac{\left(K+\frac{4}{3}G\right)}{\Delta Z_{min}}\right] \tag{4.2}$$

Where, K and G are the bulk and shear moduli, respectively; and Δzmin is the smallest width of adjoining zone in the normal direction.

The notation max [ ] indicates the maximum value among all zones adjacent to the interface, accounting for potential variability in adjacent materials. However, if one material is significantly stiffer than the other, Equation (4.2) should be applied to the softer side. This ensures that the interface stiffness, set at ten times the soft-side stiffness, minimally impacts system compliance, as the deformability of the system is dominated by the softer material.

When the physical normal and shear stiffnesses are less than ten times the equivalent stiffness of adjacent zones, using physical values poses no issues. However, if the ratio

exceeds ten, solution time may significantly increase without substantial changes in system behavior. In such cases, reducing the supplied values of normal and shear stiffnesses can enhance solution efficiency.

Joint properties are typically obtained from laboratory testing, such as triaxial and direct shear tests. These tests provide essential data for joint friction angle, cohesion, dilation angle, tensile strength, as well as joint normal and shear stiffnesses.

The interface parameters are chosen based on the material properties of each side of the interface. Key parameters for the sealant layer are listed in Table 4.5. Additionally, interface stiffness values for the model and adjacent zones are presented in Table 4.6.

Table 4.5: Sealant parameters based on the specification provided in data sheet.

Parameters	C (Pa)	φ (°)	Shear Resistance (Pa)	Tensile Stress (Pa)
Values	4.45E+4	-	1.1E+6	1.1E+6

Table 4.6: Interface parameters to be used in the model based on the material parameters and zone dimensions.

Interface	ΔZ min (m)	Equivalent Stiffness	kn & ks (Pa)	C (Pa)	φ (°)	Shear Resistance (Pa)	Tensile Stress (Pa)
Soil - Plexi-galss	0.005	1.65E+9	3.30E+11	-	15	-	
Soil – Flexible sealant	0.005	2.37E+7	4.74E+10	-	15	-	
Plexi-glass – Flexible sealant	0.02	4.74E+7	4.74E+8	-	-	1.1E+6	1.1E+6

4.2.2 Available and recommended moving mechanisms

Based on the literature review section of this study, the common types of mechanisms used for the laminar soil containers and the recommended one through this study are:

1- Flexible Sealant Mechanism (FSM.)

2- Roller Bearing Mechanism (RM.)

3- Roller Bearing and Flexible Sealant Mechanism (R&FSM.)

In this section, three different movement mechanisms for the box are studied, and the results are compared with those from the Free-Field analysis. The mechanism that best matches the results of the numerical modeling will be selected as the optimal choice for the box. As mentioned earlier, the input motion frequency for all analyses will be 8 Hz.

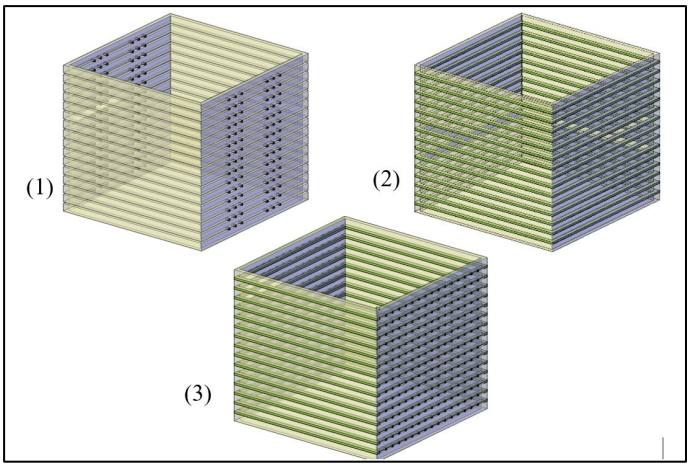

Figure 4.8: Conceptual design of laminar container using 1- Roller Mechanism (RM.) 2- Flexible Sealant Mechanism (FSM.) 3- Roller and Flexible Sealant Mechanism (R&FSM.).

4.2.3 Flexible Sealant Mechanism (FSM.)

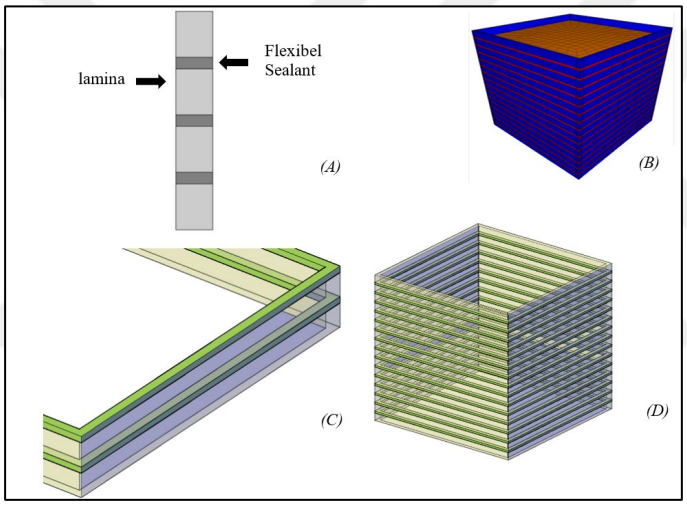

Figure 4.9: (A) Flexible Sealant mechanism used between the laminas (FSM.) (B) Laminar soil container model with the Flexible Sealant mechanism (FSM.)(FLAC3D) (C) Laminar soil container moving mechanism (D) Flexible Sealant mechanism laminar soil container scheme.

Given that each box has different boundary conditions based on its specifications, free vibration analysis is conducted for each mechanism to determine the natural frequency of the system.

The free-vibration analysis of the complete box shows a natural frequency of 20 Hz, closely matching the values obtained from the Free-Field model with extensive boundary conditions. After subjecting the box to dynamic motion, results were recorded at various points throughout the depth of the box, as presented in Figure 4.13.

4.2.4 Roller Bearing Mechanism (RM.)

The performance of the box using only roller bearings as movable separators between the laminas is presented in Figure 4.10. In modeling the roller bearings, the materials were assumed to have stiffness equal to Plexi-Glass. Certainly, a much stiffer material could be considered to ensure the time-dependent performance of the box.

4.2.5 Roller Bearing and Flexible Sealant Mechanism (R&FSM.)

Before assessing the box's deformation under the weight of soil material, it is crucial to evaluate the compression of the sealant during the box's assembly process. The sequential manufacturing involves placing each pair of laminar frames on top of each other and securing them together, repeating this process until the box reaches its full height of 1.6 m.

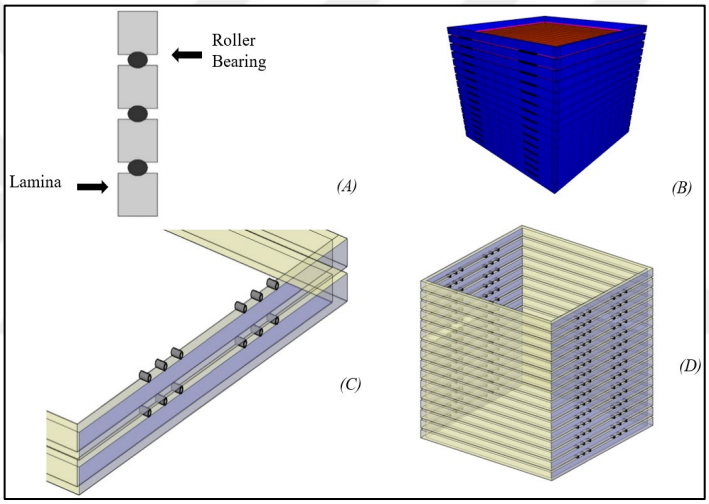

Figure 4.10: (A) Roller mechanism used between the laminas (RM.) (B) Laminar soil container model with the Roller mechanism (RM.) (FLAC3D) (C) Laminar soil container moving mechanism (D) Roller mechanism laminar soil container schematic.

The maximum deformation and compression occur at the lowest sealant layer, with a compression value of 3.6 mm, approximately 18% of the sealant layer thickness. After pouring the soil inside the box, the sealant compresses by about 3.8 mm, which accounts for 19% of the sealant layer thickness. Therefore, the sealant layer will have a thickness of approximately 1.6 cm after manufacturing the box and preparing the soil sample in the lower layer.

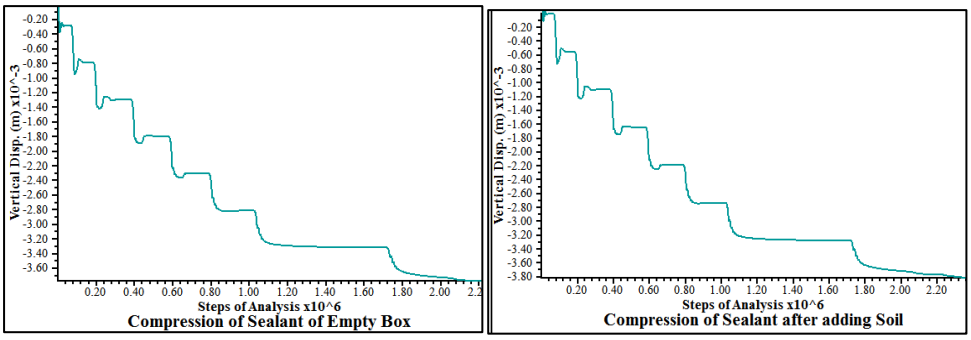

Figure 4.11: Vertical displacement on top of the lowest sealant layer under the vertical loading during construction of the box by 20 cm layers (2 laminas in each step) after completion of the box and after putting in the box in steps of 30 cm adding material.

Based on the effects of the vertical loads on the sealant compression, between the Plexi-Glass layers, and in order to decrease the effect of compression on the performance of the box during the application of the vibration load to the box, it is decided to use other mechanisms like roller bearings to prevent the layers from compression and helping the laminas to perform with a safe performance.

Although, the existence of roller bearings will help the laminas for transferring their weight to the base with the least effect on the vibration capacity of the moveable layers, it would be required to do some numerical simulation to study the performance of different mechanisms. The final design of the box may use a combination of different moving mechanisms.

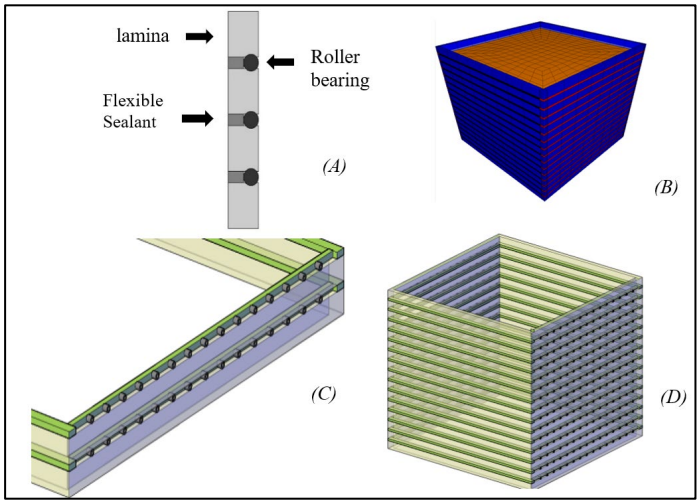

Figure 4.12: (A) Roller and Flexible Sealant mechanism used between the laminas (R&FSM.) (B) Laminar soil container model with the Roller and Flexible Sealant mechanism (R&FSM.) (FLAC3D) (C) Laminar soil container moving mechanism (D) Roller and Flexible Sealant mechanism (R&FSM.) laminar soil container scheme.

The free vibration analysis of the box using the combination of Flexible Sealant and Roller Bearings (R&FSM.) as lamina separators shows a higher natural frequency,

which closely approximates the values obtained from the Free-Field analysis of the Box-Sized model. Therefore, it is anticipated that the dynamic analysis results will align more closely with the numerical modeling results of the Free-Field Box-Sized models. The recorded results within the depth of the container are presented in Figure 4.13.

4.2.6 Deciding on the proper moving mechanism

In Figure 4.13, the container's performance is compared with previous analyses, specifically Free Field and Deep-Soil results. All values are centered around the box, using an input motion frequency of 8 Hz and acceleration of 0.3g. Among the mechanisms tested, only the box employing a combination of roller bearings and flexible sealants closely resembles the Free-Field results.

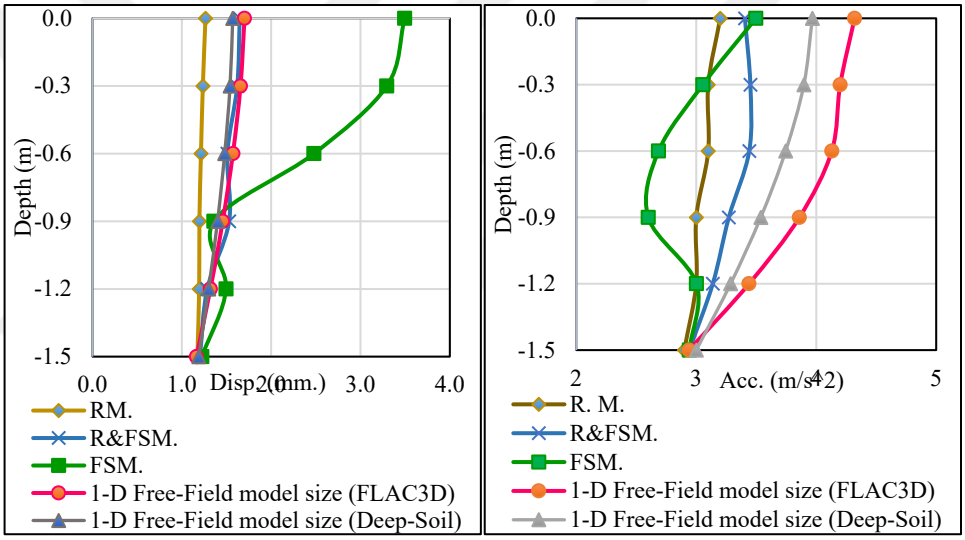

Figure 4.13: Maximum. Displacement and Acceleration comparison obtained in 3D for different moving mechanisms and 1D free field analysis.

Based on the results presented thus far, it can be concluded that the optimal mechanism for constructing the box would be a combination of roller bearings with flexible sealants as separators between the laminas. This approach eliminates the vertical compression effects on the performance of the flexible sealant and provides an impermeable boundary for the box, which is crucial when testing saturated samples.

4.3 Addition of Horizontal and Vertical External Support System to the Soil Container

Upon reviewing the results and aiming to optimize the container's performance in a single direction, we modified the boundary conditions and re-verified the outcomes.

Specifically, we tested scenarios with horizontal support only, vertical support only, and both horizontal and vertical support simultaneously to determine which configuration best approximated the expected results. For each scenario, we focused on results from a single cycle between 2.0 to 2.125 seconds, assessing whether the performance closely matched that of the 1-D free-field model (FLAC3D), as depicted in Figure 4.14.

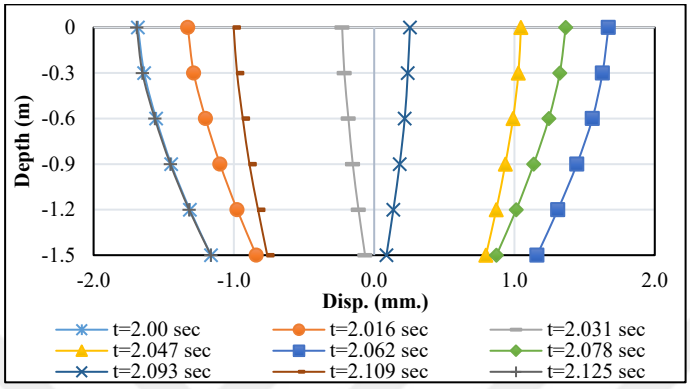

Figure 4.14: 1 cycle performance of the 1-D free-field model (FLAC3D).

4.3.1 Vertically supported FSM. container

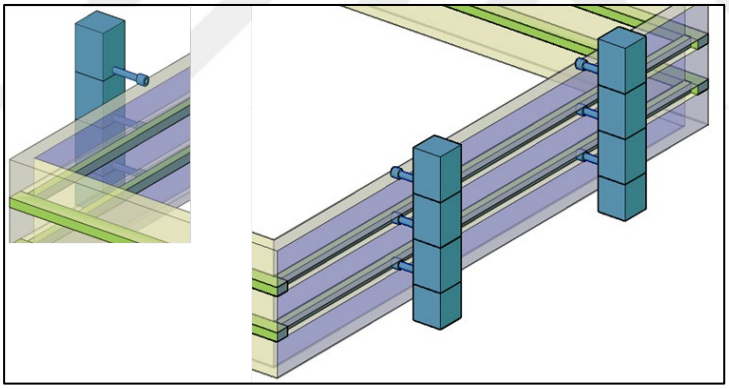

Figure 4.15: Vertical support system scheme for the laminar soil container.

In the first case, the container is modeled with only a sealant moving mechanism and supported vertically. This setup resembles the combination of roller and sealant moving mechanism (R&FSM), which prevents compression of the sealant layer between the laminas. The results of the model analysis are provided in Figures 4.16 and 4.17.

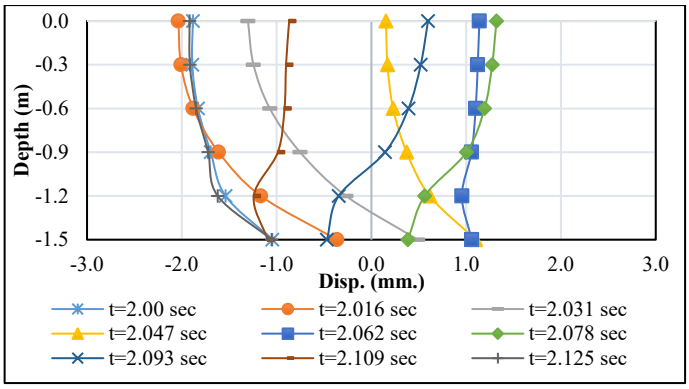

Figure 4.16: Lateral displacement of the vertically supported FSM. model in one cycle at the center.

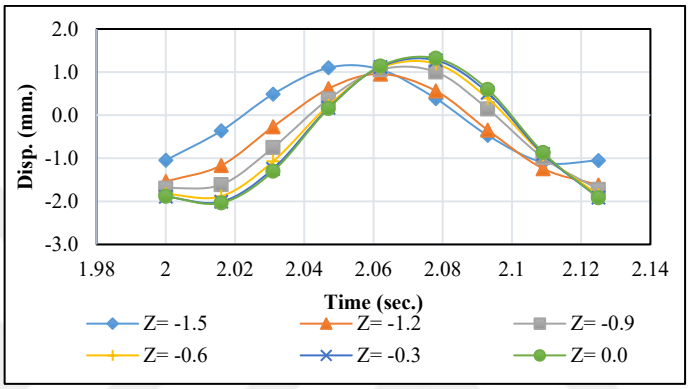

Figure 4.17: Lateral displacement of the vertically supported FSM. model in different depth in one cycle at the center.

4.3.2 Horizontally supported FSM. container

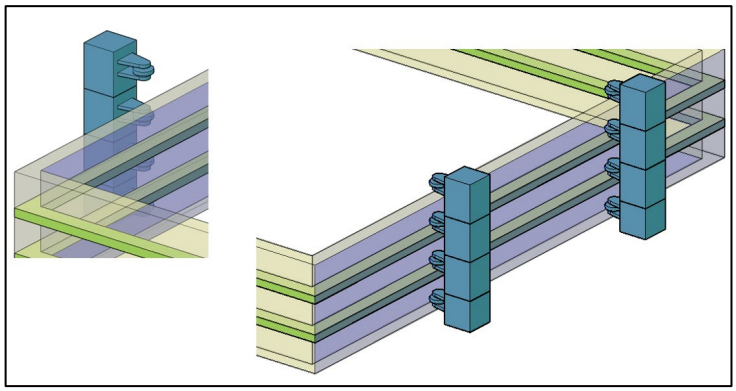

Figure 4.18: Horizontal support system scheme for the laminar soil container.

The second case involves supporting the container only horizontally. This setup aims to prevent lateral movements and rotation of the laminas, resembling conditions where lateral support is crucial. However, the performance of the container between 2.0 to 2.125 second does not closely match the results observed in the 1-D free-field model (Figures 4.19, 4.20).

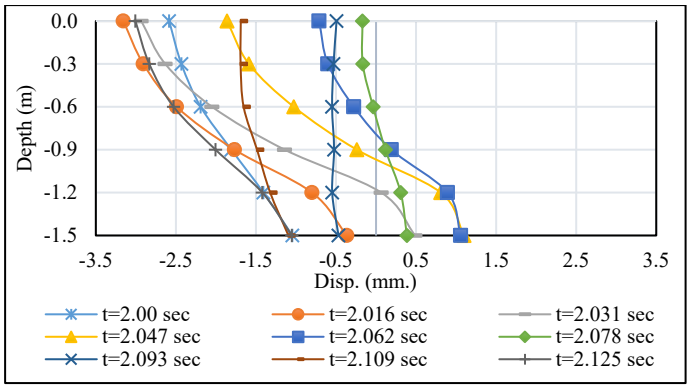

Figure 4.19: Lateral displacement of the horizontally supported FSM. model in one cycle at the center.

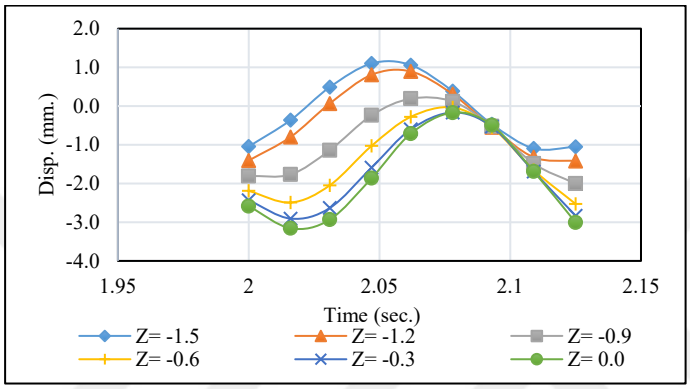

Figure 4.20: Lateral displacement of the horizontally supported FSM. model in different depth in one cycle at the center.

4.3.3 Horizontally and vertically supported FSM. container

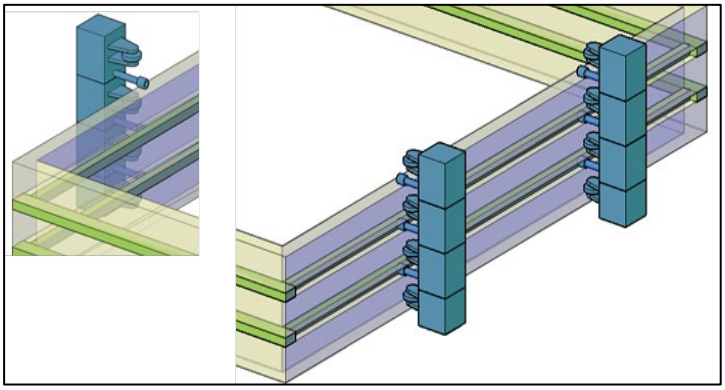

Figure 4.21: Horizontal and vertical support system scheme for the laminar soil container.

In the third case, the combination of lateral supports in both horizontal and vertical directions will be studied. This setup includes roller bearings between the laminas and beside each lamina. The results closely resemble those observed for vertically supported container boundaries. However, the addition of horizontal supports enhances stability during testing and provides lateral support for the container (Figures 4.22, 4.23).

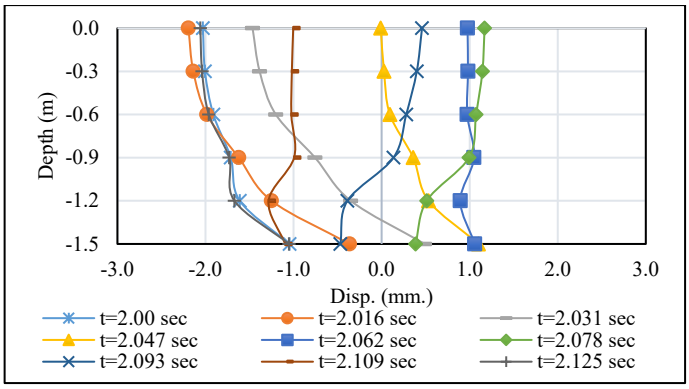

Figure 4.22: Lateral displacement of the vertically and horizontally supported FSM. model in one cycle at the center.

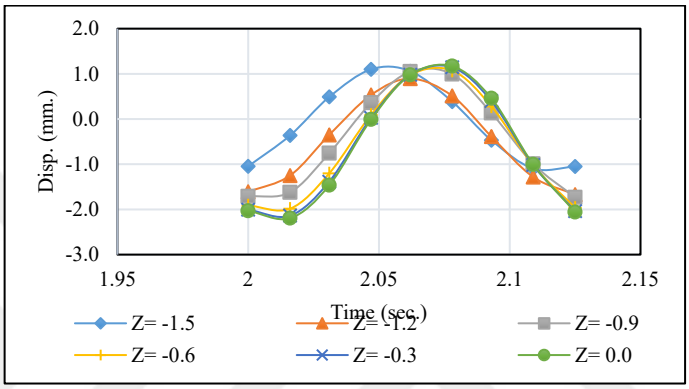

Figure 4.23: Lateral displacement of the vertically and horizontally supported FSM. model in different depth in one cycle at the center.

Through studies to verify the effect of the boundary support system on the container's performance, the following conclusions were drawn:

- The container modeled with vertical and horizontal supports resembles the free-field model more closely.
- Vertical support significantly influences the container, leading to performance closer to that of the free-field model.
- Vertical support prevents compression of the sealant and allows it to function freely like the R&FSM model.
- Vertical support bears the container's weight and allows the soil to dictate the model's performance.
- Horizontal support prevents the laminas from rotating around the frame's centerline.
- Together, vertical and horizontal support linearizes the movement of the laminas in the direction of the input motion.

4.4 Numerical Evaluation of the Container Performance During the Application of Dynamic Loads

Prior to conducting laboratory tests on the models within the container, it was decided to assess the performance of the test setup through numerical modeling for various interactions between the soil and structure. The schematic model of the structural elements and their specifications are provided in Figure 4.24. The performance of the numerical model under the influence of these structural elements was studied, and the results are presented for each location of the structural elements. These results are compared with the scenario where no structural elements or piles are present in the container.

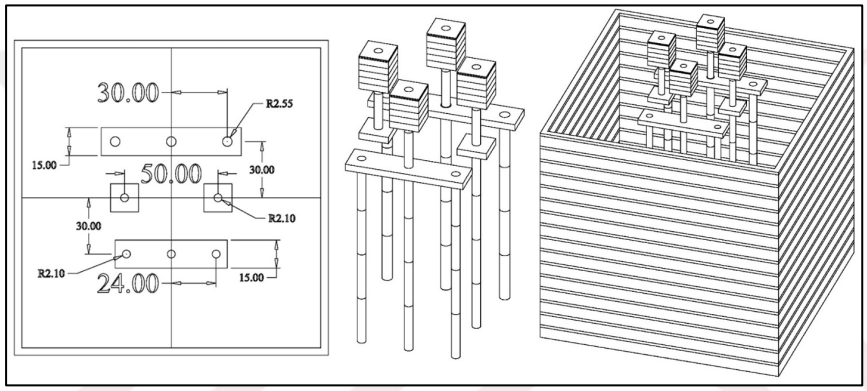

Figure 4.24: Test setup element's location and specifications.

The generated numerical model for studying soil-structure interaction is shown in Figure 4.25, along with the monitored points used to compare the model's performance across different study cases.

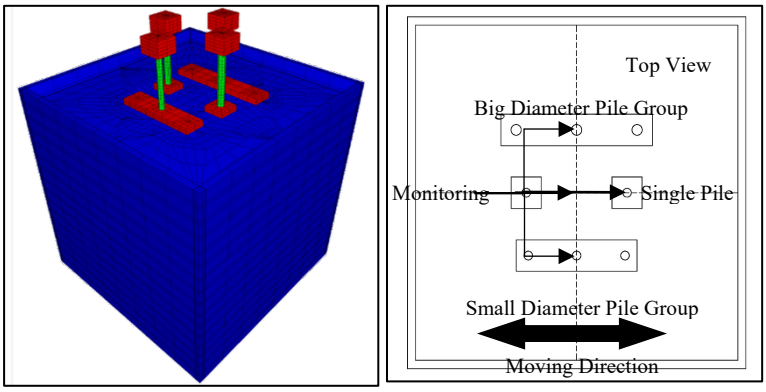

Figure 4.25: Generated numerical model for soil structure interaction study and the monitoring points.

The applied sinusoidal motion in the dynamic analysis includes an acceleration amplitude of 0.3g with a frequency content of 8 Hz. The duration of the motion is limited to 4.5 seconds due to the extended analysis time and the size of the model.

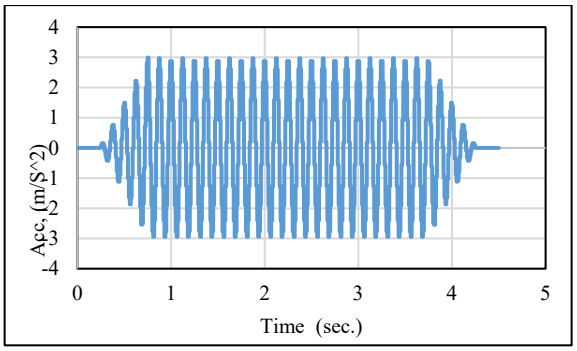

Figure 4.26: Applied sinusoidal motion to the model for SSI study.

4.4.1 Case without Structural Element or Pile (Free-Field Soil Model)

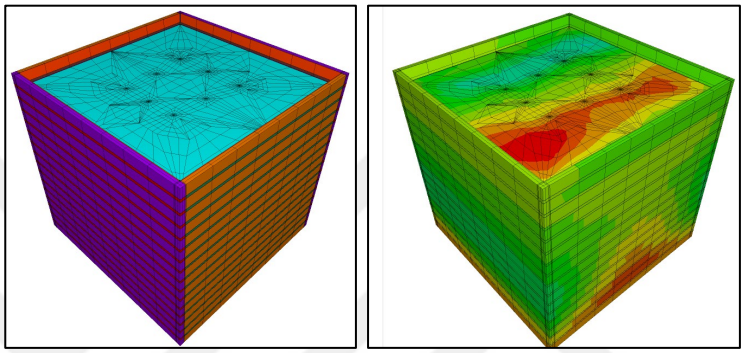

Figure 4.27: Genereated model and deformed mesh after analysis for the numerical evaluation of the container with only soil element.

The results obtained throughout the depth of the container show consistent displacement values for various points where the test models are located, as depicted in Figure 4.28. However, due to boundary effects on the soil model inside the container, the acceleration values vary, though they exhibit similarities (Figure 4.29).

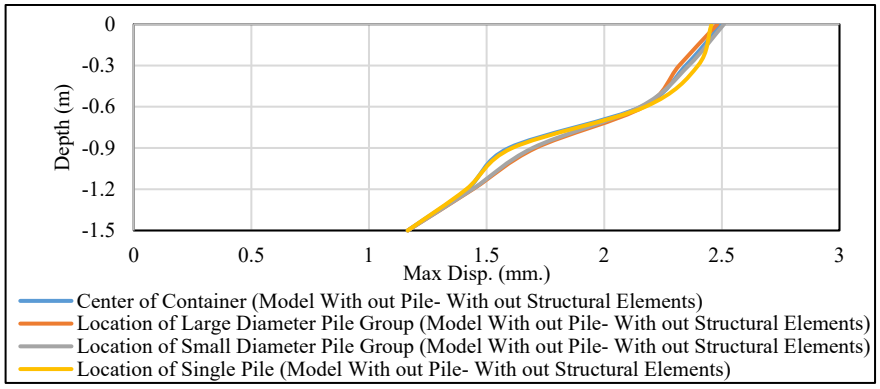

Figure 4.28: Comparison of the displacements of different points in the soil for the model without pile and structural elements.

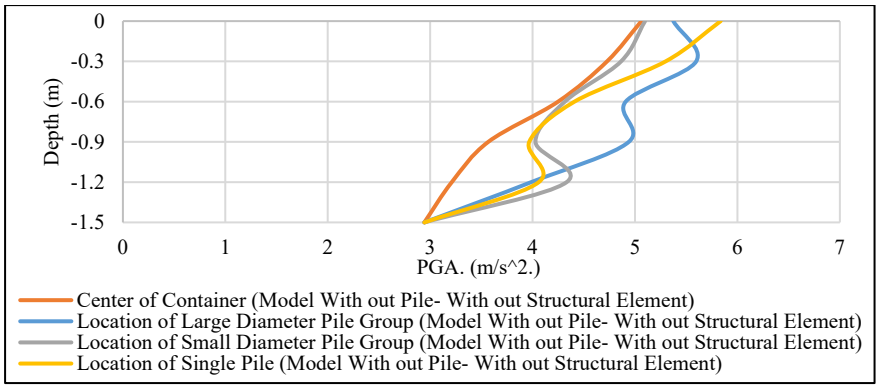

Figure 4.29: Comparison of the accelerations of different points in the soil for the model without pile and structural elements.

4.4.2 Case with a single pile, with and without super structure

The generated model and the deformed model after the analysis are presented in Figure 4.30. The models compare two scenarios: one with only a single pile in the soil and another where a superstructure is connected to the pile with a pile cap element. The length of the piles is selected to be 1.0 meter, with their base approximately 0.5 meters from the base of the container.

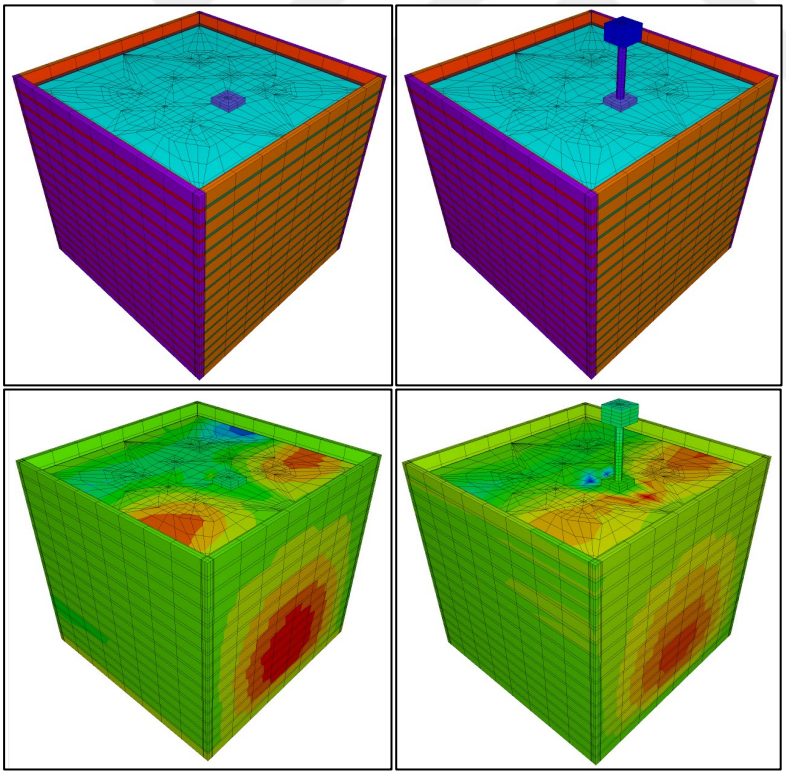

Figure 4.30: Genereated model and deformed mesh after analysis for the soil sample with single pile and effect of the SDOF system.

The container model shows nearly identical lateral displacement for every point throughout the depth. However, adding the pile to the model slightly affects the soil's

performance, exhibiting less deformation compared to the soil in the center of the model, especially when influenced by the superstructure on the pile (Figure 4.31).

It can be concluded that the single pile itself did not have a significant effect on the displacement relative to the center point of the container. However, adding the superstructure amplifies the acceleration values obtained from the pile location, resulting in higher acceleration values at that point (Figure 4.32).

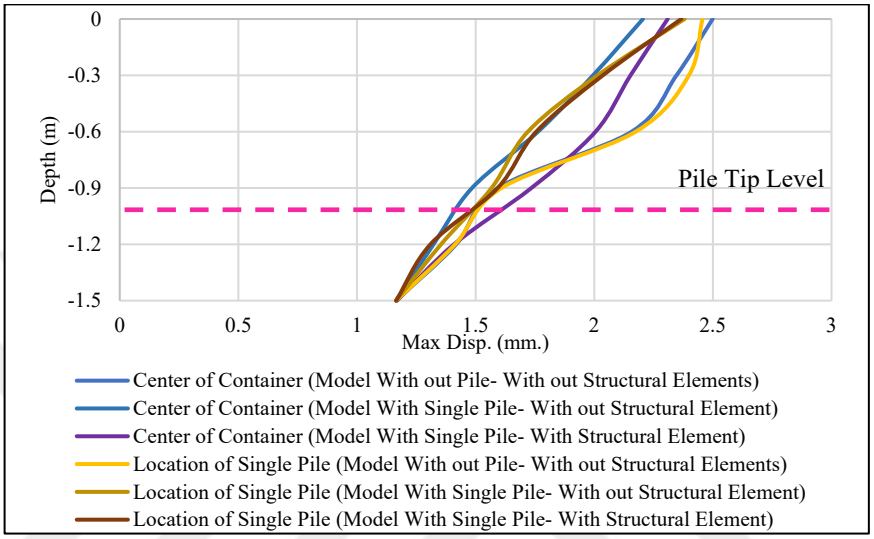

Figure 4.31: Comparison of the displacement of different points in the soil container for the soil sample with single pile and effect of the SDOF system.

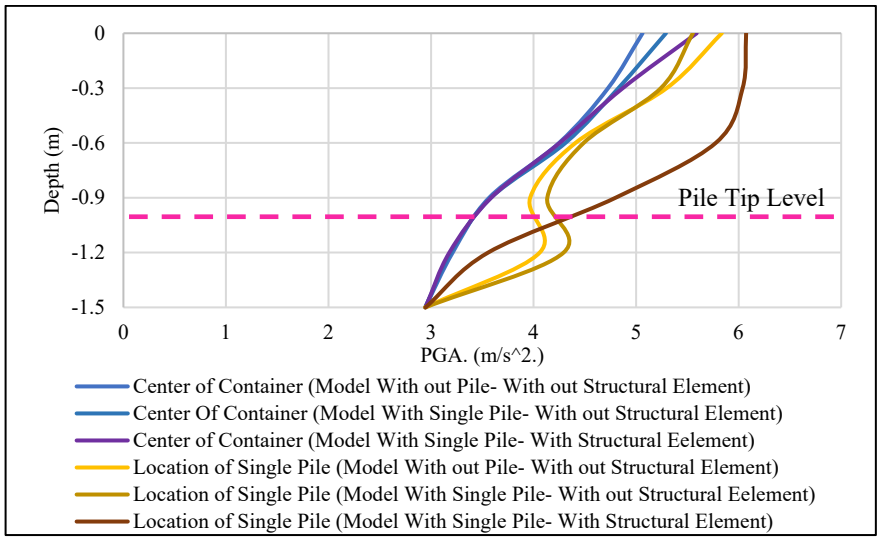

Figure 4.32: Comparison of the acceleration of different points in the soil container for the soil sample with single pile and effect of the SDOF system.

4.4.3 Case with small diameter pile group, with and without super structure

The generated model and the deformed model after analysis are presented in Figure 4.33. The models compare two cases: one where there is only a small diameter pile

group in the soil, and another where the superstructure is connected to the pile group with a pile cap element.

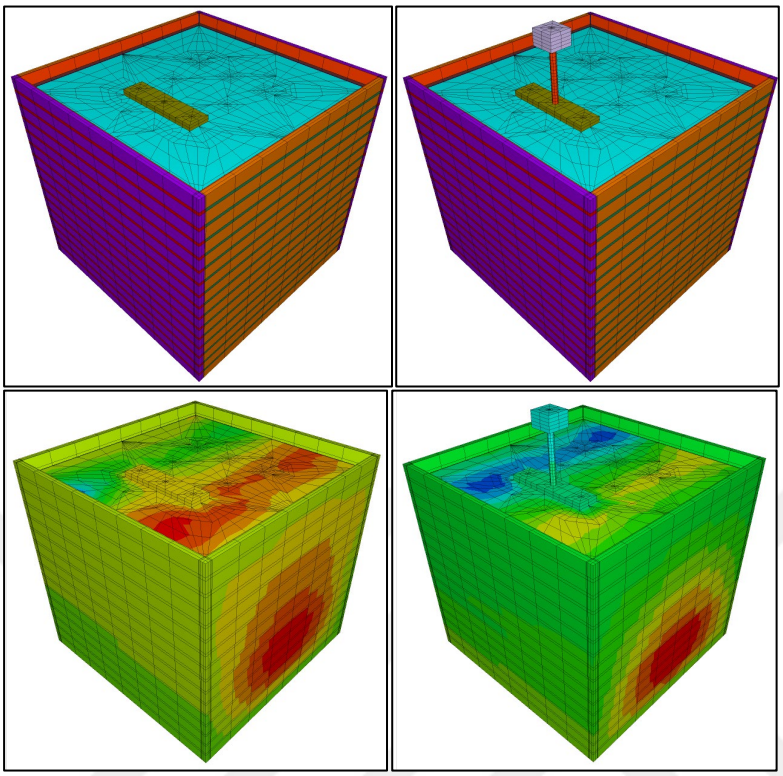

Figure 4.33: Genereated model and deformed mesh after analysis for the soil sample with small diameter pile group and effect of the SDOF system.

The displacement values for different points and models at various depths reflect similar responses in the middle of the soil model and at locations where no pile elements are present. However, when piles are in contact with the soil, their deformation differs from the surrounding soil. In this scenario, the superstructure (SDOF) system results in less amplification of the applied motion compared to the response of the pile group alone (Figure 4.34).

This trend is similarly observed in the acceleration values, where the SDOF system causes less amplification compared to the case with only piles in the system (Figure 4.35).

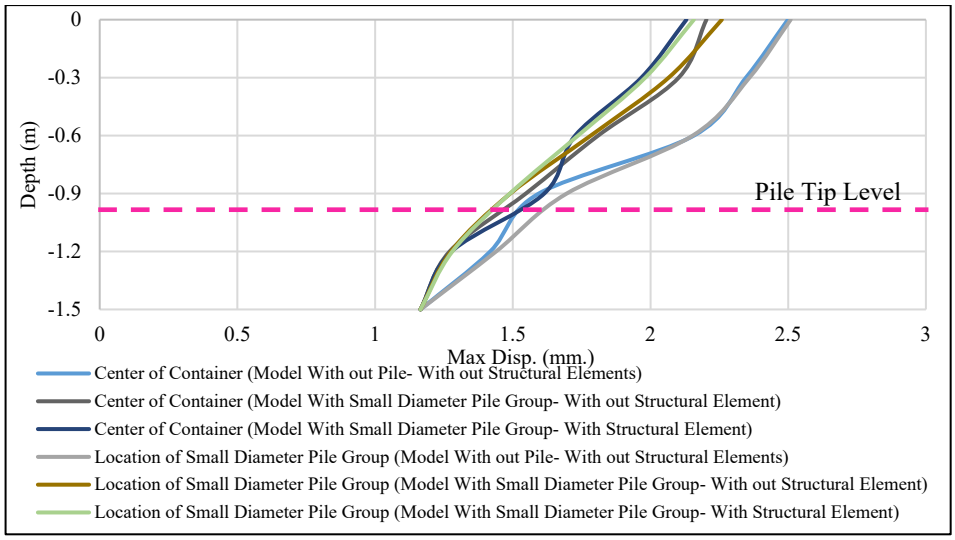

Figure 4.34: Comparison of the displacement of different points in the soil container for the soil sample with small diameter pile group and effect of the SDOF system.

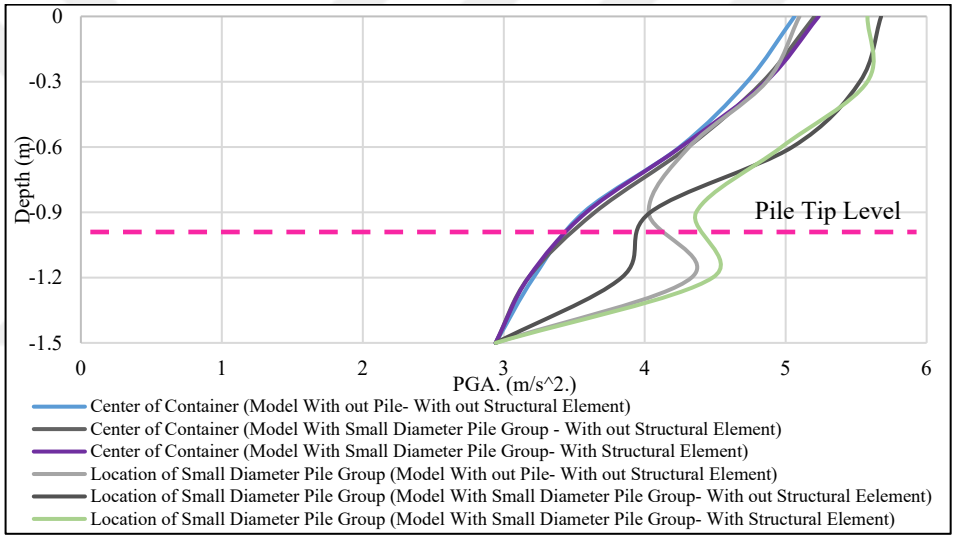

Figure 4.35: Comparison of the acceleration of different points in the soil container for the soil sample with small diameter pile group and effect of the SDOF system.

4.4.4 Case with large diameter pile group, with and without super structure

The generated model and the deformed model after analysis are presented in Figure 4.36. These models compare two cases: one with only a large diameter pile group in the soil, and another where the superstructure is connected to the pile group with a pile cap element.

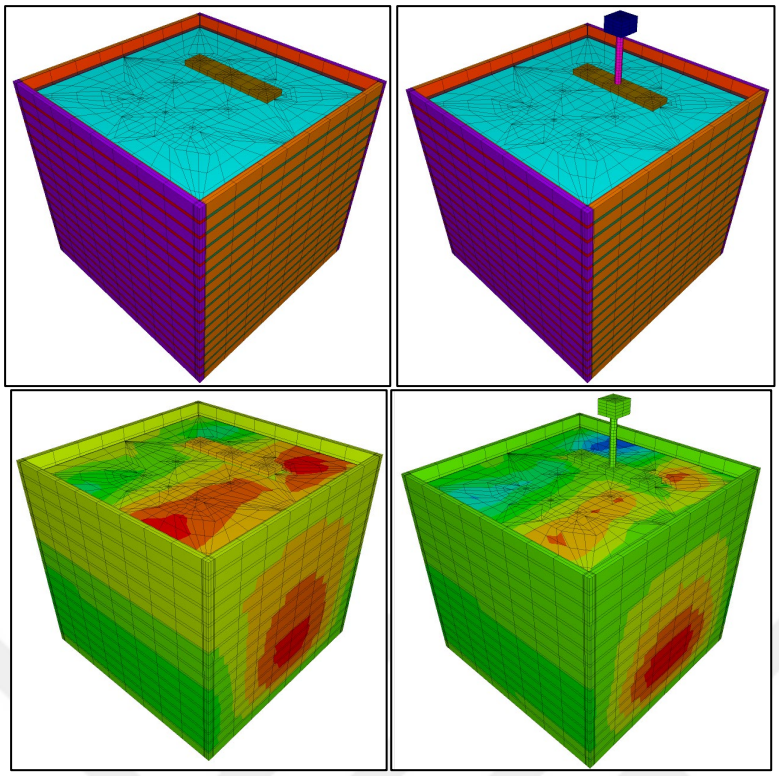

Figure 4.36: Genereated model and deformed mesh after analysis for the soil sample with large diameter pile group and effect of the SDOF system.

The displacement values at various points within the soil model, including the middle and locations near the pile groups, exhibit similar patterns. When the pile groups interact with the soil, their deformation resembles that of the surrounding soil. In such cases, the presence of the superstructure (SDOF) system has minimal effect on the amplified motion compared to the response of the pile groups at the surface (Figure 4.37).

However, the acceleration responses show significant influence from both the pile groups and the SDOF system connected to them. The SDOF system mitigates amplification compared to scenarios where only the pile groups are present in the system (Figure 4.38).

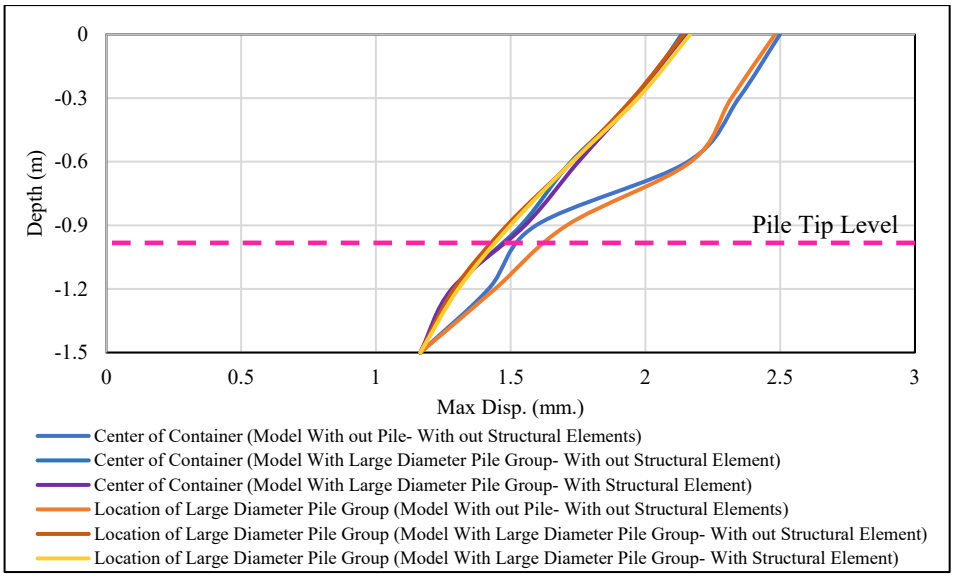

Figure 4.37: Comparison of the displacement of different points in the soil container for the soil sample with large diameter pile group and effect of the SDOF system.

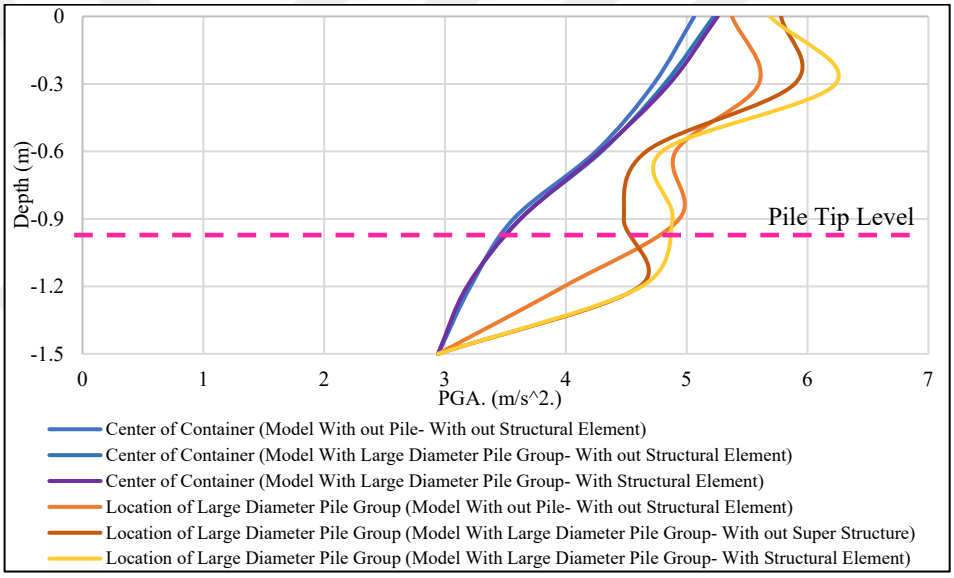

Figure 4.38: Comparison of the acceleration of different points in the soil container for the soil sample with large diameter pile group and effect of the SDOF system.

4.4.5 Case with all pile groups and super structures

The generated model and the deformed model after the analysis are presented in the Figure 4.39. The models compare the cases where there are a SDOF system connected to a large diameter pile group, small diameter pile group, single pile in the soil through a pile cap element.

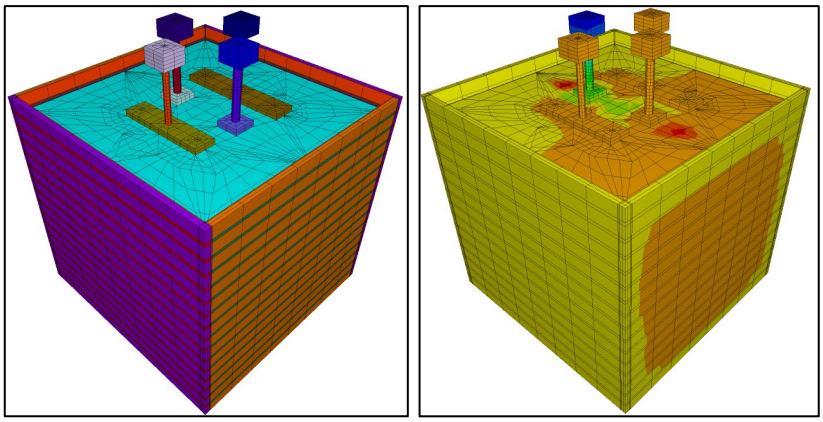

Figure 4.39: Genereated model and deformed mesh after analysis for the soil sample with large and small diameter pile groups and single piles with the effect of SDOF system.

The displacement values at different depths correspond to the observed behavior at each type of pile-supported system in the model. The influence of the superstructure (SDOF) system is evident in the amplified deformations near the soil surface. Notably, pile groups with larger diameters exhibit reduced amplification responses due to their higher rigidity. Conversely, connections to softer single pile supports result in greater deformation amplification, as depicted in Figure 4.40.

Similar trends are observed in the acceleration responses of the model, as shown in Figure 4.41.

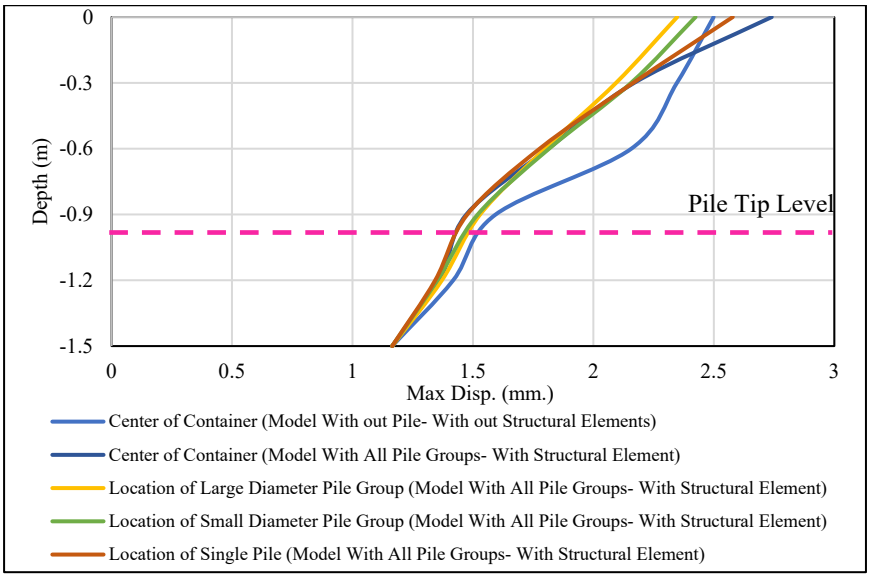

Figure 4.40: Comparison of the displacement of different points in the soil container for the soil sample with large and small diameter pile groups and single piles and effect of the SDOF system.

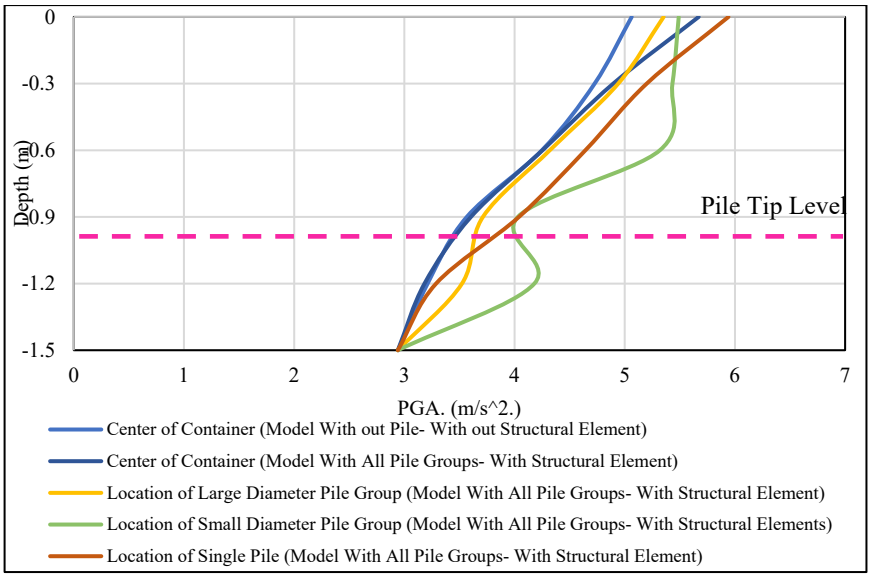

Figure 4.41: Comparison of the acceleration of different points in the soil container for the soil sample with large and small diameter pile groups and single piles and effect of the SDOF system.

4.5 Discussions and Conclusions

In this chapter the following key notes are verified and studied:

1- The performance of the soil with the free field booundary condition is studied through numerical modelling and the range of appliable dynamic sinusoidal motion is confirmed for the purpose of verification and design of the laminar soil container.

2- Laminar soil containers with different mechanisms of movement are modeled using FLAC3D software and through the result a new concept for the mechanism of movement is developed.

3- An enhanced mechnaism of movement which uses the roller bearing and flexible sealant meterial between the laminas is found to be the best performing mechanism to represent the free field boundary.

4- The effect of lateral support system on the behavior of laminar soil container is studied and it was found that the vertical support in addition to lateral support will provide better response of the laminar soil container.

5- In initial evaluation of the test setups in the laminar soil container was carried out and the effect of SDOF system on different types of pile supported foundations are studied.

5. SHAKING TABLE TESTS ON THE NEWLY DESIGNED AND MANUFACTURED ENHANCED TRANSPARENT IMPERMEABLE LAMINAR (ETILAM) SOIL CONTAINER

After extensive testing and laboratory studies on the materials intended for the laminar container, the final design for manufacturing has been completed. Figure 5.1 illustrates the finalized design of the container, showcasing its structural elements and features. Figure 5.2 shows the manufactured laminar soil container and its mechanism of movement to be used on the shaking table for the dynamic soil testing. Details outlining the container's mechanisms for facilitating movement are presented in Figure 5.3.

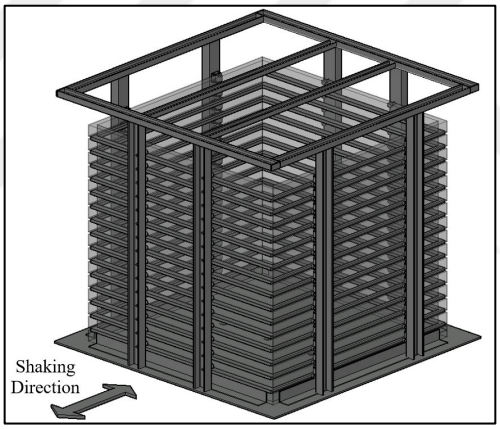

Figure 5.1: Laminar soil container scheme.

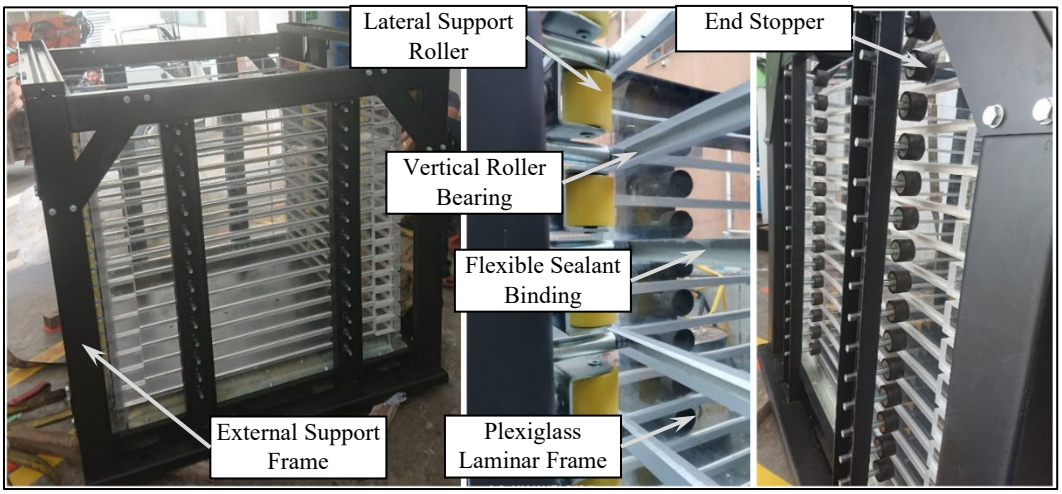

Figure 5.2: Enhanced Transparent Impermeable Laminar (ETILam) Soil Contianer and components of mechanism of movement .

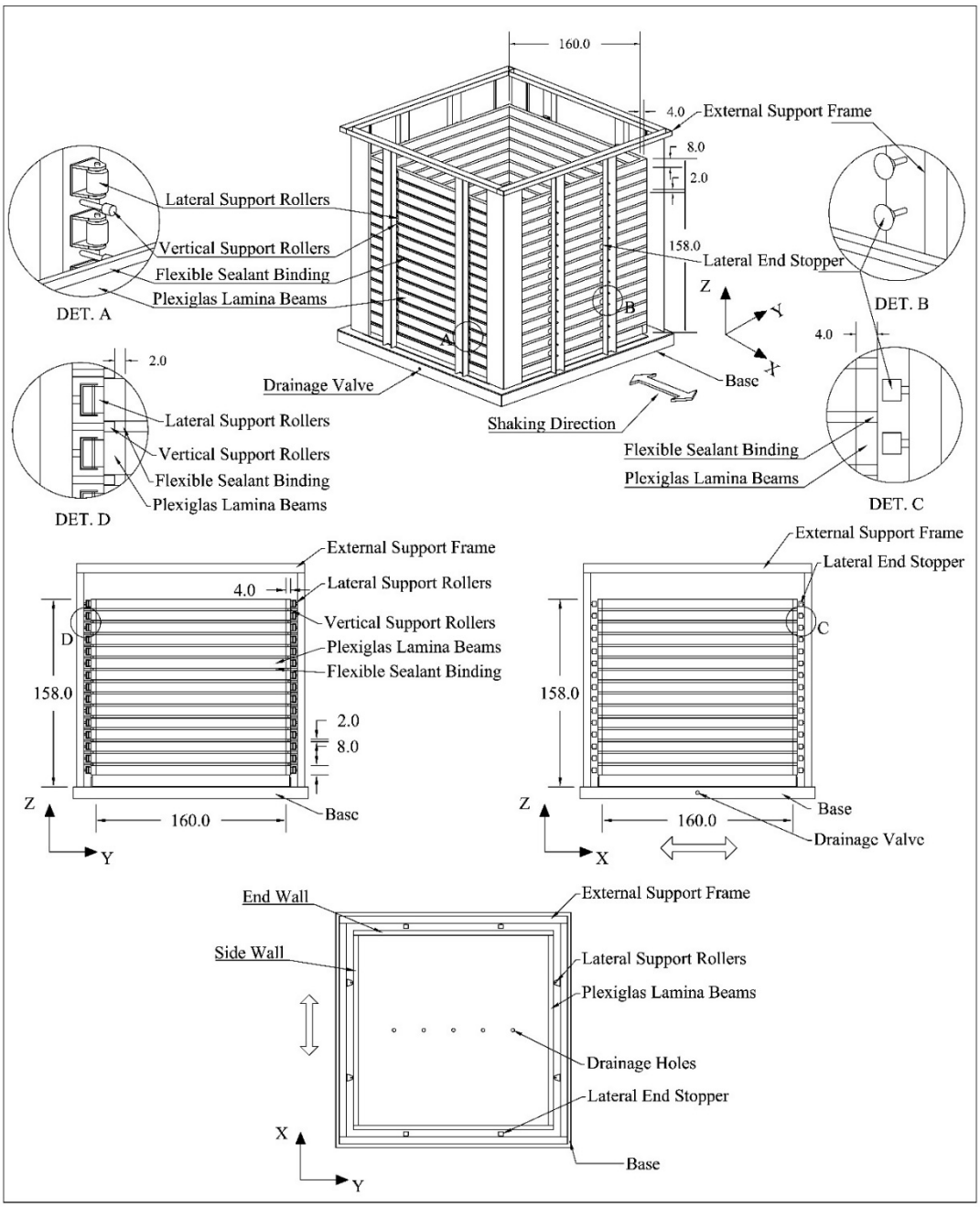

Figure 5.3: Details of the ETILam soil container manufactured for the laboratory tests.

5.1 Laboratory Test on the Laminar Container in Empty Condition

To evaluate the performance of the empty container, a sinusoidal motion was applied to the shaking table. Figure 5.4 illustrates the laminar container mounted on the shaking table in preparation for testing. The motion had an input acceleration of 0.32g and a frequency of 2 Hz applied at the base of the container, with the response recorded at the lamina located 1.20 meters above the base. The response records are presented in Figure 5.5. It was observed that the motion was amplified, indicating that the

container effectively transmitted the motion to the higher laminas without additional damping effects.

Figure 5.4: Testing the laminar soil container in empty condition on the shaking table.

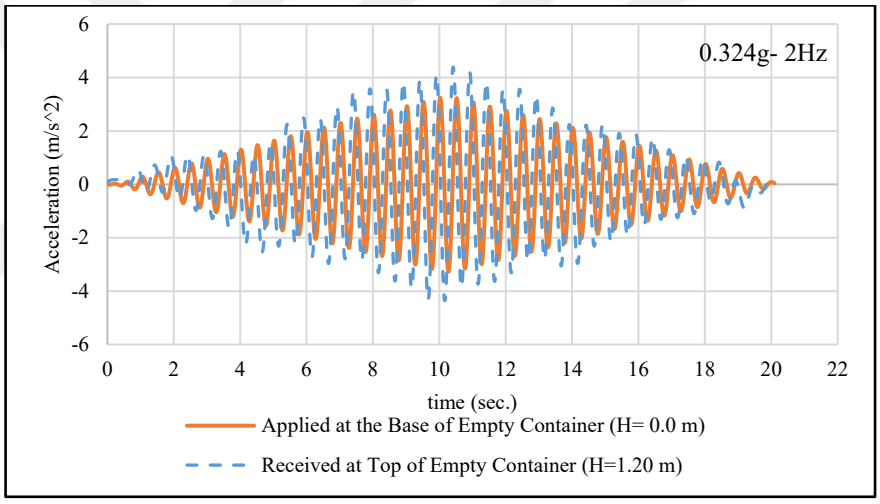

Figure 5.5: Performance of the laminar soil container on shaking table under dynamic loading through laboratory test.

5.2 Sand Pluviation Mechanism

Before mounting the sand pluviation mechanism on top of the laminar soil container, it was necessary to ensure the controlled passage of sand through the sieve holes. The sieve mechanism is designed with two interchangeable hole-pattern plates that slide over each other. The upper plate can be adjusted to achieve the desired relative density during sand pluviation in the container. For each layer of sand, the frame surrounding the sieves is filled with sand. After sliding and aligning the sieve plates to match the holes, the sand flows through them. It's important to note that based on previous

laboratory tests, the hole pattern of the upper sieve plate must be adjusted to achieve the intended relative density of the soil sample inside the container.

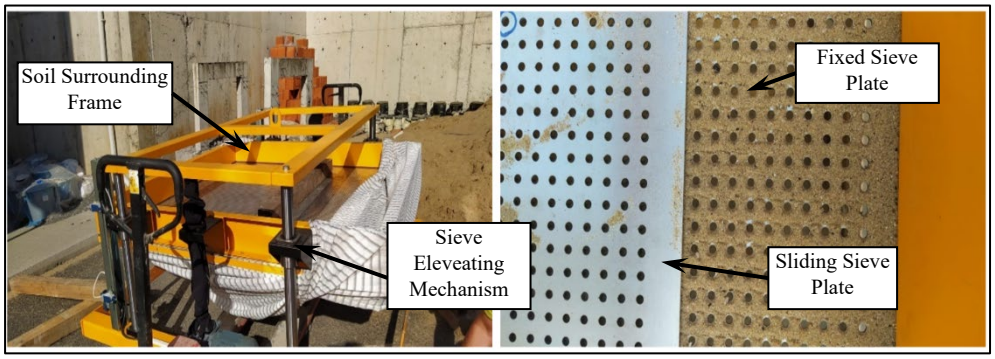

Figure 5.6: Testing the sand pluviation mechanism and accumulated sand between the sieves.

The sand transfer to the pluviation system involves attaching vacuum barrels to a vacuum pump, filling them with sand, and then emptying them onto the sieves (Figure 5.7).

Figure 5.7: Prepared and tested vacuum barrels for transferring the sand on the sand pluviation mechanism.

5.3 Shaking Table Tests on the ETILam Soil Container Including Only Soil

To conduct tests on the shaking table, the sand material was transferred over the container and poured into the sand pluviation mechanism multiple times. Each transfer was weighed to determine the mass of sand located in the container, allowing for calculation of the relative density. Sensors, positioned according to predetermined locations shown in Figure 5.8, were carefully arranged in the correct orientation during the placement of sand samples to ensure proper connection with the surrounding sand. After filling the container to the intended depth, the sensors were detached from the support beam above the container, and the surface was then trimmed appropriately. The soil sample was prepared in two different densities: dense sand and loose to

medium dense sand above the dense layer. These layers were separated by colored sand placed near the container wall and visible through the Plexiglas. The procedure for preparing the test sample is detailed in Figures 5.9 to 5.12.

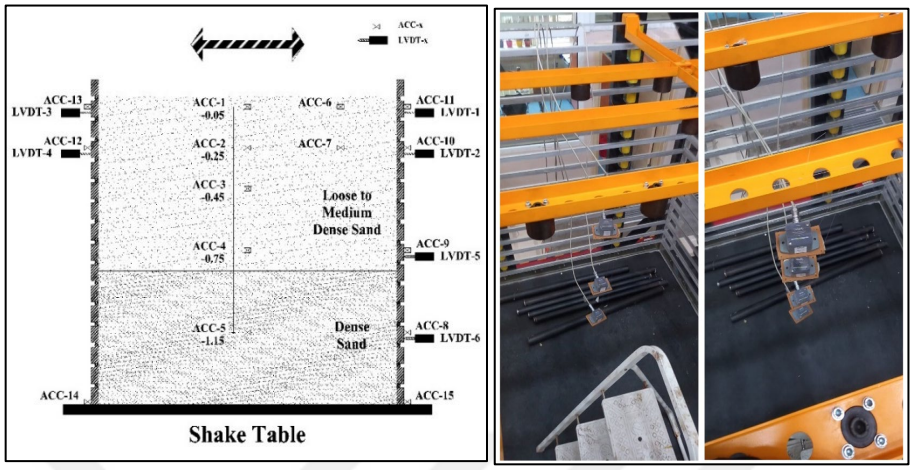

Figure 5.8: Sensor pattern in the laminar container and locationg the sensors prior to sand pluviation.

Figure 5.9: Transferring the sand over the laminar soil container and pouring on the sand pluviation mechaanism.

Figure 5.10: Weighing the tanks prior to the pouring the sand and uniform scattering the sand on the sieves.

Figure 5.11: Aligning the buried sensors in the sand sample and separating the dense sand layer from the upper loose layer through a colored sand layer.

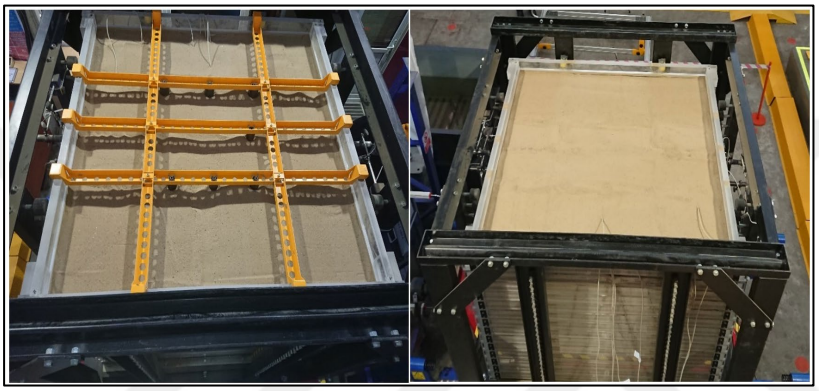

Figure 5.12: Separating the buried sensors from the support beam and trimmimg the surface of the soil sample in the container.

The container and the soil sample inside were subjected to various sinusoidal motions, with responses recorded by accelerometers and LVDT (Linear Variable Differential Transformer) sensors placed inside the container and on its sidewall. Each loading step in the procedure resulted in settlements in both the loose and dense layers of the soil sample, causing them to compact.

The specifications of the applied dynamic load recorded at ACC-15 on the shaking table, the received response at the top of the soil sample at ACC-1, and the changes in relative density of the soil during the tests are presented in Table 5.1. The range of settlement after performing the tests is shown in Figure 5.13.

The accelerometer records of the applied motion to the laminar soil container, obtained from ACC-15 on the shake table, are presented in Figure 5.14. Figure 5.15 illustrates the comparison between the motion applied to the shake table and the motion received on top of the soil layer for various applied conditions. It is evident that increasing the motion amplitude and frequency results in higher amplification of the input motion.

Table 5.1: Dynamic load and response specifications and the changes in the relative density of the soil sample.

Sample No. 1							
Dynamic Load Specifications				Soil Sample Parameters Change During Tests			
Test No.	Frequenc y	Applied PGA (m/s2)	Received PGA (m/s2)	Dr%, Layer 1 (0 to -85 cm)		Dr%, Layer 2 (-85 to -150 cm)	
				Initial	Final	Initial	Final
T1-1	2	1.77	1.94	34	43	68	68
T1-2	2	2.65	3.43	43	53	68	72
T1-3	3	2.44	4.75	53	65	72	76

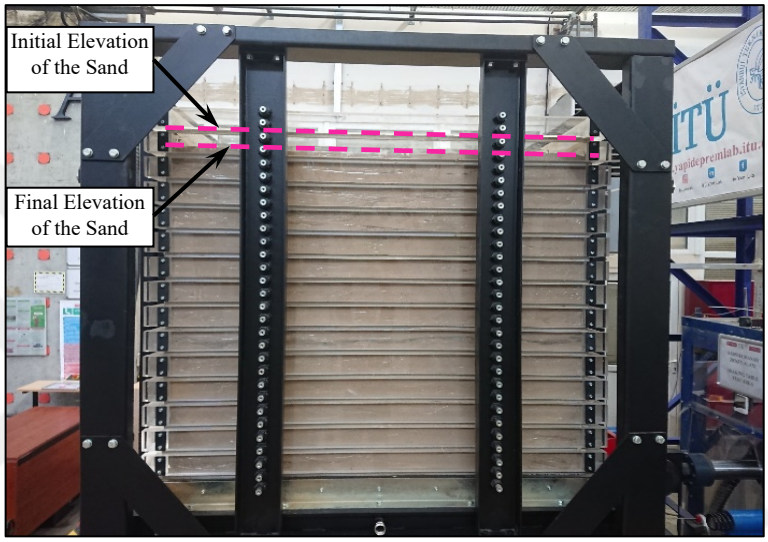

Figure 5.13: Settlement on the soil sample after applying the dynamic loads to the laminar soil container.

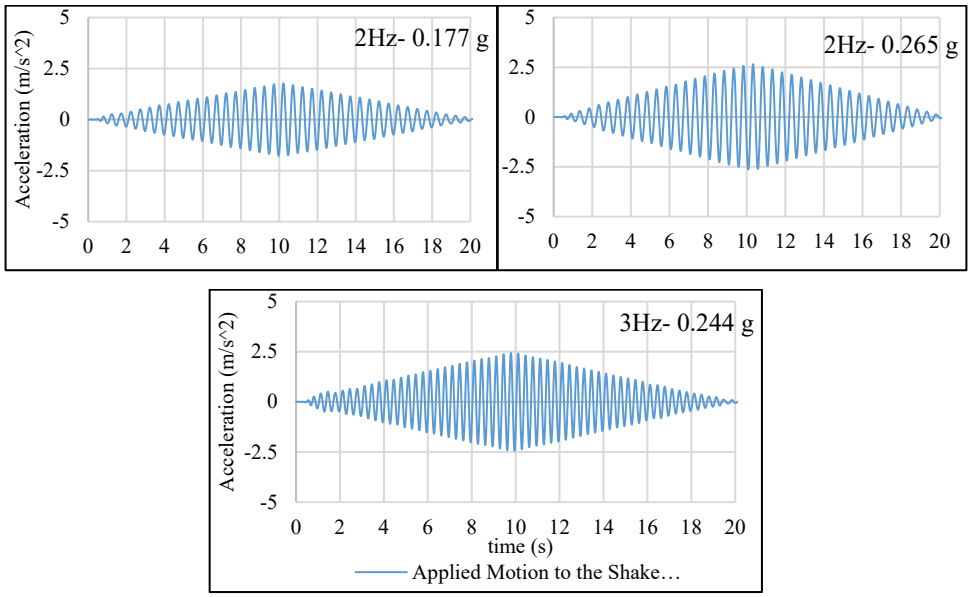

Figure 5.14: Applied motions to the base of the laminar soil container (ACC-15) for different tests.

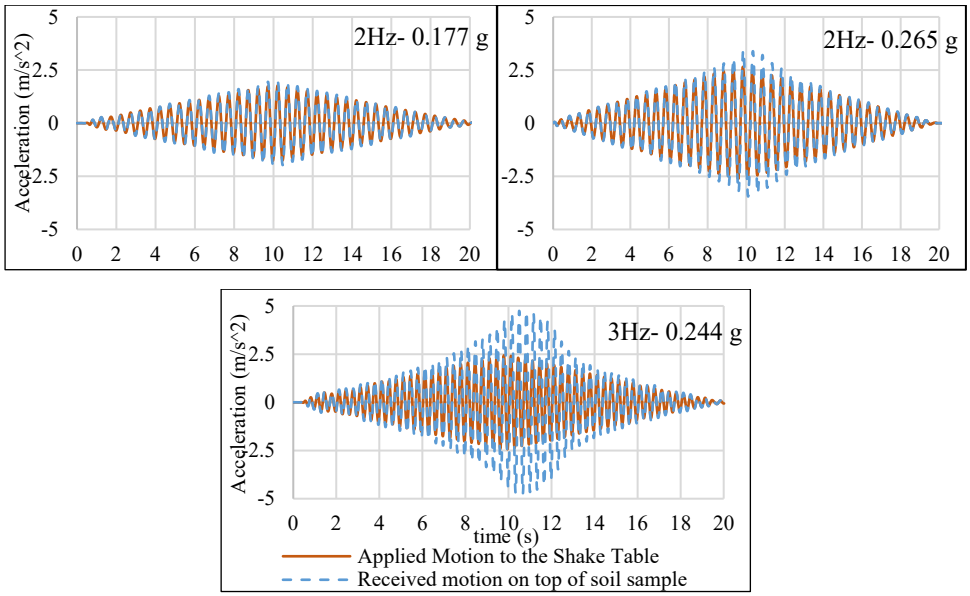

Figure 5.15: Comparison of the applied motion to the laminar box (ACC-15) and received response at top of the soil sample (ACC-1) for different applied dynamic loads.

The specifications of the tests performed in the laboratory on the first test setup to study the performance of the soil inside the container are summarized in Table 5.2.

Table 5.2: Laboratory test specifications performed on the first test sample/

First Test Set	Test Model	Dr (%)	PGA (g)	F (Hz)	Duration (sec)
T1-1	Free Field	25 % - 40 %	0.2	2	20
T1-2		40 % - 55 %	0.3	2	20
T1-3		55 % - 65 %	0.3	3	20
T1-4		65%>	0.2	3	20
T1-5			0.2	3	6
T1-6			0.3	3	6
T1-7			0.3	4	20
T1-8			Tabas	-	
T1-9			Northridge	-	
T1-10			LomaP	-	

5.4 Shaking Table Tests on the ETILam Soil Container with Single Degree of Freedom System (SDOF) on Shallow Foundation

To evaluate the performance of a single degree of freedom (SDOF) system on the soil layer, a surface foundation and SDOF test setup were placed on the soil surface. This setup aimed to study the transmitted motion applied by the shaking table to both the foundation and the SDOF mass. The SDOF mass simulated prototype models with fundamental frequencies of 1 Hz and 2 Hz. Accordingly, the models were designed to replicate these superstructure frequencies as detailed in Table 5.3, scaled at a ratio of 10:1 between prototype and model dimensions. The specific motion parameters

applied during the tests are summarized in Table 5.4, and the model setup is illustrated in Figure 5.16.

Table 5.3: Frequency content of the superstructure during laboratory tests.

	Prototype Super Structure	Laboratory Super Structure
Test Setup	Fundamental Frequency (Hz)	Fundamental Frequency (Hz)
Structural Element	1	5.62
	2	11.24

Table 5.4: Laboratory test specifications performed on the first test sample.

First Test Set	Test Model	Dr (%)	PGA (g)	F (Hz)	Duration (sec)
T1-11	Surface Foundation and Structure	65%>	0.2	2	20
T1-12			0.3	2	20
T1-13			0.3	3	20
T1-14			0.2	3	20
T1-15			0.2	3	6
T1-16			0.3	3	6
T1-17			Tabas		

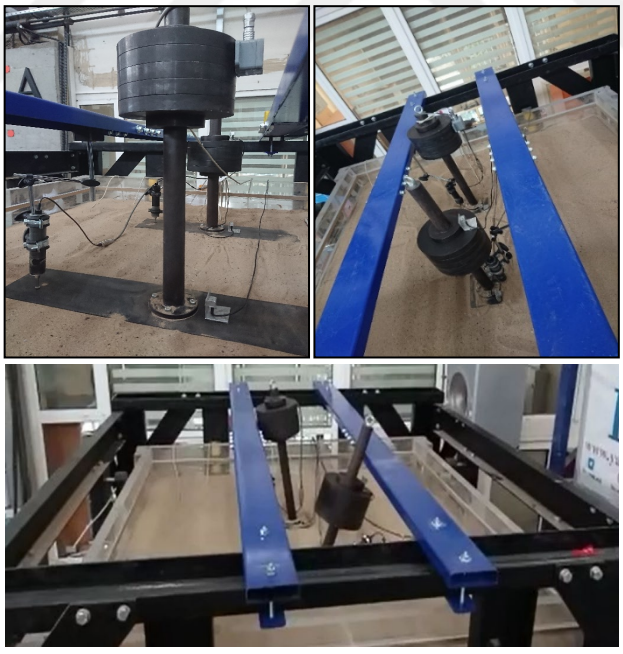

Figure 5.16: Performing the laboratory tests on the surface foundation with a SDOF superstructure.

5.5 Shaking Table Tests on the ETILam Soil Container with SDOF System with Group Piles and Single Piles

5.5.1 Pile model elements and test setups

The test setup which is planned to be located in the box during the dynamic tests, is supposed to include as many test samples and piles as possible without being affected by the boundaries of the container. It is tried to locate the elements as far as they do not have any affect on performance of each other. The sample pile elements are supposed to represent the diameter of piles equal to 1.00 meter and 0.65 meter. Also, the depth of the piles is selected to be 1 meter. Two different super structures are planned to be located on the piles and also on the surface of the sand in the container representing the frequencies of 1 and 2 Hz for the prototype model. Again the prototype to model ratio is selected to be 10 times in length. The details of the model and parameters of the pile elements are summarized in Table 5.5.

Table 5.5: Properties of the test model based on the prototype dimensions.

	Prototype Pile Specifications		Laboratory Setup Pile Specifications		
Test Setup	Pile Depth (m)	Pile Diameter (m)	Pile Depth (m)	Pile Outer Diameter (m)	Pile Inner Diameter (m)
Big Diameter Pile Group	10	1	1	0.05	0.038
Small Diameter Pile Group	10	0.65	1	0.04	0.037
Single Pile	10	0.65	1	0.04	0.037

5.5.2 Preparing the test setup and applying the dynamic loads

To conduct laboratory tests on the pile-supported single degree of freedom system, strain gauges need to be attached to the pile models. Given the limitation in the number of sensors and data logger channels, it was decided to place strain gauges on one side of the middle piles in the group and also on the single pile system. To validate the responses obtained from the strain gauges, additional strain gauges were attached on the opposite side at two different elevations on each pile element. The prepared pile elements are depicted in Figure 5.17. It is important to note that the pile elements have two different rigidity parameters, representing prototype concrete piles with diameters of 0.65 meters and 1.00 meters; one of each type is equipped with strain gauges.

Figure 5.17: Prepared model pile elements and attached strain gauges on them.

The pile formations and their locations within the group setups are illustrated in Figure 5.18. To secure the piles in their intended positions, a specially designed support beam was placed on the laminar box, ensuring proper guidance for the piles at their specified locations.

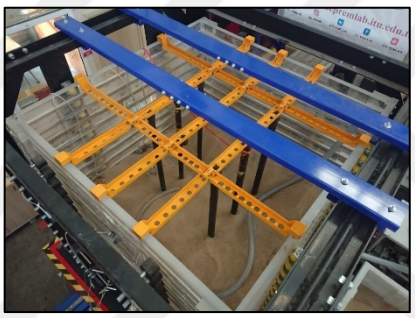

Figure 5.18: Prepared beam element structure to assemble the pile elements on the exact required point.

The straing gauge cables are connected so that there would be no problem in their functioning during the tests.

Figure 5.19: Mounted pile elements on the support beam and buried into the lower dense sand.

After filling the laminar box with sand to achieve the intended relative density and placing the accelerometer sensors in their designated locations, the pile cap, which is designed to connect the piles together to function as a group system, is attached to the piles.

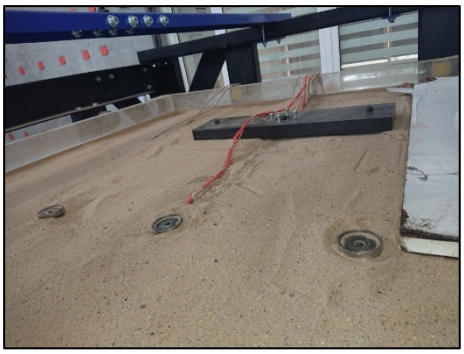

Figure 5.20: Filled container with the sand and conncted cap pile element on the piles.

The superstructure model, designed to function as a single degree of freedom system, is attached to the pile cap plate to transfer the dynamic movements to the supporting system.

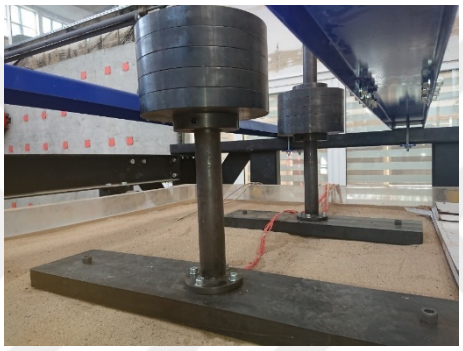

Figure 5.21: Mounted SDOF system on the pile group system.

After preparing the test setup, the accelerometers and LVDT (Linear Variable Differential Transformer) sensors are attached to the moving mass and the pile cap. These sensors are used to record the vertical movement of the pile cap during dynamic loading. It should be noted that, in order to allow the superstructure to perform with two different periods (equal to 0.5 and 1.0 seconds of the prototype), the elevation of the mass is adjusted for each test set.

Figure 5.22: Mounted sensores on the superstructure system for the SDOF system with 1 and 2 Hz of response frequecy on pile group model.

The same procedure was applied for the single pile setup, where the SDOF system was attached to the single cap pile connected to the middle pile, which was monitored by the strain gauges on the pile body. In this case, the elevation of the mass was adjusted to achieve different performing periods of the SDOF system.

Figure 5.23: Mounted sensores on the superstructure system for the SDOF system with 1 and 2 Hz of response frequecy on single pile model.

Each test set was subjected to a series of dynamic harmonic motions as well as earthquake record motions. The details of these test sets are summarized in Table 5.6.

The applied sinusoidal loads have frequencies of 1, 2, and 3 Hz with acceleration input values of 0.2g and 0.3g. Additionally, scaled earthquake motions from Tabas, Northridge, and Loma Prieta outcrop motions were used. To process the results from each test, filtering and baseline correction were applied to the records using MATLAB. The outcomes from the accelerometers positioned in the middle of the soil container are summarized as acceleration values and integrated displacement values varying with depth. These values are presented for each test setup in the subsequent sections.

The first test setup aimed to prepare the sand sample in a loose condition. However, the intense initial motion of the shaking table caused the sample to become denser, altering the test conditions from the expected values. The locations of the sensors are presented in Figure 5.24.

During the tests, a total of 15 accelerometers, 16 strain gauges, and 6 LVDTs were used to monitor the performance of the soil sample, laminar container, and structural elements. Each pile group consisted of 3 pile elements with identical structural and rigidity parameters. The cap pile is a continuous plate that ensures simultaneous movement of the piles through the head connections. As previously mentioned, the lower 65 centimeters of the soil in the box were filled with dense sand to serve as the supporting layer for the pile elements.

During the initial test, the soil sample experienced increasing densification after each load case. The changes in density are detailed in Table 5.7, providing a basis for evaluating soil parameters for further analytical assessments or numerical modeling studies.

Table 5.6: Summary of the performed tests on the SDOF test setup.

Second Test Set	Tets Model	Dr (%)	PGA (g)	F (Hz)	Duration (sn)	Received Results	
						Small Diameter Structure	Large Diameter Structure
T2-1	Group Pile Structures with Small and Large Diameter- Super-Structure Freq. 2 Hz	40 % - 45 %	0.2	2	6	✓	✓
T2-2		40 % - 45 %	0.3	2	6	✓	✓
T2-3		45 % - 50 %	0.2	3	6	✓	✓
T2-4		55 % - 60 %	0.3	3	6	✓	✓
T2-5		55 % - 60 %	Tabas	-	-	✓	✓
T2-6		55 % - 60 %	Northridge	-	-	✓	✓
T2-7		55 % - 60 %	LomaP	-	-	✓	✓
Third Test Set	Tets Model	Dr (%)	PGA (g)	F (Hz)	Duration (sn)		
T3-1	Group Pile Structures with Small and Large Diameter- Super-Structure Freq. 2 Hz	60%>	0.2	1	6	✓	✓
T3-2			0.3	1	6	✓	✓
T3-3			0.2	2	6	✓	✓
T3-4			0.3	2	6	✓	✓
T3-5			0.2	3	6	✓	✓
T3-6			0.3	3	6	✓	✓
T3-7			Tabas	-	-	✓	✓
T3-8			Northridge	-	-	✓	✓
T3-9			LomaP	-	-	✓	✓
Forth Test Set	Tets Model	Dr (%)	PGA (g)	F (Hz)	Duration (sn)		
T4-1	Group Pile Structures with Small and Large Diameter- Super-Structure Freq. 1 Hz	60%>	0.2	1	6	✓	✓
T4-2			0.3	1	6	✓	✓
T4-3			0.2	2	6	✓	✓
T4-4			0.3	2	6	✓	✓
T4-5			0.2	3	6	✓	✓
T4-6			0.3	3	6	✓	✓
T4-7			Tabas	-	-	✓	✓
T4-8			Northridge	-	-	✓	✓
T4-9			LomaP	-	-	✓	✓
Fifth Test Set	Tets Model	Dr (%)	PGA (g)	F (Hz)	Duration (sn)		
T5-1	Single Pile Structures with Small and Large Diameter- Super-Structure Freq. 2 Hz	60%>	0.2	1	6	✓	✓
T5-2			0.3	1	6	✓	✓
T5-3			0.2	2	6	✓	✓
T5-4			0.3	2	6	✓	✓
T5-5			0.2	3	6	✓	✓
T5-6			0.3	3	6	✓	✓
T5-7			Tabas	-	-	✓	✓
T5-8			Northridge	-	-	✓	✓
T5-9			LomaP	-	-	✓	✓
Sixth Test Set	Tets Model	Dr (%)	PGA (g)	F (Hz)	Duration (sn)		
T6-1	Single Pile Structures with Small and Large Diameter- Super-Structure Freq. 1 Hz	60%>	0.2	1	6	✓	✓
T6-2			0.3	1	6	✓	✓
T6-3			0.2	2	6	✓	✓
T6-4			0.3	2	6	✓	✓
T6-5			0.2	3	6	✓	✓
T6-6			0.3	3	6	×	✓
T6-7			Tabas	-	-	×	✓
T6-8			Northridge	-	-	×	✓
T6-9			LomaP	-	-	×	✓

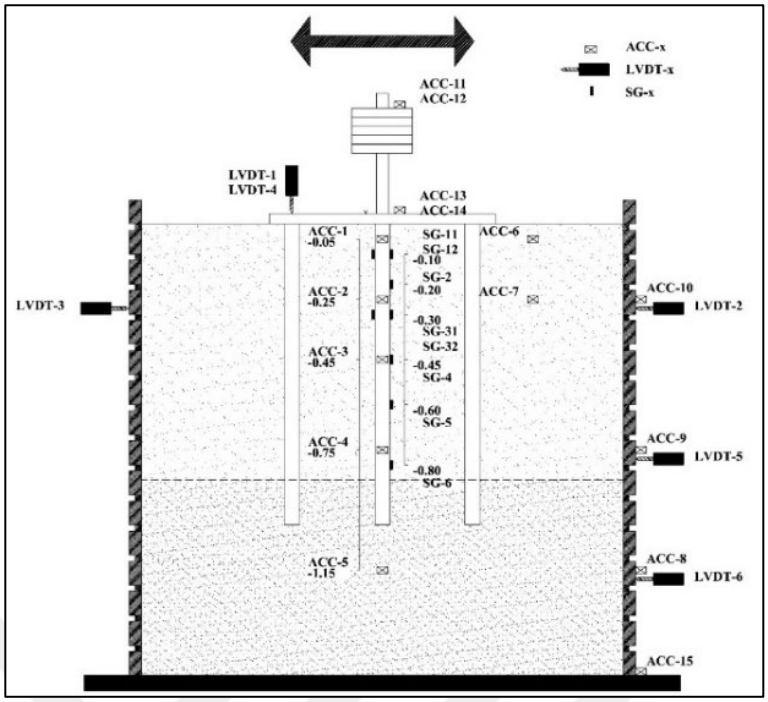

Figure 5.24: Location of the sensores in the test setups including the pile group system.

Table 5.7: Soil parameter change during the performing of the second set of dynamic laboratory tests.

Layer 1 (0 to -85 cm)							
Test No.	2-1	2-2	2-3	2-4	2-5	2-6	2-7
Weight of the Sand (kg)	3176.00	3176.00	3176.00	3176.00	3176.00	3176.00	3176.00
Height (m)	0.83	0.83	0.82	0.81	0.81	0.80	0.80
Volume (m^3)	2.11	2.11	2.10	2.06	2.06	2.05	2.05
Settlement (cm)	0.00	0.00	0.50	1.50	0.00	0.30	0.20
Dry Density (kg/m^3)	1503.79	1503.79	1512.96	1541.15	1541.15	1546.91	1550.78
Gs	2.65	2.65	2.65	2.65	2.65	2.65	2.65
e	0.76	0.76	0.75	0.72	0.72	0.71	0.71
e max	0.91	0.91	0.91	0.91	0.91	0.91	0.91
e min	0.57	0.57	0.57	0.57	0.57	0.57	0.57
Dr %	43.5	43.5	46.6	56.0	56.0	57.9	59.2
Layer 2 (-85 to -150 cm)							
Weight of the Sand (kg)	2585.60	2585.60	2585.60	2585.60	2585.60	2585.60	2585.60
Height (m)	0.63	0.63	0.63	0.63	0.63	0.63	0.63
Volume (m^3)	1.61	1.61	1.61	1.61	1.61	1.61	1.61
Settlement (cm)	0.00	0.00	0.00	0.00	0.00	0.00	0.00
Dry Density (kg/m^3)	1603.17	1603.17	1603.17	1603.17	1603.17	1603.17	1603.17
Gs	2.65	2.65	2.65	2.65	2.65	2.65	2.65
e	0.65	0.65	0.65	0.65	0.65	0.65	0.65
e max	0.91	0.91	0.91	0.91	0.91	0.91	0.91
e min	0.57	0.57	0.57	0.57	0.57	0.57	0.57
Dr %	75.6	75.6	75.6	75.6	75.6	75.6	75.6

The motion parameters applied in the second test are presented in Table 5.8, which define the input motions and also verify the obtained results in each structural setup.

Table 5.8: Specifications of the applied loads to the container in the second test set.

Second Test Set	Tets Model	Dr (%)	PGA (g)	F (Hz)	Duration (sn)	Received Results	
						Small Diameter Structure	Large Diameter Structure
T2-1	Group Pile Structures with Small and Large Diameter- Super-Structure Freq. 2 Hz	40 % - 45 %	0.2	2	6	✓	✓
T2-2		40 % - 45 %	0.3	2	6	✓	✓
T2-3		45 % - 50 %	0.2	3	6	✓	✓
T2-4		55 % - 60 %	0.3	3	6	✓	✓
T2-5		55 % - 60 %	Tabas	-	-	✓	✓
T2-6		55 % - 60 %	Northridge	-	-	✓	✓
T2-7		55 % - 60 %	LomaP	-	-	✓	✓

The results of the second test set are summarized using accelerometer records to illustrate changes in acceleration and displacement with depth (see Figures 5.25). Values obtained from earthquake records are presented separately (see Figures 5.26). The findings indicate that increasing input frequencies or acceleration values amplify the soil sample's response at the surface.

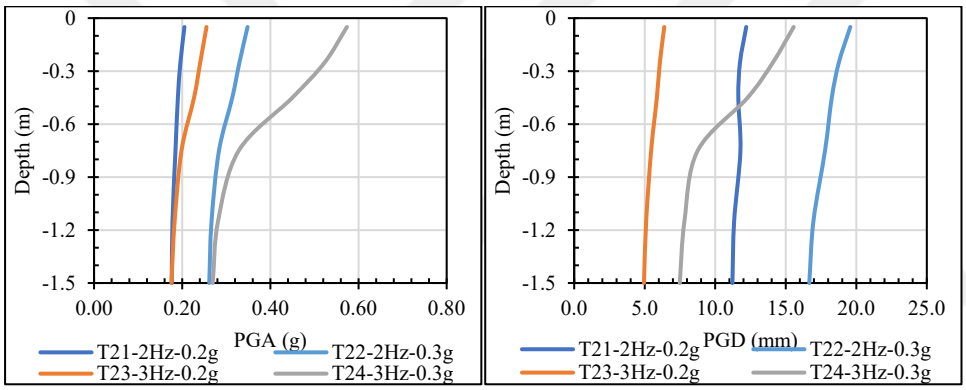

Figure 5.25: The recorded values by the accelerometers located at the center of the container after applying sinusoidal motion for the second test set.

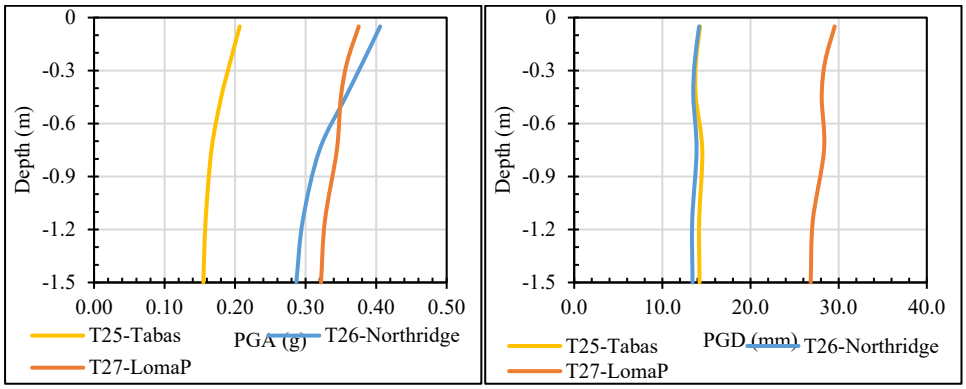

Figure 5.26: The recorded values by the accelerometers located at the center of the container after applying earthquake motion for the second test set.

Since the sole parameter affecting the records is the density of the soil sample in the container, and given that the density did not change after the second test setup, the records are nearly identical for the same input motion across different test cases.

In each test setup, the influence of the structural elements on the sensor records located at the middle of the container is negligible, with only slight variations observed between the values obtained in each setup. The fundamental frequency effect of the SDOF system is studied in test setups 3 and 4. The details of these tests are summarized in Table 5.9, and the results are presented in Figures 5.27 to 5.30. The acceleration values recorded at the cap pile increase in response to the applied motion characteristics and the natural frequency of the SDOF system.

Table 5.9: Specifications of the applied loads to the container in the third and forth test set.

Third Test Set	Tets Model	Dr (%)	PGA (g)	F (Hz)	Duration (sn)	Received Results	
						Small Diameter Structure	Large Diameter Structure
T3-1	Group Pile Structures with Small and Large Diameter- Super-Structure Freq. 2 Hz	60%>	0.2	1	6	✓	✓
T3-2			0.3	1	6	✓	✓
T3-3			0.2	2	6	✓	✓
T3-4			0.3	2	6	✓	✓
T3-5			0.2	3	6	✓	✓
T3-6			0.3	3	6	✓	✓
T3-7			Tabas	-	-	✓	✓
T3-8			Northridge	-	-	✓	✓
T3-9			LomaP	-	-	✓	✓
Forth Test Set	Tets Model	Dr (%)	PGA (g)	F (Hz)	Duration (sn)		
T4-1	Group Pile Structures with Small and Large Diameter- Super-Structure Freq. 1 Hz	60%>	0.2	1	6	✓	✓
T4-2			0.3	1	6	✓	✓
T4-3			0.2	2	6	✓	✓
T4-4			0.3	2	6	✓	✓
T4-5			0.2	3	6	✓	✓
T4-6			0.3	3	6	✓	✓
T4-7			Tabas	-	-	✓	✓
T4-8			Northridge	-	-	✓	✓
T4-9			LomaP	-	-	✓	✓

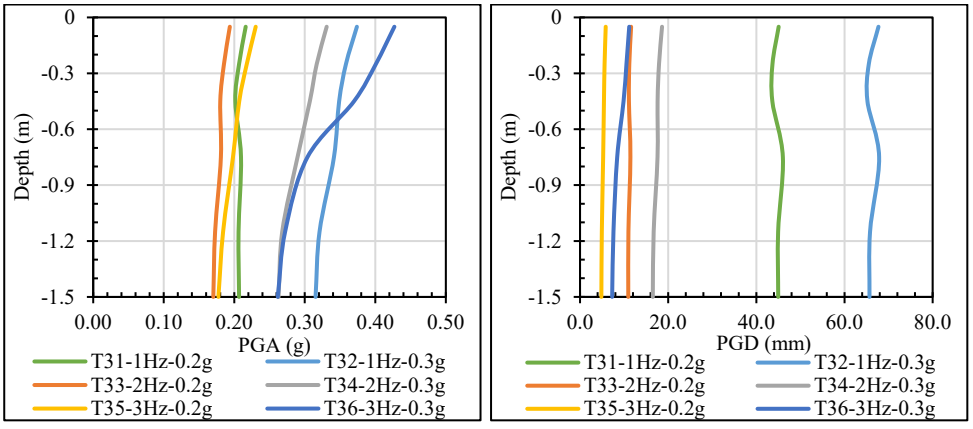

Figure 5.27: The recorded values by the accelerometers located at the center of the container after applying sinusoidal motion for the third test set for the SDOF system with 2Hz frequency.

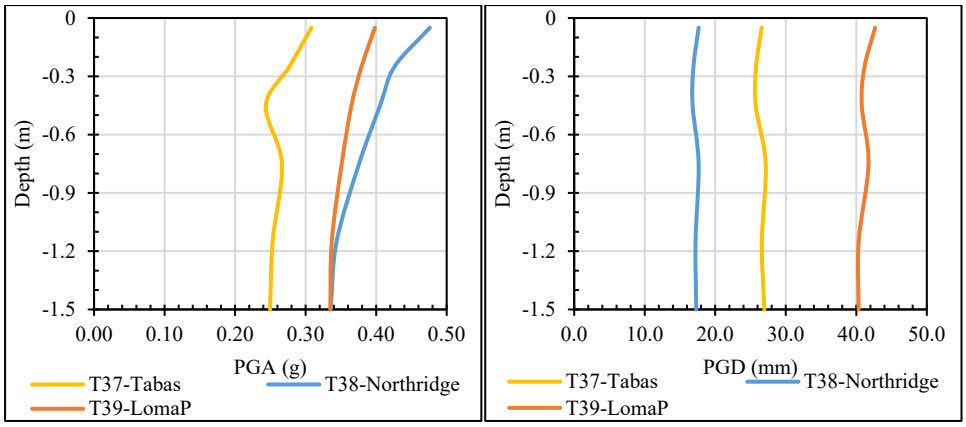

Figure 5.28: The recorded values by the accelerometers located at the center of the container after applying earthquake motion for the third test set for the SDOF system with 2Hz frequency.

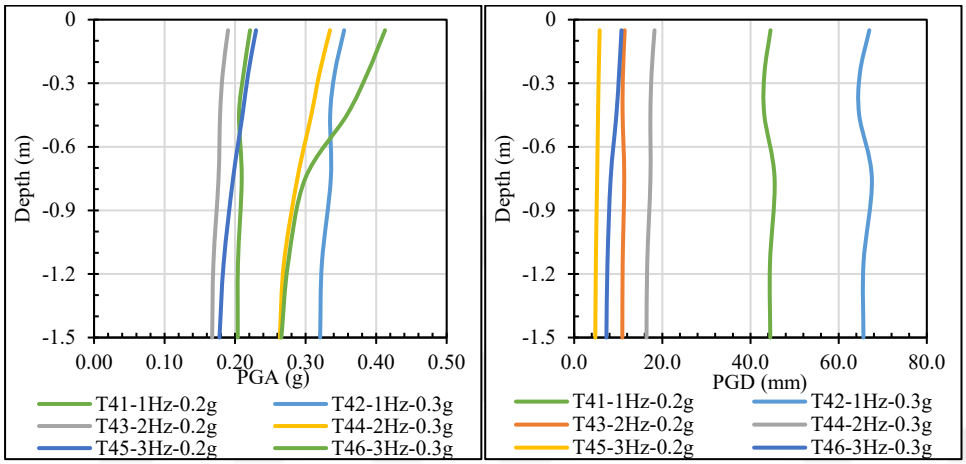

Figure 5.29: The recorded values by the accelerometers located at the center of the container after applying sinusoidal motion for the forth test set for the SDOF system with 1Hz frequency.

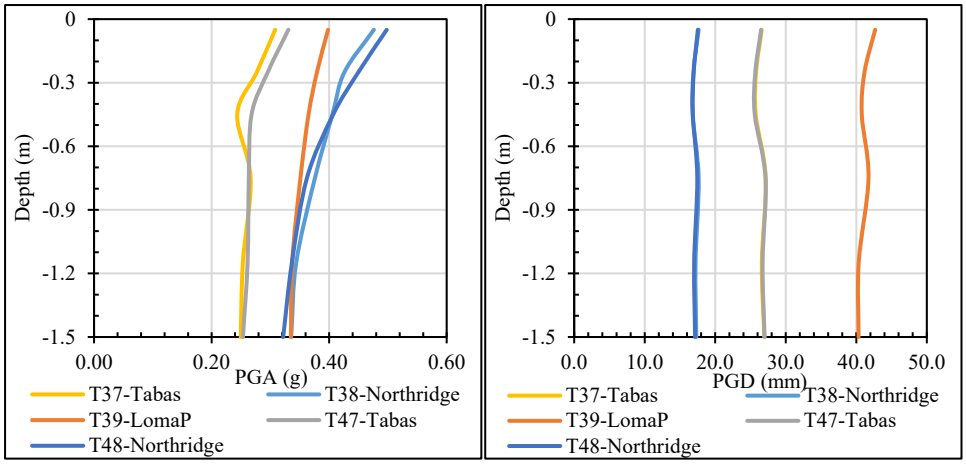

Figure 5.30: The recorded values by the accelerometers located at the center of the container after applying earthquake motion for the forth test set for the SDOF system with 1Hz and 2Hz frequency.

The test conditions selected for the group pile system were also applied to the single pile support system and the SDOF system connected to the cap piles. As mentioned in the sample preparation section, the SDOF system was connected to the single pile

through a single cap pile, and the sensors were attached to the structures as presented in Figure 5.31.

The specifications for each test setup are summarized in Table 5.10. It should be noted that the small diameter pile setup was damaged during testing and did not yield any results for the setup with an SDOF system frequency of 1 Hz. The recorded results obtained from the sensors are summarized in Figures 5.32 to 5.35.

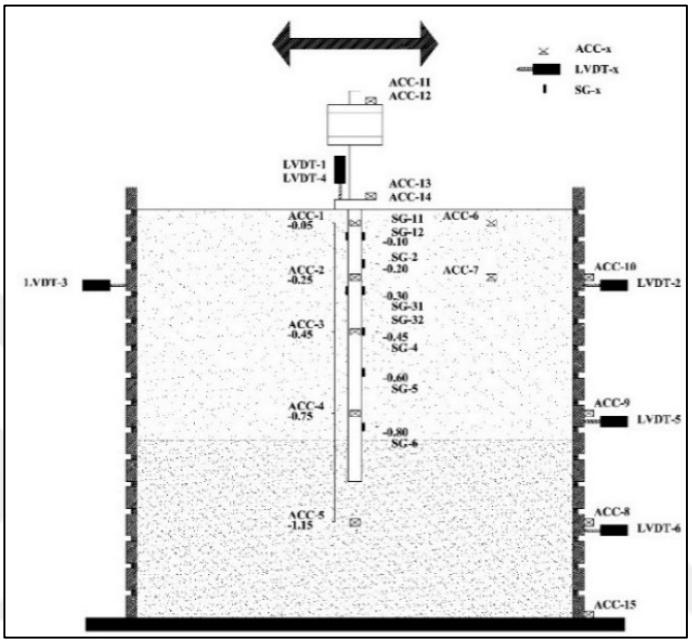

Figure 5.31: Location of the sensores in the test setups including the single pile system.

Table 5.10: Specifications of the applied loads to the container in the fifth and sixth test set.

Fifth Test Set	Tets Model	Dr (%)	PGA (g)	F (Hz)	Duration (sn)	Received Results	
						Small Diameter Structure	Large Diameter Structure
T5-1	Single Pile Structures with Small and Large Diameter- Super-Structure Freq. 2 Hz	60%>	0.2	1	6	✓	✓
T5-2			0.3	1	6	✓	✓
T5-3			0.2	2	6	✓	✓
T5-4			0.3	2	6	✓	✓
T5-5			0.2	3	6	✓	✓
T5-6			0.3	3	6	✓	✓
T5-7			Tabas	-	-	✓	✓
T5-8			Northridge	-	-	✓	✓
T5-9			LomaP	-	-	✓	✓
Sixth Test Set	Tets Model	Dr (%)	PGA (g)	F (Hz)	Duration (sn)		
T6-1	Single Pile Structures with Small and Large Diameter- Super-Structure Freq. 1 Hz	60%>	0.2	1	6	✓	✓
T6-2			0.3	1	6	✓	✓
T6-3			0.2	2	6	✓	✓
T6-4			0.3	2	6	✓	✓
T6-5			0.2	3	6	✓	✓
T6-6			0.3	3	6	×	✓
T6-7			Tabas	-	-	×	✓
T6-8			Northridge	-	-	×	✓
T6-9			LomaP	-	-	×	✓

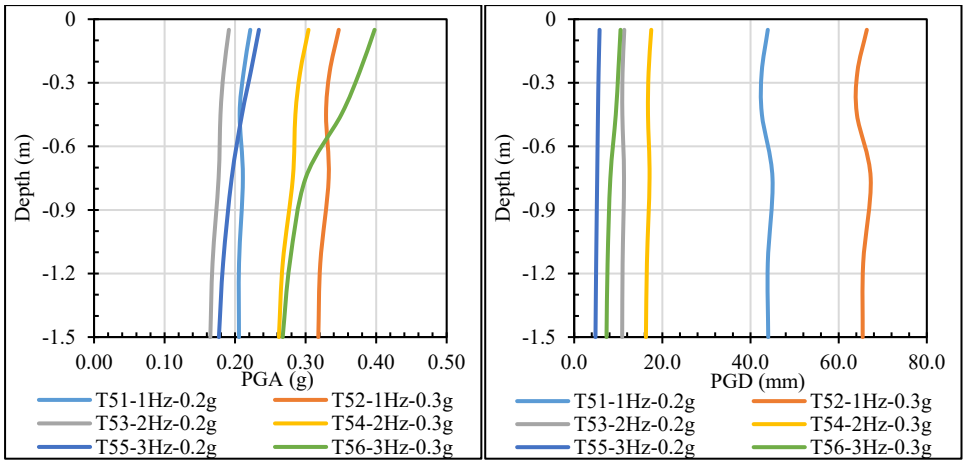

Figure 5.32: The recorded values by the accelerometers located at the center of the container after applying sinusoidal motion for the fifth test set for the SDOF system with 2Hz frequency.

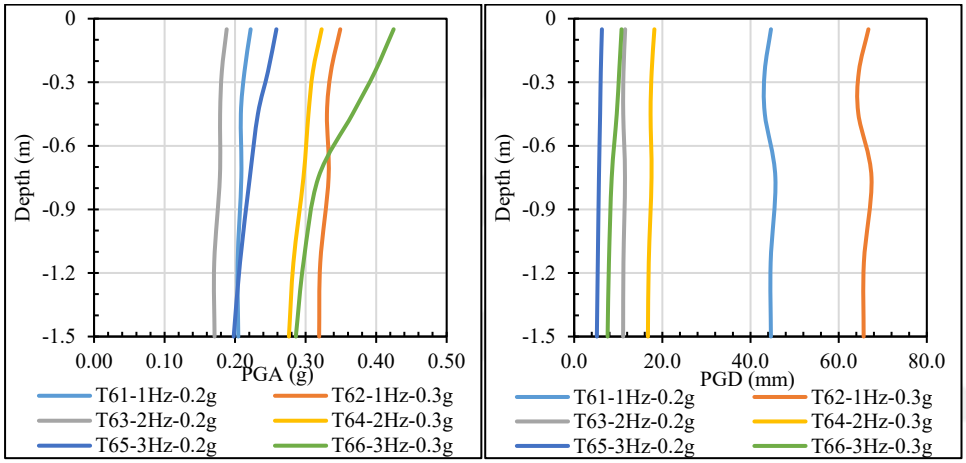

Figure 5.33: The recorded values by the accelerometers located at the center of the container after applying sinusoidal motion for the sixth test set for the SDOF system with 1Hz frequency.

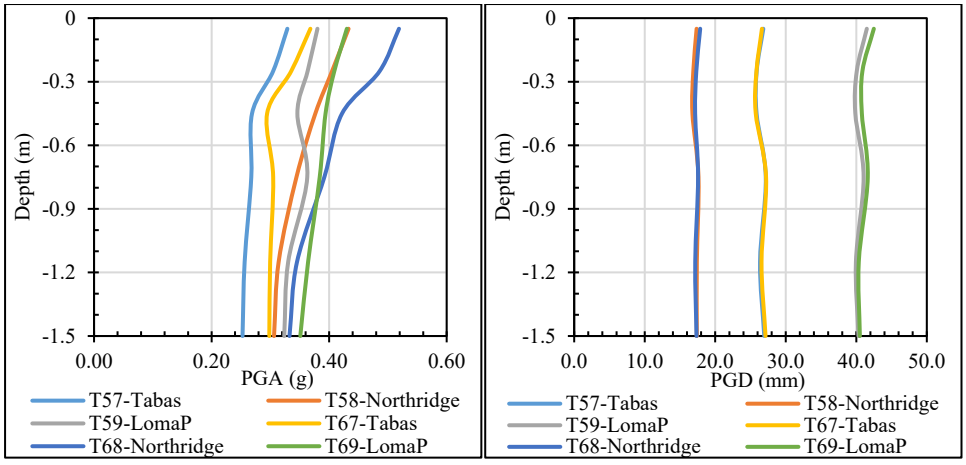

Figure 5.34: The comparison of the recorded values by the accelerometers located at the center of the container after applying earthquake motion for the fifth and sixth test set for the SDOF system with 1Hz and 2Hz frequency.

Figure 5.35 represents the responses obtained for the large diameter pile group and single pile supported systems. It is evident that the applied and transferred motions

were identical across different test setups. However, during the 3rd test series, where the soil was softer compared to the 5th series, greater acceleration amplification of the input motion was observed on the soil surface.

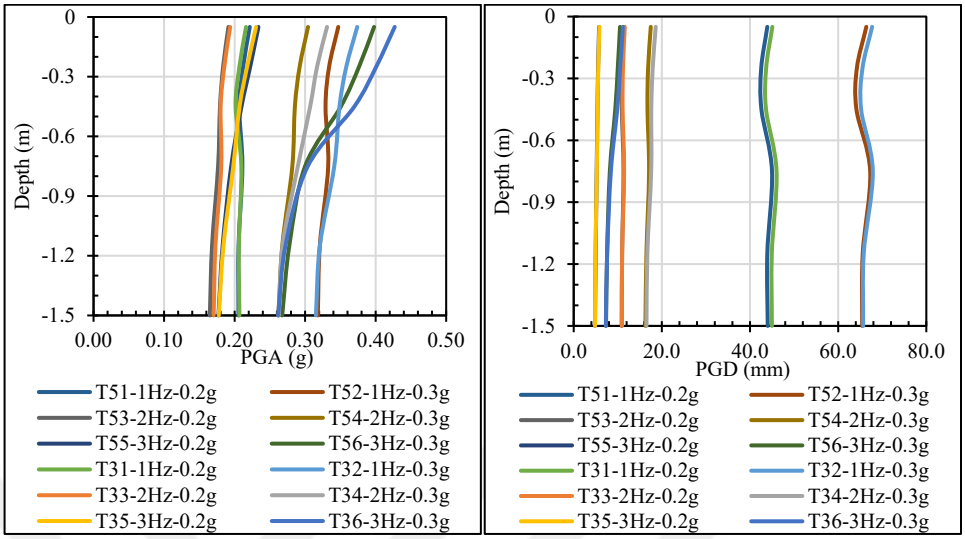

Figure 5.35: The comparison of the recorded values by the accelerometers located at the center of the container after applying sinusoidal motion for the large diameter pile group and single pile for the SDOF system with 2Hz frequency.

5.6 Discussions and Conclusions

1- An Enhance Transparent Impermeable Laminar (ETILam) Soil Container is designed and manufactured based on the laboratory tests and numerical models presented in the previous chapters.

2- The performacne of the ETILam soil container is studied through a series of laboratory tests on the soil sample in the laminar soil container and some portion of the resulting performance is presented.

3- A test setup is designed and manufactured to represent pile supported SDOF system as prototype conditions.

4- A series of laboratory test setups are prepared to study the performance of pile supported SDOF system and soil structure interaction (SSI) and some of the results are presented.

6. COMPARISON OF THE NUMERICAL MODEL RESULTS WITH THE LABORATORY TEST RESULTS

6.1 Comparing the Numerical Results with the EITLam Soil Container Test in Empty Condition

The results from laboratory tests conducted on the empty box under sinusoidal loading were previously presented. Now, to validate the model generated in FLAC3D, the results from the numerical model are compared with those obtained from the laboratory tests.

The responses of the laboratory test were recorded on the lamina located 1.2 meters from the base of the container. The comparison between the input motion and the received motion at the top of the container is presented in Figure 6.1(A). The response of the numerical model at corresponding points is shown in Figure 6.1(B). It can be concluded that the numerical model closely replicates the response of the laminar container itself, with nearly identical recorded responses observed at the top of the container.

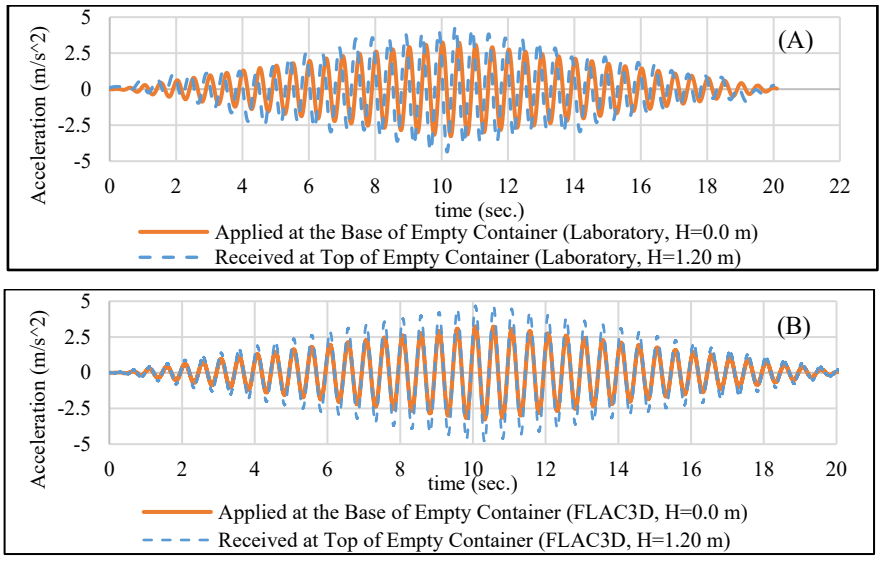

Figure 6.1: Performance of the laminar soil container on shaking table under dynamic loading through (A) laboratory test (B) numerical modelling.

6.2 Comparison of the Numerical Results with the EITLSC Test for Free Field Tests

To compare the results of the laboratory tests with the numerical model, analyses were conducted using dynamic loads with identical acceleration and frequency contents as those applied to the soil container during laboratory tests. The model performance closely matched the laboratory results only at an acceleration of 0.177g and a frequency of 2 Hz, as illustrated in Figure 6.2.

The divergence between the numerical model's response and the expected laboratory test results with increasing acceleration and frequency content of the motion could stem from several factors. These include the use of a Mohr-Coulomb soil model in the numerical analysis, which exhibits damping effects when the model undergoes plastic behavior under significant deformations. Another factor could be the influence of hysteresis damping in the model, particularly its higher damping ratios at greater strain levels. Adjustments to the soil model, including soil parameters and damping values, may be necessary to explore variations in the model's performance. However, verifying the soil model and conducting analytical studies on the behavior of numerical soil models lie beyond the scope of this dissertation. Therefore, only comparisons with laboratory results are presented for similar numerical cases.

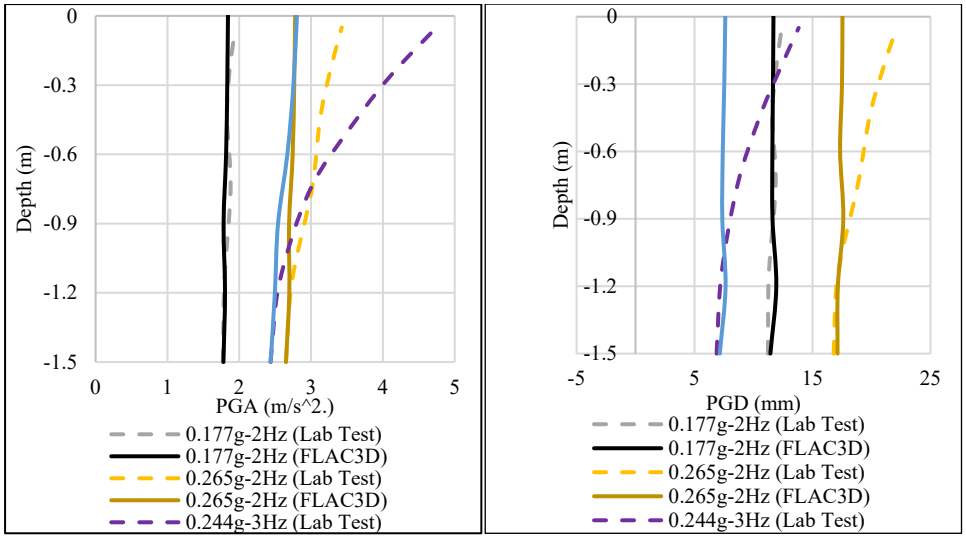

Figure 6.2: Comparison between the results of laboratory tests and numerical modeling (FLAC3D).

Given the discrepancies in the FLAC3D numerical model's response under high acceleration and frequency inputs, a comparative evaluation of the soil layer was conducted using DEEPSOIL software. The analysis in DEEPSOIL revealed that employing the equivalent linear analysis method yielded results similar to those

obtained from the FLAC3D model. However, selecting the non-linear non-masing analysis method in DEEPSOIL resulted in a response closer to the laboratory test results. The comparative responses from these analyses are illustrated in Figure 6.3.

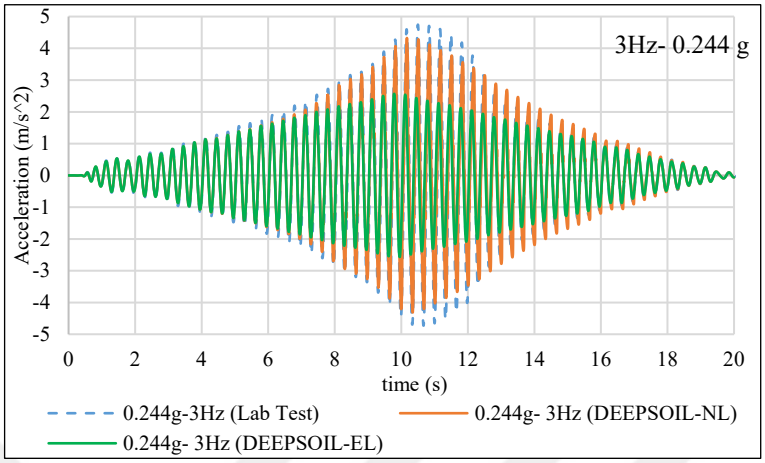

Figure 6.3: Comparison between the results of laboratory tests and numerical modeling (DEEPSOIL).

6.3 Discussions and Conclusions

1- The performance of the ETILam Soil Container in the empty condition was compared with the numerical model results and it was found that the numerical model results resemble the laboratory test result.

2- The results obtained from the laboratory tests are compared with the numerical model results for the case where soil is tested in the ETILam Soil Container and it was found that by increasing the input motion frequency and acceleration, the numerical model does not represent the laboratory test results and it will require more detailed analytical studies on the soil models in the software.

3- The laboratory tests results are compared with the DEEPSOIL model which shows proper resemblance to the nonlinear non masing analysis method.

7. DISCUSSIONS AND CONCLUSIONS

The presented study presented a new method for evaluation of laboratory soil tests with the purpose of designing an enhanced transparent impermeable laminar (ETILam) soil container. Through this study a comprehensive review was carried out on the soil test setups and multiple types of laminar soil containers were studied. Based on the details of available containers in the literature, a new mechanism of movement for the laminar soil container was developed and new concept of design process was proposed. The efforts resulted in the manufacturing of the ETILam soil container.

The process of the study provide multiple outcomes which are summarized as the following key notes:

1- The key aspects and essential characteristics for laboratory tests setups and the effect of soil container boundary condition on the performance of the test setup were studied.

2- Different types of soil containers and their specifications are studied and the laminar soil containers are selected as the best performing type of containers for the laboratory test setups.

3- Effective limitations which should be considered during the design of a laminar soil container were evaluated and the initial design concept was developed.

4- Based on the initial design concept of the laminar soil container, the potential materials were tested through laboratory tests and their characteristic parameters were evaluated to be used through numerical modelling steps. The selected materials for the laminar soil container were Plexiglas and flexible sealant paste named Sikaflex Pro3.

5- The performance of the lamina frame under the maximum stresses induced during dynamic loadings is verified using structural software, and the locations of lateral support points are determined.

6- In order to prepare the required soil sample with the proper relative density a new method was developed for evaluating the relative density of the soil based on the

diameter of the sieve opening and height of the raining. The results of this study let to designing a new sand pluviation mechanism.

7- Through numerical modelling the effect of boundary type and expansion was studied on the soil sample and based on the results obtained from applying different sinusoidal motions to the model, the proper motion was selected for the purpose of numerical evaluations of the laminar soil container design.

8- Based on the reviews on the available containers and their mechanism of movement, different numerical models were developed and the performance of them were compared with the free field tests responses. The enhanced mechanism of movement was developed to provide more resembling response to the free field condition. This mechanism uses roller bearing and flexible sealant mechanism of movement between the laminas.

9- The effect of lateral support system on the behavior of laminar soil container is studied and it was found that the vertical support in addition to lateral support will provide better response of the laminar soil container.

10- Expected performance of the laminar soil container during laboratory was studied based on the generated model. The soil structure interaction performance was evaluated and the effect of SDOF system on the soil performance was studied.

11- Design procedure through numerical modelling resulted in design and manufacturing of the Enhance Transparent Impermeable Laminar (ETILam) Soil Container. The performance of the ETILam soil container is evaluated through tests on the empty container on shaking table and with soil samples during multiple tests.

12- For studying the soil structure interaction (SSI) effect a test setup is designed and manufactured to represent pile supported SDOF system as prototype conditions. A series of laboratory test are performed on pile supported SDOF system and some of the results are presented.

13- The performance of the ETILam Soil Container in the empty condition was compared with the numerical model results and it was found that the numerical model results resemble the laboratory test result.

14- The results obtained from the laboratory tests on the soil sample inside the container are compared with the numerical model results and it was found that by

increasing the input motion frequency and acceleration, the numerical model does not represent the laboratory test results and it will require more detailed analytical studies on the soil models in the software.

REFERENCES

Alaie, R., Chenari, R. J. (2018), Design and performance of a single axis shake table and a laminar soil container. *Civil Engineering Journal, 4, no. 6, 1326-1337.*

Anastasopoulos, I., Georgarakos, T., Drosos, V., Giannakos, S., Gazetas, G. (2009), Towards a reversal of seismic capacity design: Part B, Shaking-table testing of bridge pier-foundation system. *Paper presented at 3rd Greece-Japan Workshop on Seismic Design, Observation, and Retrofit of Foundations, Santorini: National Technical University of Greece.*

Bandini, V., Cascone, E., Biondi, G., Di Filippo, G., Ingegneri, S., Casablanca, O., Genovese, F. (2019), The shaking table with laminar box of the University of Messina. *Paper presented at 7th ICEGE International Conference on Earthquake Geotechnical Engineering.*

Bhattacharya, S., Lombardi, D., Dihoru, L., Dietz, M.S., Crew, A.J., Taylor, C.A., (2012). Model container design for soil-structure interaction studies, *Role of Seismic Testing Facilities in Performance-Based Earthquake Engineering", SERIES Workshop, Geotechnical, Geological and Earthquake Engineering, vol. 22, Springer Science & Business Media*, *Chapter 8, 135-158.* DOI 10.1007/978-94-007-1977-4_8.

Brennan, A. J., Madabhushi, S. P. G. (2002). Design and performance of a new deep model container for dynamic centrifuge testing. *Paper presented at International Conference on Physical Modelling in Geotechnics, Balkema,* Rotterdam, The Netherlands, St Johns NF, Canada, 2002.

Brennan, A. J., Madabhushi, S. P. G., & Houghton, N. E. (2006) Comparing laminar and equivalent shear beam (ESB) containers for dynamic centrifuge modelling. *Paper presented at 6th International Conference on Physical Modelling in Geotechnics, vol. 6*.

Campbell, D.J., Cheney, J.A., Kutter, B.L. (1991)**.** Boundary effects in dynamic centrifuge model tests. *Paper presented at International Conference Centrifuge 1991*, Boulder, Colorado.

Cengiz, C., Guler, E. (2017), Design of a novel laminar box for evaluating the seismic performance of soils. *Paper presented at 6th International Young Geotechnical Engineers' Conference*.

Cengiz, C., Guler, E. (2018). Shaking table tests on geosynthetic encased columns in soft clay. *Geotextiles and Geomembranes, 46, no. 6, 748-758.*

Cengiz, C., Guler, E. (2020). A laminar box apparatus for 1 g testing of granular columns embedded in soft clay. *International Journal of Physical Modelling in Geotechnics, 20, no.1, 38-54.*

Chau, K. T., C. Y. Shen, and X. Guo. (2008). Nonlinear seismic soil–pile–structure interactions: shaking table tests and FEM analyses. *Soil Dynamics and Earthquake Engineering, 29, 300-310. https://doi.org/10.1016/j.soildyn.2008.02.004.*

Chunxia, H., Hongru, Z., Guoxing, C., Zhilong, S. (2008). Design and performance of a large-scale soil laminar shear box in shaking table test. *Paper presented at 14th World Conference on Earthquake Engineering*.

Coelho, P. A. L. F., Haigh, S. K., Madabhushi, S. G. (2003). Boundary effects in dynamic centrifuge modelling of liquefaction in sand deposits. *Paper presented at the 16th ASCE Engineering Mechanics Conference,* University of Washington, Seattle, USA, July.

Ecemis, N. (2013). Simulation of seismic liquefaction: 1-g model testing system and shaking table tests. *European journal of environmental and civil engineering, 17, no. 10, 899-919.*

Eseller-Bayat, E., Nateghi, A., Viand, A. S., Jadidoleslam, M. (2016). Numerical modelling of liquefaction tests of fully saturated sands in CSSLB. *Paper presented at 4th International Conference on New Developments in Soil Mechanics and Geotechnical Engineering,* Near East University, Nicosia, North Cyprus.

Fardis, M. N., Rakicevic, Z. T. (Eds.). (2011). Role of Seismic Testing Facilities in Performance-Based Earthquake Engineering, *SERIES Workshop, Geotechnical, Geological and Earthquake Engineering, vol. 22, Springer Science & Business Media, Chapter 8, 135-158.* DOI 10.1007/978-94-007-1977-4_8.

Funahara, H., Fujii, S. Tamura, S. (2000). Numerical Simulation of Pile Failure in Liquefied Soil Observed in Large-scale Shaking Table Test, *Paper presented at 12th World Conference on Earthquake Engineering,* Auckland, New Zealand, Reference No. 927.

Goit, C. S., Saitoh, M., Mylonakis, G. (2013). Applicability of principle of superposition in obtaining horizontal impedance functions of pile groups under soil nonlinearity. *Paper presented at 4th International Conference on Computational Methods in Structural Dynamics and Earthquake Engineering, COMPDYN*, National Technical University of Athens, January.

Goit, C. S., Saitoh, M. (2014). Model tests on horizontal impedance functions of fixed-head inclined pile groups under soil nonlinearity. *Journal of Geotechnical and Geoenvironmental Engineering, 140, no. 6.*

Hushmand, B., Scott, R. F., Crouse, C. B. (1988). Centrifuge liquefaction tests in a laminar box. *Geotechnique, 38, no. 2, 253-262.*

Itasca Consulting Group, Inc. (2019), *FLAC3D - Fast Lagrangian Analysis of Continua in Three-Dimensions, Ver. 7.0. Minneapolis: Itasca.*

Jurabchian, A., (2003). Design and Construction of a Laminar Box for 1g Shaking Table Test. *Master's thesis*, Sharif University of Technology.

Kahraman, I. (2013). Seismic liquefaction: 1-G model testing system and shake table tests. *Master's thesis,* İzmir Institute of Technology.

Kokusho, T., Iwatate, T. (1979). Scaled model tests and numerical analyses on nonlinear dynamic response of soft grounds. *Paper presented at Proceedings of the Japan Society of Civil Engineers, vol. 1979, no. 285, May*.

Kramer, S.L. (1996). Geotechnical Earthquake Engineering. *Prentice Hall, Upper Saddle River.*

Lee S., Choo Y., Kim D. (2011). Performance evaluation of equivalent shear beam (ESB) model container for dynamic geotechnical centrifuge tests. *Soil Dynamics and Earthquake Engineering, 44, 2013, 102–114.*

Lei, H., Hu, Y., Han, Q., Zheng, G., Zhao, B., Du, Y. (2020). Design and test verification of a cylindrical 3D laminar shear soil container for use on shaking tables. *Soil Dynamics and Earthquake Engineering, 139.*

Madabhushi S.P.G., Butler G., Schofield A.N., (1998). Design of an equivalent shear beam (ESB) container for use on the US Army centrifuge, *Centrifuge 98, Balkema, 117-122.*

Meymand, P. J. (1998). Shaking table scale model tests of nonlinear soil-pile-superstructure interaction in soft clay. *PhD dissertation*., University of California, Berkeley.

Meymand, P., Reimer, M., Seed, R. (2000). Large scale shaking table tests of seismic soil-pile interaction in soft clay. *Paper presented at 12th World Conference of Earthquake Engineering, New Zealand, 5, no. 0915, January*.

Mohsan, M., Kiyota, T., Munoz, H., Nihaaj, M., Katagiri, T. (2018). *Fabrication and Performance of Laminar Soil Box with Rigid Soil Box for Liquefaction Study. Bulletin of ERS, no. 51*

Pamuk, A., Gallagher, P. M., Zimmie, T. F. (2007). Remediation of piled foundations against lateral spreading by passive site stabilization technique. *Soil Dynamics and Earthquake Engineering, 27, no.9, 864-874.*

Paolucci, R., Shirato, M., Yilmaz, M. T. (2007). Seismic behaviour of shallow foundations: Shaking table experiments vs numerical modelling. *Earthquake Engineering & Structural Dynamics, 37, no.4, 577-595.*

Prasad, S. K.,(1996) Evaluation of deformation characteristics of 1-G model ground during shaking using a laminar box, *Doctoral thesis*, University of Tokyo, Japan.

Prasad, S. K., Towhata, I., Chandradhara, G. P., Nanjundaswamy, P. (2004). Shaking table tests in earthquake geotechnical engineering. *Current science, 1398-1404.*

Qin, X., Cheung, W. M., Chouw, N., Larkin, T., Ching, S. W. C. (2013). Study of soil-structure interaction effect on ground movement using a laminar box. *Paper presented at New Zealand Society for Earthquake Engineering Conference, April*.

Shirato, M., Kouno, T., Asai, R., Nakatani, S., Fukui, J., Paolucci, R. (2008). Large-scale experiments on nonlinear behavior of shallow foundations subjected to strong earthquakes. *Soils and foundations, 48, no. 5, 673-692.*

Suzuki, H., Tokimatsu, K., Sato, M., Abe, A. (2006). Factor affecting horizontal subgrade reaction of piles during soil liquefaction and lateral spreading. *Paper presented at Workshop on Seismic performance and simulation of pile foundations in liquefied and laterally spreading ground.*

Suzuki, H., Tokimatsu, K., Sato, M., Tabata, K. (2008) Soil-pile-structure interaction in liquefiable ground through multi-dimensional shaking table tests using e-defense facility. *Paper presented at the 14th World Conference on Earthquake Engineering,* Beijing, China, October.

Tabata, K., Sato, M. (2018). Cyclic Behavior at Small Shear Deformations of Non-Liquefiable Sand Ground Obtained from Horizontal 1-D and 2-D E-Defense Tests. *Paper presented at Geotechnical Earthquake Engineering and Soil Dynamics V: Slope Stability and Landslides, Laboratory Testing, and In Situ Testing (pp. 160-170).* Austin, Texas, June 10–13.

Tabata, K., Sato, M. (2010). E-Defense shaking table test on the behavior of liquefaction-induced lateral spreading of large-scale model ground with a pile-foundation structure behind quay wall. *Paper presented at 5th International Conference on Recent Advances in Geotechnical Earthquake Engineering and Soil Dynamics.* San Diego, California, May 24-29.

Tabatabaiefar, S. H. R., Fatahi, B., Samali, B. (2014). Numerical and experimental investigations on seismic response of building frames under influence of soil-structure interaction. *Advances in structural Engineering, 17, no. 1, 109-130.*

Tabatabaiefar, H. R. (2016). Detail design and construction procedure of laminar soil containers for experimental shaking table tests. *International Journal of Geotechnical Engineering, 10, no. 4, 328-336.*

Takahashi, A., Takemura, J., Suzuki, A., Kusakabe, O. (2001). Development and performance of an active type shear box in a centrifuge. *International Journal of Physical Modelling in Geotechnics, 1, no. 2, 1-17.*

Takahashi, A. (2002), Soil pile interaction in liquefaction induced lateral spreading of soils. *PhD diss.,* Tokyo Institute of Technology.

Thevanayagam, S., Kanagalingam, T., Reinhorn, A., Tharmendhira, R., Dobry, R., Abdoun, T., El Shamy, U. (2009). Laminar box system for 1-g physical modeling of liquefaction and lateral spreading. *Geotechnical Testing Journal, 32, no. 5.*

Tokimatsu, K., Suzuki, H. (2004). Porewater pressure response around pile and its effects on py behavior during soil liquefaction. *Soils and Foundations, 44, no. 6, 101-110.*

Turan, A., Hinchberger, S. D., El Naggar, H. (2008). Design and commissioning of a laminar soil container for use on small shaking tables. *Soil Dynamics and Earthquake Engineering, 29, no. 2, 404-414.*

Turan, A., Hinchberger, S. D., El Naggar, M. H. (2013). Seismic soil–structure interaction in buildings on stiff clay with embedded basement stories. *Canadian Geotechnical Journal, 50, no. 8, 858-873.*

Ueng, Tzou-Shin, Wang, Ming-Huei, and Ming-Horng Chen. (2000). Large biaxial shear box on shaking table. *Paper presented at ISRM (International Society for Rock Mechanics) International Symposium,* Melbourne, Australia, November.

Ueng, T. S., Chen, M. H., Wang, M. H., and Ho, W. C. (2001). Large-scale shear box soil liquefaction tests on shaking table (I)—Development of the large biaxial shear box. *Report No. NCREE-01-011,* National Center for Research on Earthquake Engineering, Taiwan.

Ueng, T. S., Chen, M. H., Wang, M. H. (2002). A Two-dimensional large-scale shear box on shaking Table. *Paper presented at International Conference on Physical Modelling in Geotechnics*, St. John, Newfoundland, Canada. 10-12 July.

Ueng, T. S., Chen, C. H., Peng, L. H., and Li, W. C. (2003), Large-scale shear box soil liquefaction tests on shaking table (II)—Preparation of large sand specimen and preliminary shaking table tests. *Report No. NCREE-03-042,* National Center for Research on Earthquake Engineering, Taiwan.

Ueng, T. S., Wang, M. H., Chen, M. H., Chen, C. H., Peng, L. H. (2006). A large biaxial shear box for shaking table test on saturated sand. *Geotechnical Testing Journal, 29, no. 1, 1-8.*

Ueng, T. S. (2006). Inference of behavior of saturated sandy soils during earthquakes from laboratory experiments. *Journal of GeoEngineering, 1, no. 1, 1-9.*

Van Laak, P. A., Taboada, V. M., Dobry, R., Elgamal, A. W. (1994). Earthquake centrifuge modeling using a laminar box. *Dynamic Geotechnical Testing II. ASTM International.*

Yang, H. J., Elfass, S., Norris, G. (2010). Settlement behavior of a shallow foundation in dry sand under simulated earthquake motion on a biaxial shake table. *Paper presented at GeoFlorida 2010: Advances in Analysis, Modeling & Design,* February.

Yoo, M.T., Han, J. T., Choi, J. I., Kwon, S.Y., (2017). Development of dynamic pile behavior predicting method considering kinematic load effect by centrifuge tests. *Bull Earthquake Eng., Vol 15 Issue 3, 967-989*

Yoo, M.T., Choi, J. I., Han, J. T., Kim, M.M., (2013). Dynamic p-y curves for dry sand from centrifuge tests. *Journal of Earthquake Engineering., Vol 17 No.7, 1082-1102*

Zayed, M., Luo, L., Kim, K., McCartney, J. S., Elgamal, A. (2017). Development and performance of a laminar container for seismic centrifuge modeling. *Paper presented at Third International Conference on Performance-Based Design in Earthquake Geotechnical Engineering (PBD-III),* Vancouver, Canada, July.

Zeng, X., Schofield, A. N. (1996). Design and performance of an equivalent-shear-beam container for earthquake centrifuge modelling. *Geotechnique, 46, no. 1, 83-102.*

APPENDICES

APPENDIX A: Table A1

APPENDIX A

Table A. 1: Laminar soil containers published in literature and their specifications

Reference	Dimensions, L x W x H, mm3	Dimension of Motion and Test Type	Ranges of Applied Frequency or Period and Acceleration or Displacement	Soil Type	Applied Tests	Design Specifications	Key Notes and Results Regarding the Performance of Laminar Container
Kokusho T. and Iwatate T. 1979 Central Research Institute of Electric Power Industry	1200x500x1005	1-D, 1-G	8~25 Hz, 1.44~0.72 s, 0.215 g or 406 gal	sand	nonlinear dynamic response of the soil	1- Rectangular shape 2- Roller bearings between the laminas 3- Use of 1 mm thickness membrane	-
Hushmand et al. 1988 California Institute of Technology	356x 178x 256	1-D, N-G	-	sand	liquefaction phenomenon	1- Rectangular shape 2- Roller bearings between the laminas	1- Bearings reduced friction coefficient of the plates from about 0·04 (Teflon coated without bearings) to a measured value of 0·013 2- Virtually identical pp at the one-third height at the center of the box 3- Similar settlement in the center and at the side of the top surface in the dry sand 4- Desired one-dimensional response of the laminar box is attained.
Van Laak et al. 1994	457x 254x 254	1-D, N-G	-	dry and saturated sand	verification of one-dimensional response of the soil	1-Rectangular shape 2- Made of 39 rectangular aluminum rings on roller bearings	1- Development of a correction for the influence of lateral inertia of the container on the soil model response
Prasad et al. 1996 S J College of Engineering and Technology	1000x 500x1000	1-D, 1-G	sinusoidal, 2 Hz, 0.4~1.5 g	Toyoura sand	excess pore water pressure, ground amplification, scaling factors, boundary effects	1- Rectangular shape 2- Made of 11 laminas separated by bearing 3- Short length of each lamina is designed in a way that the beam could rotate around its axial axis to represent the deformation of the adjacent soil 4-Use of provision to apply pre-loading to improve the contact between the bearings and the layers and to provide restraint against lateral deflection of long side or upward movement of layers 5- Use of 10 mm thick porous stone at the base as filter and water distributer 6- Use of 2 mm thickness membrane 7- Use of raining method in preparing the model	1- The rotating side, vertical to the movement direction, reduces the boundary effect and provides a pure shear condition for the soil element and eliminates the rocking effect 2- The rectangular shape has the advantage to reduce friction due to longitudinal displacement and lateral buckling possibility 3-Free movement of soil along the transverse cross section 4- Providing a factor to nullify the effect of inertia of the mass of the box 5- An acceleration level of 0.5 g or more is better to cause slip between laminas to efficiently utilize the box 6-If it would be required to achieve very high frequency, higher level of acceleration would be adequate 7- Since the membrane was not attached to the box, it did not have much effect on results

Table A. 1 (continued): Laminar soil containers published in literature and their specifications

Reference	Dimensions, L x W x H, mm3	Dimension of Motion and Test Type	Ranges of Applied Frequency or Period and Acceleration or Displacement	Soil Type	Applied Tests	Design Specifications	Key Notes and Results Regarding the Performance of Laminar Container
Meymand et al. 1998 University of California, Berkeley	2300 (D,H) x2000	2-D, 1-G	Sinusoidal type (sweep wave) and earthquake time histories, 0.05 ~ 1.0 g	kaolinite, bentonite, type C fly ash	soil-pile-superstructure interaction	1- Circular shape 2- Connection of top ring to the base by steel pipes to prevent the overturning of the container 3- A neoprene rubber membrane is hung from the top ring and clamped at the base 4-Woven Kevlar straps are arrayed in circumferential bands around the exterior of the membrane	1- The container provides the desired properties of lateral flexibility in simple shear and radial stiffness 2- Laterally flexible but radially stiff to provide quasi-free field response 3- Providing the laminar box design concepts to allow for multi-directional shaking 4- Free field response of the model was compared with SHAKE 91 results
Funahara et al. 2000 Taisei Research Institute	11600x 3100x 6000	1-D, 1-G	Rinkai wave (maximum acceleration 310 gal)	Kasumigaura sand	pile behaviors in a liquefied soil	1- Rectangular shape 2- Constructed of 29 rectangular frames made of H-shaped steel members (200 mm x 200 mm) 3- Use of 3 mm thick rubber membrane for waterproofing and protecting the rollers from the soil 4- Steel pipes with an outer diameter of 200 mm as rollers and Teflon sheets were placed between each of the container frames	1- Behavior of pile foundation structure in unsaturated sand could be reproduced by a centrifuge test, while considering a large-scale test as a prototype.
Ueng el al. 2000 National Taiwan University	1888x 1888x 1520	2-D, 1-G	sinusoidal 1~8 Hz, 10 sec., 0.03~0.15 g,	Vietnam sand (Ueng el al. 2001, 2002, 2003, 2006)	dynamic response of the soil	1- Rectangular shape 2- Composed of 15 layers of sliding frames 3- A maximum displacement of ±150 mm is allowed for each layer in both X and Y directions 4- Use of 2mm thick silicone rubber membrane to provide a watertight shear box 5- Sample prepared by wet sedimentation method from a large pluviation device	1- The movement of each layer of the frames is independent of other frames 2- Two-dimensional shaking induces higher porewater pressure generation and deeper liquefaction depth than those under the one-dimensional shaking of the same acceleration magnitude 3- The multidirectional shaking causes larger settlements of sand 4- The volumetric strain of the sand after liquefaction decreases with the relative density of the sand while it increases with shaking duration.
Takahashi et al. 2001 Tokyo Institute of Technology	450x 200x 325	1-D, N-G	sinusoidal	dense Toyoura sand	seismic performance of the piles in liquefiable soil (Takahashi, 2002)	1- Rectangular shape with active boundary 2- Consisting of a laminar box and three actuators 3- Made of 13 laminas with aluminum profile 4- Use of roller bearing between laminas 5- The loading rods are connected to three laminas at different levels 6- The displacement between the laminas are transferred by plate springs 7- Use of external columns with rollers, to prevent out of plane displacement 8- Use of roughened sheets by glued sand particles, on the end walls and base of the box to develop shear stress on the boundaries	1- Narrower box would have better performance on testing loose sand 2- Friction between the laminas does not have significant effect on the performance of the box 3- If the difference between the measured and target displacements be normalized by target displacement, smaller values of target displacement creates smaller normalized differences 4- The pile response is very sensitive to the displacement and type of ground motion 5- The box has adequate capability in modelling of intended strain field in the soil 6- The stress is different from free field stress condition

Table A. 1 (continued): Laminar soil containers published in literature and their specifications

Reference	Dimensions, L x W x H, mm3	Dimension of Motion and Test Type	Ranges of Applied Frequency or Period and Acceleration or Displacement	Soil Type	Applied Tests	Design Specifications	Key Notes and Results Regarding the Performance of Laminar Container
Brennan and Madabhushi 2002 University of Cambridge	653x 253x 427	1-D, N-G	0~50 Hz, 4sec. (Coelho, P., 2003)	sand	saturated sample, buried structures (tunnel)	1- Rectangular shape 2-Rubber layers between aluminum rectangular hollow section frames	1- To ensure the Ko conditions, the sides of the container are designed to be stiff 2- Studs are installed through the end walls to increase the safety and in case required to vertically pre-stress the rings 3- Side walls are covered with glass sheets to ensure a frictionless surface. 4- Rough shear sheets are attached to the end walls to provide shear stresses. 4- As the shear stress distribution does not match the required deformation profile, the adjustment of the thickness of rubber layers with depth is desirable.
Jurabchian 2003 Sharif University of Technology	1000x 1000x 1000	1-D, 1-G	-	Toyoura sand	dynamic response of the soil	1- Cubic shape 2- Made of 24 laminas composed of hollow profiles of 40 mmx 40 mmx 2 mm 3- Use of 12 ball bearings in each layer to allow sliding between laminas with the gap of 3 mm 4- Use of Teflon layers to polish the surface of the aluminum profiles 5- Use of base plate under the box with the dimension of 1500 mmx 1500 mmx 2 mm 6- Use of 2 mm membrane inside the box 7- Use of side guides within 15 cm distance from the box	1- Natural frequency of the first mode of the laminar shear box with different densities for small strains, is in the range of 20-35 Hz 2- A coefficient is defined to eliminate the inertia effect by the container walls 3- Use of static pull out test to define the friction coefficient 4- As the density of the model decreases, the need for the flexible container increases
Tokimatsu and Suzuki 2004 National Research Institute for Earth Science and Disaster Prevention (NIED)	12000x3500x 5500	1-D, 1-G	2 Hz, 0.2g	Nikko sand	pile performance in liquefying sand	-	-

Table A. 1 (continued): Laminar soil containers published in literature and their specifications

Reference	Dimensions, L x W x H, mm3	Dimension of Motion and Test Type	Ranges of Applied Frequency or Period and Acceleration or Displacement	Soil Type	Applied Tests	Design Specifications	Key Notes and Results Regarding the Performance of Laminar Container
Pamuk et al. 2007 Columbia University	710x 355x 355	1-D, N-G	2 Hz, 0.25 g	Nevada sand	piled foundations against lateral spreading	1- Rectangular shape 2- Made of 38 rectangular rings of high strength aluminum alloy 3- Use of Teflon sheets for bearing cages that are constructed to maintain proper alignment and spacing 4- Relative displacement of 3.0 mm with respect to adjacent frame providing a total overall shear strain of up to 20%. 5- Model utilizes 23 accelerometers, 8 displacement transducers (LVDT) and 8 pore water pressure transducers (PP)	-
Chau K.T. et al. 2008 The Hong Kong Polytechnic University	1400x 900x 1700	1-D, 1-G	sinusoidal waves, fundamental frequency of the system, 20 ~ 90 sec., 0.02 ~ 0.2 g	poorly graded river sand	soil-pile-structure interaction	1- Rectangular shape 2- Made of 32 laminar rectangular steel frames made of rectangular hollow sections of 50 mmx 50 mmx 2.8 mm 3- To allow sliding, two 1-mm-thick layers of Teflon are glued to the top and bottom of each steel frame section 4- Frictional coefficient between two Teflon surfaces is found equal to 0.126 5- The bottom frame section is welded to a bottom steel plate of 12 mm thickness 6- A 3-D frame with cross bracing is used to limit the maximum translation, providing a reference for displacement measurements 7- Use of electric hammer to compact soil layers of 154 mm in 11 layers	1- The dynamic shear modulus is higher than the static shear modulus due to dynamic condition and also the friction between laminas
Chunxia et al. 2008 Nanjing University of Technology	3000x 1500x 1808	1-D, 1-G	El Centro (0.12g).	sand	investigate the behavior of composite foundation of stone columns	1- Rectangular shape 2- Consists of fifteen rigid rectangular laminar frames (made from welded 100×100×3mm square steel pipe) 3- External support buries the weight of the container by being connected through bearings and transfers the load off the table	1- Laminar box does not impose significant boundary effects and is able to maintain 1-D soil column behavior
Shirato et al. 2008 Public Works Research Institute	4000x 4000x 2100	1-D, 1-G	Sinusoidal type (sweep wave), 50 gal 1995 Kobe, 812 gal	Toyoura sand (Paolucci, 2007)	performance of shallow foundation	1- Cubic shape	-

Table A. 1 (continued): Laminar soil containers published in literature and their specifications

Reference	Dimensions, L x W x H, mm3	Dimension of Motion and Test Type	Ranges of Applied Frequency or Period and Acceleration or Displacement	Soil Type	Applied Tests	Design Specifications	Key Notes and Results Regarding the Performance of Laminar Container
Suzuki et al. 2008 National Research Institute for Earth Science and Disaster Prevention (NIED)	8000(D, H) x6500	2-D, 1-G	0.1 ~ 1.0 s, 0.3 ~ 3.0 m/s^2	dry Albany sand	soil-pile-structure interaction	1- Circular shape 2- Made of 41 stacked ring frames that provide two-dimensional shear deformation	1- Generation of excess pore water pressure (EPWP) and soil pile structure interaction (SPSI) depend on the maximum acceleration and the type of the input motions 2- The bending strain in a pile group, becomes the largest in the leading pile but the smallest in the following pile 3- All the pile heads yield with the largest input acceleration
Turan et al. 2008 The University of Western Ontario	900x 450x 807	2-D, 1-G	0.12 ~ 0.7 g	synthetic clay	performance of the laminar container, dynamic response of the soil (Turan et al. 2013)	1- Rectangular shape 2- Laminas are supported individually by linear bearings and steel guide rods connect them to an external frame 3- To fix the soil layer on shaking table, a 10 mm thick epoxied surface wooden plate, is bolted to shaking table 4- Interior of the container is lined with thin latex sheets 5- Test setup utilizes 7 accelerometers and 1 laser displacement transducer	1- Friction between laminas and membrane effects are uniform along the depth of the container and also, insignificant compared to the shear resistance of the soil 2- The flexible boundaries of the laminar container functions appropriately 3- Comparing the experimental and numerical results, laminar box and soil model performs well in 1-G condition 4- As the mass of the soil is higher than the mass of the table, the frequency of the soil is predominant over the table frequency
Anastasopoulos I. et al. 2009 National Technical University of Athens	1600x 1000x 1000	1-D, 1-G	30 cycle, 1~2 Hz, 0.4 g	Longstone (M34) sand	benefits of soil failure for protecting the superstructure	1- Rectangular shape, Transparent 2- Roller bearings between the laminas 3- 24 octagon-shaped aluminum I-beams, each 0.25 m wide and 0.30 m deep 4- The ratio of ring weight to saturated soil weight in each ring is about 11 % 5-Maximum horizontal sliding of 36 mm relative to the adjacent laminate 6- Maximum shear strain could be 15%	1- Realistic simulation of dynamic soil response 2- Allowing the soil to deform freely 3- Allowing direct observation of deformation as box is transparent on one side 4- Image analysis techniques (such as Particle Image Velocimetry – PIV) are applicable
Thevanayagam et al. 2009 University at Buffalo NEES	5000x 2750x 6200	2-D, 1-G	2 Hz,35 sec., 0.01~0.3 g	Ottawa sand	liquefaction-induced lateral spreading	1- Octagonal shape 2- Made of 24 laminas stacked on top of each other supported by ball bearings 3- Use of hydraulic pumping to fill the container 4- Use of safety cables in 5 different levels to prevent the excess lateral movement of the laminas over 36 mm 5- Use of 1.1 mm rubber membrane inside the container 6- Using sample buckets during the filling of the container to evaluate the in-situ density	1- The laminar box system performed well. 2- Obtaining 30% to 40% of relative density by maintaining 60 cm height of the water over the sand to represent the underwater sedimentation in river beds, harbors and lakes 3- The system properly transfers the applied motion to the container in the shaking direction 4- During the tests, excess lateral spreading of the soil and container damaged the instrumentations

Table A. 1 (continued): Laminar soil containers published in literature and their specifications

Reference	Dimensions, L x W x H, mm3	Dimension of Motion and Test Type	Ranges of Applied Frequency or Period and Acceleration or Displacement	Soil Type	Applied Tests	Design Specifications	Key Notes and Results Regarding the Performance of Laminar Container
						7- Use of cone penetration test to verify the uniformity of the filling 8- Tests utilize more than 400 sensors including; 48 accelerometers, 21 displacement transducers (LVDT), 20 pore water pressure transducers (PP) and 4 digital cameras	5- 40% of vertical settlement occurs during the shaking and the rest during the pore water pressure dissipation
Tabata et al. 2010 National Research Institute for Earth Science and Disaster Prevention (NIED)	16000x 4000x 5000	2-D, 1-G	30 sec, 5.69 m/s^2	Albany silica sand	pile foundation and liquefaction phenomenon	1- Rectangular shape 2- 836 sensors monitor the behavior and the three-dimensional displacement 3- Digital video cameras observe the large displacements	1- The overturning is mainly caused by pile inertial force and not by the influence of backfill ground deformation
Yang et al. 2010 University of Nevada, Reno	3048x 3048x 1829	1-D, 1-G	1 Hz, 0.1~0.5 g	Ione utility sand	settlement of shallow foundation	1- Rectangular shape 2- Rubber layers between aluminum frames	1- Large box can diminish boundary effects and provide space for shallow foundation to extend the passive zone 2- Design of the box provides certain level of lateral flexibility and avoids the external pressure 3- Input motion and the real achieved one on shaking table are not identical both in acceleration values and wave shape 4- Homogeneous quality of the model has significant effect on the different settlement under the shallow foundation
Lee S. et al. (2011) Korea Institute of Nuclear Safety (KINS)	490x 490x 630	1-D, N-G	0.054~0.375 g	Silica sand	dynamic response of the soil, pile behaviour (Min-Taek Yoo, et al., 2013,2017)	1- Rectangular shape 2- Made of 10 aluminum alloy laminas with a 60 mm height, stacked on top of each other supported by ball bearings 3- Rubber layers of 3 mm between aluminum frames 4- Sand Paper is used on the end wall to provide friction to the adjacent soil.	1- The design intends to match the deflection of each frame with the soil column at the middle 2- The rubber layers seal the container boundary and support the shearing behaviour of the frames and soil 3- The shear sheets on the end wall reduce the rubber layer discontinuous deflection

Table A. 1 (continued): Laminar soil containers published in literature and their specifications

Reference	Dimensions, L x W x H, mm3	Dimension of Motion and Test Type	Ranges of Applied Frequency or Period and Acceleration or Displacement	Soil Type	Applied Tests	Design Specifications	Key Notes and Results Regarding the Performance of Laminar Container
Goit et al. 2013 Saitama University	1200x 800x 1000	1-D, 1-G	9 ~ 35 Hz, 0.2~2.0 m/s^2	Gifu sand	pile-to-pile horizontal interaction factors and impedance functions	1- Rectangular shape 2- Roller bearings between the laminas	1- Local nonlinearity and resonant behavior of soil have a significant impact on both the interaction factors and the impedance functions 2- Principle of superposition is applicable under nonlinear conditions
Nurhan Ecemis 2013 Izmir Institute of Technology	1600x 380x 1500	1-D, 1-G	2 Hz, 12 sec, 0.05~0.56 g	sand	liquefaction phenomenon (Kahraman, I., 2013)	1- Rectangular shape 2- Roller bearings between the laminas	1- Static pull out test of the empty container shows that the friction between the rollers and the laminates are small (free field condition) 2- Soil sample is prepared by the hydraulic filling method (creating loose sand prone to liquefaction) 3- A good agreement is achieved between the computed and measured settlements 4- In contrast to the acceleration time, the computed excess pore pressures are in a good agreement with the measured values 5- Measurements and computed results show that the liquefaction at each test occurs more or less at the same time throughout the depth
Qin et al. 2013 The University of Auckland	800x 800x 300	1-D, 1-G	ground motion is based on the Japanese design spectrum for hard soil condition	dry sand	effect of soil structure interaction on horizontal displacement	1- Cubic shape, Transparent 2- Two transparent plexiglasses were installed as the longitudinal faces of the box	1- Vertical propagation of horizontal shear waves from the bedrock to the surface of the soil can be simulated 2- Peak acceleration increases when the wave propagates to the surface of soil 3- Soil structure interaction effect can reduce the excitation at the interface between the structure and soil 4- Soil response is smaller than what happens in the free-field site

Table A. 1 (continued): Laminar soil containers published in literature and their specifications

Reference	Dimensions, L x W x H, mm3	Dimension of Motion and Test Type	Ranges of Applied Frequency or Period and Acceleration or Displacement	Soil Type	Applied Tests	Design Specifications	Key Notes and Results Regarding the Performance of Laminar Container
Tabatabaiefar et al. 2014 University of Technology Sydney	2100 x 1300x 1100	1-D, 1-G	30~56.5 s, 0.229~0.843g	synthetic clay mixture	response of building frames under influence of soil structure interaction	1- Rectangular shape 2- Rubber layers between aluminum rectangular hollow section frames 3- Use of aluminum hollow profiles to build the lamina frames 4- Use of absorbing layers of Polystyrene foam sheets on end walls of the soil container to simulate viscous boundaries in the free field condition 5- Attaching gravelly soil particles to the bottom of the soil container to provide friction between the timber base plate, as the bedrock, and the in-situ soil, preventing the soil to slip over base plate	1- Defining the fundamental natural frequency of the container by applying Sine Sweep tests 2- Satisfying Taylor's conditions (Taylor, 1997)
Cengiz and Güler 2017 University of Bristol	900x 900x 1932	1-D, 1-G	0.5~5 Hz, 35,40 s, 0.0735~0.82 g	Kaolinite clay	geosynthetic encased columns	1- Rectangular shape 2- Use of guide rods through sigma profiles 3- Transferring the laminas load to an external frame 4- Use of surcharge unit for clay consolidation	1- The response of the GECs is dependent on both the loading frequency and the amplitude of the dynamic base excitation 2- The highest reinforcement strains are observed for a frequency range of 1–2 Hz
Zayed et al. 2017 University of California San Diego	241x 381x 266	1-D, N-G	sinusoidal,100 and 130 Hz, 40 cycles, 0.05 g	dry sand	dynamic response of the soil	1- Rectangular shape 2- Roller bearings mounted to an external frame	1- The container provides lets the deformation of loose sand during shaking 2- The container provides proper rigidity to maintain Ko condition during spin-up and plane-strain boundary conditions during shaking
Muhammad MOHSAN et al. 2018 University of Tokyo	1000x 400x 700	1-D, 1-G	sinusoidal, 10 Hz, 3 s, 90 cyc, amp. 300 gal	silica sand 5	liquefaction phenomenon	1- Rectangular shape 2- Use of 17 laminas 3- Roller bearing are used to separate the laminas 4- Use of 2 mm thickness rubber membrane inside the box 5- Laminas are made of High strength aluminum hollow box section 6- Each lamina is guided by the 4 linear bearings that allows the movement of the lamina in one direction 7- Use of 11 porous stones for injecting/extracting the water for saturation/desaturation 8- A 15 mm solid steel base is attached to avoid the movement at soil-base plate interface	1- Soil requires fewer loading cycles to liquefy compared to the soil in rigid box 2- Pore water pressure development starts before the time that was observed in the rigid soil box 3The observed settlements are higher in the laminar soil container compared to the tests in rigid soil box

Table A. 1 (continued): Laminar soil containers published in literature and their specifications

Reference	Dimensions, L x W x H, mm3	Dimension of Motion and Test Type	Ranges of Applied Frequency or Period and Acceleration or Displacement	Soil Type	Applied Tests	Design Specifications	Key Notes and Results Regarding the Performance of Laminar Container
Alaie et al. 2018 University of Guilan	700x 500x 950	1-D, 1-G	sinusoidal, 5 Hz, 1~20 mm	sand of the Caspian Sea	producing stress-strain data at different shear strain amplitudes	1- Rectangular shape 2- Ball bearings used between the laminas 3- Use of thin flexible plastic membrane to prevent soil penetration into the gaps between laminas 4- Wooden base plate with rough surface used to prevent sliding at the soil-base plate interface	1- Assuming one-dimensional shear beam behavior, Shear stress–strain hysteresis was calculated 2- Results were in agreement with the empirical trends 3- The evaluated shear modulus and damping ratio showed low confinement behavior in shake table models 4- Modulus reduction trend seems higher than the conventional curves, probably due to the densification of sand 5- Damping characteristics is in match with the benchmark curves found in literature for sand materials 6- A scatter was found in the damping ratio data which was the result of low confinement in 1-g
Bandini et al. 2019 University of Messina	6000x 1500x 2000	1-D, 1-G	earthquake loads	sand	dynamic response of the soil	1- Rectangular shape 2- Made of 18 aluminum rectangular hollow section rings, stacked with rubber EPDM (Ethylene-Propylene Diene Monomer) and polyzene sheets 3- Use of abrasive paper sheet on the base to aid the transmission of shear waves 4- Use of abrasive paper sheet on the end walls to enable generation of shear stress 5- Lateral walls covered with two layer sheets lubricated with hexagonal boron nitride 6- A rigid steel frame and a system of steel roller bearings used to restrain lateral deformations and preventing unwanted torsional movement 7- Use of pluviator for preparing the soil specimen 8- Use of laser tracker system (Leica AT930) to measure the coordinates of 56 points on the side walls and 26 points on the shaking table platform	1- During sand filling stages and deformation of the walls of the container, plane strain conditions verified properly 2- Higher range of frequencies originated form the devices and machinery affect the results and cause differences between target motion and measured one

Table A. 1 (continued): Laminar soil containers published in literature and their specifications

Reference	Dimensions, L x W x H, mm3	Dimension of Motion and Test Type	Ranges of Applied Frequency or Period and Acceleration or Displacement	Soil Type	Applied Tests	Design Specifications	Key Notes and Results Regarding the Performance of Laminar Container
Lei H. et al. 2020 Tianjin University	2000(D,H) x1800	3-D, 1-G	El Centro (0.1-0.8g)	medium dense sand	dynamic response of the soil	1- Circular shape 2- Made of 18 aluminum circular rings separated with 3D limit connectors 3- A highly elastic membrane used to cover the inner wall of the container 4- Guardrails used to constraint the excessive horizontal movement of the container	1- Performance of the container is verified through numerical modelling 2- The natural frequency and damping ratio of the container is much different from soil sample 3- The boundary effect is evaluated by calculating the error factor

CURRICULUM VITAE

Name Surname: Omid BAGHERI

EDUCATION

B.Sc.: 2008, University of Mohaghegh Ardabili, Civil Engineering Department

M.Sc. : 2012, Tarbiat Modares University, Geotechnical Engineering Department

PROFESSIONAL EXPERIENCE AND REWARDS:

Awarded Full-Scholarship for the whole B.Sc. Courses, University of Mohaghegh Ardabili (2003 – 2008).

Awarded Full-Scholarship for the whole M.Sc. Courses, Tarbiat Modares University (2010 – 2012).

TÜBİTAK Researcher, No. 119M624., Funded by The Scientific and Technological Research Council of Turkey (September 2019- September 2022).

BAP scholarship , No. 42629., Funded by Financial Coordination Office for Research Projects of Istanbul Technical University (September 2020- September 2022).

Short- Term Student Exchange Grant for Studying in Japan offered by Tokyo Institute of Technology (July 2019- September 2019).

PUBLICATIONS, PRESENTATIONS AND PATENTS ON THE THESIS:

O. Bagheri and E. E. Eseller-Bayat, Laminar Soil Container's Performance Study for Dynamic Laboratory Tests: Comprehensive Review and Numerical Verification, KSCE Journal of Civil Engineering (2024) 28(7):2705-2721, DOI 10.1007/s12205-024-1122-4